Investigation of Environmental Influences on Mycotoxin Production in *Alternaria alternata* and the Biosynthesis of Alternariol Sulfate

Zur Erlangung des akademischen Grades eines

DOKTORS DER NATURWISSENSCHAFTEN

(Dr. rer. nat.)

von der KIT-Fakultät für Chemie und Biowissenschaften

des Karlsruher Instituts für Technologie (KIT)

genehmigte

DISSERTATION

von

Adetoye W. Adeyemo, M.Sc

1. Referent: PD Dr. Markus Schmidt-Heydt
2. Referent: Prof. Dr. Reinhard Fischer
Tag der mündlichen Prüfung: 15.07.2025

Eidesstattliche Erklärung

Hiermit versichere ich, dass ich die vorliegende Arbeit eigenständig verfasst und keine anderen als die angegebenen Hilfsmittel oder Quellen verwendet habe. Die wörtlich oder inhaltlich übernommenen Stellen sind als solche kenntlich gemacht. Die Regeln zur Sicherung guter wissenschaftlicher Praxis am Karlsruher Institut für Technologie (KIT), in der gültigen Fassung vom 05.10.2021, wurden beachtet.

List of Abbreviations

AOH	Alternariol
AOH-S	Alternariol sulfate
ALS	Altenusin
ALN	Altenuene
AME	Alternariol monomethyl ether
ATX	Altertoxin
DCBR	Dichloran-Bengalrot-chloramphenicol-Agar
DMSO	Dimethyl sulfoxide
DoxI	putative extradiol dioxygenase
DSMZ	German collection of microorganisms and cell cultures
EFSA	European food safety authority
EMEM	Eagle's minimum essential medium
EndoPG	Endopolygalacturonase
GDP	Guanosindiphosphat
GTR	General time reversible
HOG	High osmolarity glycerol
HPLC	High-performance liquid chromatography
HSA	Human Serum Albumin
ITS	Internal transcribed spacer
MG	Malt-glucose
nm	Nanometer
PCR	Polymerase chain reaction
PDA	Potato dextrose agar
PEG	Polyethylenglycol
pks	Polyketidsynthase
ROS	Reactive oxygen species
RPB2	second largest subunit of RNA polymerase II
sgRNA	Single guide RNA
SULT	Sulfotransferase
TBE	TRIS-Borat-EDTA-Puffer
TeA	Tenuazoic acid
TLC	Thin layer chromatographie
TMHMM	Transmembrane Helices Hidden Markov Model
UV	Ultraviolet
WST	Water-soluble tetrazolium
YES	Yeast extract sucrose

Abstract

Even though *A. alternata* has major potential to cause health risks for consumers due to its ubiquitous and toxigenic nature; to date, the lack of data prevents the introduction of federal limits. While monitoring recommendations for AOH, AME, and TeA were provided by the European Commission, these only applied to specific foods, such as processed tomato products and cereal-based foods for infants and young children. Hence, to recommend or advise on federal limits, data on toxin occurrence and the feasibility of modifying the synthesized amounts of toxins must be generated.

This thesis is subdivided into three parts: first, the identification of *A. alternata*; second, the change in mycotoxin production due to environmental stress factors; and third, the investigation of the alternariol sulfate biosynthesis as well as the infection of apples by *A. alternata*.

In this thesis, after several *Alternaria* strains were isolated, the existing means of identification were applied to assign those isolates to their corresponding species. Yet, it turned out, those means of identification were insufficient. Therefore, the concatenation of three molecular markers was compared to the extensions of the application of concatenations of four and five molecular markers. This resulted in the finding that increasing the number of markers from three to five significantly improves the precision of species assignment, while not requiring an excessive amount of additional work. Furthermore, the means of identification based on spore morphology, colony phenotype, and chemotype were compared to the newly developed system using five molecular markers. This is concluded by visible discrepancies, indicating that spore morphology, colony phenotype, and chemotype, independently, are insufficient means of identification and should therefore be used in combination with molecular markers to identify *A. alternata* strains more accurately.

Since environmental stress factors can modify toxin synthesis in fungi, the previously isolated *A. alternata* isolates were exposed to various light wavelengths, oxidative stress, different pH levels, varying temperatures, and low water activity. The mycotoxin concentrations of AOH, AME, AOH-S, TeA, ALS, ALN, and ATX-I were quantified by HPLC and compared to a negative control. It was shown that exposure to light of any wavelength generally leads to an increase in mycotoxin concentrations. However, the other external stress factors, such as the pH value of 4 or 8, the oxidative stress caused

by 5 mM H_2O_2 or 8 mM H_2O_2, as well as the lower temperature of 16 °C, resulted in significant decreases in some toxins while also causing an increase in others. Finally, an elevated temperature of 33 °C and a low water activity of 0.9 resulted in decreased concentrations of most toxins without stimulating an increase in others, making these two stress factors the most susceptible in order to design mycotoxin prevention strategies.

Due to the scarcity of research on AOH-S, this thesis investigated its biosynthesis. Since sulfotransferases are necessary for the transfer of the sulfate group to AOH, a concatenation of BLAST searches was performed through which several putative sulfotransferases were found in *A. alternata*. Using protein prediction tools, SULT2 and SULT15 were identified as belonging to the group of cytosolic SULTs, which are more likely to be involved in metabolic processes. The corresponding genes for the cytosolic SULTs *sult2* and *sult15*, as well as the corresponding gene for the membrane-bound SULT1, were inactivated using the CRISPR/Cas9 system. When examining the *Δsult2*, *Δsult15*, and *Δsult1* mutants by quantifying the synthesized mycotoxin concentrations via HPLC, it became apparent that, although changes in the metabolite profile were visible, no change in the AOH-S concentrations could be identified. This led to the conclusion that none of the genes examined codes for the SULT of interest.

When *A. alternata* infects an apple, a lesion is formed, and mycotoxins are synthesized, which migrate into the apple. Within this thesis, it was determined that while the infection remains rather superficial even after 14 days, mycotoxins migrate into the apple beyond the visible lesion, questioning any recommendations of even generously removing moldy parts to be able to eat the fruit.

In conclusion, this multidisciplinary study provides an in-depth analysis of the mycotoxin formation in *A. alternaria*. Based on the data generated in this work, recommendations for food safety and mycotoxin prevention strategies can be derived.

Zusammenfassung

Trotz des Gesundheitsrisikos, das *Alternaria alternata* aufgrund seiner ubiquitären Natur und Toxigenität für Verbraucher birgt, verhindert der Mangel an Daten bislang die Einführung gesetzlicher Grenzwerte. Die von der Europäischen Kommission formulierten Überwachungsempfehlungen für Alternariol (AOH), Tenuazonsäure TeA) Alternariolmonomethylether (AME) und) gelten lediglich für spezifische Lebensmittel, wie verarbeitete Tomatenprodukte. Um gesetzliche Grenzwerte definieren zu können, müssen daher Daten zum Toxinaufkommen, zur Toxikologie sowie zur Möglichkeit der Beeinflussung der Toxinbildung bereitgestellt werden.

Diese Thesis kann in drei Teile unterteilt werden. Zunächst die Identifikation von *A. alternata*, als nächstes wird der Einfluss den Umweltfaktoren auf die Mykotoxin Synthese haben beleuchtet und zuletzt wird die Alternariol Sulfat Biosynthese sowie die Infektion von Äpfeln durch *A. alternata* betrachtet.

In dieser Arbeit wurden zunächst mehrere *Alternaria*-Stämme isoliert und anschließend mit den vorhandenen Identifizierungsmethoden ihren jeweiligen Arten zugeordnet. Es stellte sich heraus, dass diese Methoden unzureichend waren. Daher wurde die Kombination von drei molekularen Markern mit Erweiterungen auf vier und fünf molekulare Marker verglichen. Dabei zeigte sich, dass die Erhöhung der Markeranzahl von drei auf fünf die Präzision der Artzuordnung signifikant verbessert, ohne dass ein unverhältnismäßiger Arbeitsaufwand entsteht. Des Weiteren wurden die Identifizierungsmethoden, die auf Sporenmorphologie, Koloniephänotyp und Chemotyp basieren, mit dem neu entwickelten System verglichen. Dies führte zu sichtbaren Diskrepanzen, die zeigen, dass Sporenmorphologie, Koloniephänotyp und Chemotyp, isoliert betrachtet, als Identifizierungsmittel unzureichend sind und daher nur in Kombination mit molekularen Markern zur Identifikation genutzt werden sollten.

Da Umweltfaktoren die Toxinsynthese bei Pilzen beeinflussen können, wurden die zuvor isolierten *A. alternata*-Isolate verschiedenen Lichtwellenlängen, oxidativem Stress, unterschiedlichen pH-Werten, variierenden Temperaturen und niedriger Wasseraktivität ausgesetzt. Die Mykotoxinkonzentrationen von AOH, AME, AOH-S, TeA, ALS, ALN und ATX-I wurden mittels HPLC quantifiziert und mit einer Negativkontrolle verglichen. Es zeigte sich, dass die Exposition gegenüber Licht jeglicher Wellenlänge im Allgemeinen zu einem Anstieg der Mykotoxinbildung führte.

Andere externe Stressfaktoren, wie ein pH-Wert von 4 oder 8, oxidativer Stress ausgelöst durch 5 mM H_2O_2 oder 8 mM H_2O_2 sowie eine niedrigere Temperatur von 16 °C, führten hingegen zur signifikanten Abnahme der Bildung einiger Toxine, während sich diese gleichzeitig für andere erhöhte. Letztendlich führten sowohl eine erhöhte Temperatur von 33 °C als auch eine niedrige Wasseraktivität von 0.9 zu verringerten Konzentrationen der meisten Toxine, ohne eine Zunahme anderer zu stimulieren, was diese beiden Einflussfaktoren am vielversprechendsten für die Entwicklung von Mykotoxin-Präventionsstrategien erscheinen lässt.

Aufgrund der geringen Datenlage zu AOH-S wurde im Rahmen dieser Arbeit dessen Biosynthese untersucht. Zunächst wurde eine Kombination von BLAST-Alignments durchgeführt, wodurch mehrere putative Sulfotransferasen in *A. alternata* identifiziert werden konnten. Mithilfe von Protein-Prediction-Tools konnten SULT2 und SULT15 der Gruppe der zytosolischen SULTs zugeordnet werden. Die entsprechenden Gene für die zytosolischen SULTs *sult2* und *sult15* sowie das entsprechende Gen für die membrangebundene SULT1 wurden mittels des CRISPR/Cas9-Systems inaktiviert. Bei der Untersuchung der *Δsult2*-, *Δsult15*- und *Δsult1*-Mutanten durch Quantifizierung der synthetisierten Mykotoxinkonzentrationen mittels HPLC zeigte sich, dass, obwohl Veränderungen im Metabolitenprofil sichtbar waren, keine Veränderung der AOH-S-Konzentrationen nachweisbar war. Dies führte zu dem Schluss, dass keines der untersuchten Gene für die gesuchte SULT kodiert.

Wenn *A. alternata* einen Apfel infiziert, bildet sich eine Läsion, und Mykotoxine werden synthetisiert, die in den Apfel migrieren. Innerhalb dieser Arbeit wurde festgestellt, dass die Infektion selbst nach 14 Tagen oberflächlich bleibt, die Mykotoxine jedoch über die sichtbare Läsion hinaus in den Apfel migrieren

Zusammenfassend lässt sich sagen, dass diese multidisziplinäre Studie eine eingehende Analyse der Mykotoxinbildung in *A. alternata* liefert. Basierend auf den in dieser Arbeit generierten Daten können Empfehlungen für die Lebensmittelsicherheit und Mykotoxin-Präventionsstrategien abgeleitet werden.

Content

1 Introduction

1.1 Filamentous fungi

Filamentous fungi are a vastly diverse group of eukaryotic organisms with over 70.000 different described species and an estimated 1-4 million unknown species (Blackwell, 2011). The kingdom of fungi, which is superordinated to the filamentous fungi, consists of several different phyla, most of which are Ascomycota and Basidiomycota. One crucial attribute all members of the fungal kingdom possess is the cell wall, which is composed of chitin as the major component for structural integrity, along with ß-1,3-glucans and ß-1,6-glucans (Gow et al., 2017). Fungi are heterotrophic and live as saprophytes, either in symbiosis or as parasites (Harley, 1971; Merckx et al., 2009). Saprophytic organisms decompose dead animals, plants, and microorganisms, utilizing them as a source of energy, thereby making organic compounds more readily available in their environment (Setälä & McLean, 2004). As symbiotes, fungi live in association with other organisms, such as plants, algae, or cyanobacteria (Hawksworth, 1988; Hyvärinen et al., 2002; Koide & Mosse, 2004). One of the most well-known symbioses is the mycorrhiza, a symbiosis between fungi and plant roots. In this symbiosis, the plants provide the fungi with glucose that is synthesized through photosynthesis. Meanwhile, the plant is supplied with phosphorus and nitrate due to the fungus's ability to extend the plant root surface through which these minerals can be absorbed (Read, 1999). The defining trait of filamentous fungi is the apical polar growth of their filaments, known as hyphae (Parkinson, 1994). Within the hyphae, multiple cross-walls, known as septa, can be found. These septa, along with the help of so-called Woronin bodies that can block the septal pores, can plug damaged hyphae. This blockage allows the organism to survive external physical damage (Markham & Collinge, 1987). When multiple hyphae create a network,

it´s called mycelium. While multicellular fungi like *Alternaria alternata* mostly grow polarly at their hyphal tips, unicellular fungi like the yeast *Saccharomyces cerevisiae,* which is used for baking or brewing, either reproduce by binary fission or by budding (Bullerman & Bianchini, 2007; Lahue et al., 2020) (Herskowitz, 1988; Taralova et al., 2011).

The metabolism of filamentous fungi can be separated into primary and secondary metabolism. Primary metabolism, which is the metabolism essential for the organism's survival, includes the production of basic components for growth, like amino acids and nucleic acids, as well as macromolecules. Primary metabolism also provides the fungus with energy (Chroumpi et al., 2020). Conversely, the secondary metabolism results in metabolites that the organism does not need for essential survival (Keller et al., 2005). Yet, those secondary metabolites are formed from intermediates of products synthesized in the primary metabolism, such as melanin, which is formed from malonyl-CoA (Eisenman & Casadevall, 2012). Secondary metabolites can have a plethora of different functions ranging from UV light protection by pigments such as carotenoids or melanins (Stahl & Sies, 2002) (Suthar et al., 2023), protection against radicals by antioxidants like the mycotoxin citrinin (Geisen et al., 2018; Heider et al., 2006), inhibition of the surrounding microbiome by antibiotics like penicillin (Mohr, 2016) or enhancement of the ability to infect host plants by mycotoxins such as alternariol (AOH) (Wenderoth et al., 2019). Mycotoxins will be discussed in detail in the following subsections of the chapter. Secondary metabolites are a group of compounds with tremendous variation, which include polyketides, non-ribosomal peptides, ribosomally synthesized and post-translationally modified peptides, non-alpha poly-amino acids like e-Poly lysine, terpenes, and indole terpenes, which are typically coded by a group of genes in close proximity to each other, making up a gene cluster (Ahmed et al., 2017; Bai et al., 2023; Hetrick & van der Donk, 2017; Keller & Hohn,

1997; Schmidt-Dannert, 2015; Wei et al., 2023; Wyatt et al., 2010). Due to the aforementioned secondary metabolites having significantly varying properties, filamentous fungi have become of major importance to the pharmaceutical industry. This importance is not limited to antibiotics like the beta-lactams, which include penicillins, cephalosporins, clavulanic acid, and carbapenems, but also anti-cancer compounds like the chemotherapeutic agents anguidine, fumagillin (Balsalobre et al., 2019; Carvalho et al., 2009; Hou et al., 2009; Kornienko et al., 2015). Beyond their use in the pharmaceutical industry, fungi are already a staple organism in the food industry. Some fungi have been used for food fermentation for millennia (Selhub et al., 2014). Foods such as bread and beer are fermented with Saccharomyces cerevisiae, whereas sake and soy sauce are fermented with different *Aspergillus* species (Abe & Gomi, 2007; Ali et al., 2012; Hu et al., 2022; Lodolo et al., 2008). Fungal fermentation of foods leads to longer consumablility due to the fungus's production of antimicrobial substances, such as acids and alcohols (Nout & Aidoo, 2011; Sreeramulu et al., 2000). Additionally, the fungus physically the food from being infected by other microorganisms by inhabiting the niche. Furthermore, fungal fermentation enhances digestibility and nutrient availability in foods by degrading and reconstructing non-digestible or stodgy carbohydrates, as well as hydrolyzing proteins into short-chain peptides (de Reu et al., 1995; Samtiya et al., 2021). With the rising demand for meat alternatives, plant-based or insect-based products are gaining increasing importance as protein sources. Yet, food based on mycoproteins is also emerging. Not only are mycoproteins an animal-cruelty-free alternative to meat that contains approximately 41 % more essential amino acids than most plant-based proteins, but they also offer multiple benefits beyond their nutritional value (Finnigan et al., 2019). Additional benefits are stabilizing blood insulin levels, a decrease in the necessary energy intake (Bottin et al., 2016), improvement of cholesterol levels

(Turnbull et al., 1990), and support of muscle growth (Dunlop et al., 2017). Despite the multiple possibilities of how some fungi can be used positively, there are severe issues caused by the presence of others. Plant pathogenic fungi can infect several different hosts, like fruits (Fontaine et al., 2021; Nazari et al., 2022; Thomma, 2003; Troncoso-Rojas & Tiznado-Hernández, 2014b), as well as vegetables (Farrar et al., 2004) (Singh, 2015) (Vakalounakis & Malathrakis, 1988) and even grass (Abdessemed et al., 2019; Wilson et al., 2014), which can lead to harvest losses or even to complete crop failure. Beyond that, some filamentous fungi, such as *A. alternata*, which uses plants as their hosts, are mycotoxin producers. Those contaminations cause an estimated 20 % of harvest losses yearly (Nowicki et al., 2012). This work focuses on the Ascomycota genus *Alternaria*, particularly the species *A. alternata*, a relevant plant pathogen and mycotoxin producer, thereby holding significant importance for food and feed safety (Pavicich et al., 2022).

1.2 Genus *Alternaria*

The genus *Alternaria*, which occurs ubiquitously, has more than 360 species, all known to be plant pathogens (J.-F. Li et al., 2023). *Alternaria* spp. has a black to dark brown or dark greenish phenotype (Fig 1), which is caused by its melanization of hyphae and spores (Fetzner et al., 2014) as seen in Fig. 1. *Alternaria* spores are very noticeable due to their compared to other spores large size, their club like shape with multiple septa and them being polynuclear as seen in Fig. 2 (Thomma, 2003). Currently, the phylogenetically often-changing genus *Alternaria* contains 29 sections, with the most prominent ones being the section *Alternaria*, section *brassicicola*, and section *infectoriae* (J.-F. Li et al., 2023). Multiple factors are considered when assigning species to specific sections. In the past, morphological features like conidial septation,

Figure 1: Colony phenotypes of A. alternata strains isolated in this study showing the typical black and greenish phenotypes. On the left side with the black phenotype, strain APKA can be seen and on the right the dark green phenotype of APBR can be seen. Both strains were incubated on PDA at 28°C.

conidia chain length, and chain branching, which can be seen in Fig. 3, as well as patterns of mycotoxin synthesis, were mainly used for identification (Emory G Simmons, 2007). Yet, since the early 2000s, when sequencing became more affordable, genetic markers within the genus *Alternaria* and led to many changes within the phylum (Lawrence et al., 2015). Today, molecular markers are used as the primary method of identification, while chemotyping and phenotyping play a role in combination with molecular markers to identify and assign *Alternaria* species (Adeyemo & Schmidt-Heydt, 2024). Additionally, the genus *Alternaria* can pose a health risk in multiple ways

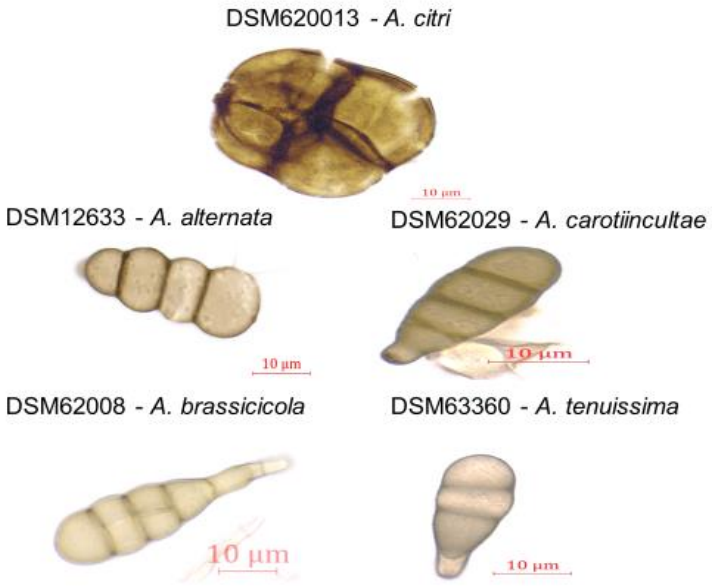

Figure 2: Morphological features of representative spores from commercial Alternaria strains bought at DSMZ

(Chain, 2011). *Alternaria* spores carry E-specific antigens on their surface, which can cause Type I hypersensitivity in susceptible individuals.

Those hypersensitivities can result in a couple of conditions that are especially present in the respiratory organs. Those conditions can include rhinitis, rhinosinusitis, and asthma, as well as forms of atopic dermatitis (Horner et al., 1995). Beyond its role as an allergen, the genus *Alternaria* poses health risks due to its toxigenic nature, which enables it to synthesize a range of mycotoxins, including alternariol and tenuazonic acid. The mycotoxins synthesized by the genus *Alternaria* will be elaborated in detail in the following subsections of this chapter.

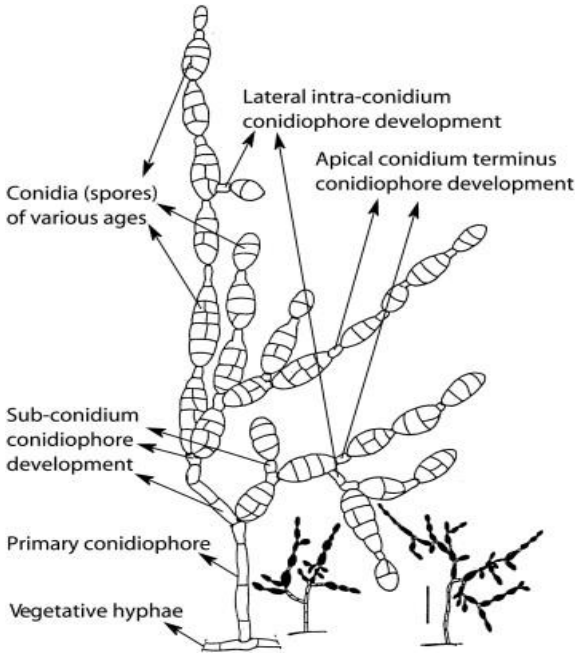

Figure 3: *Alternaria alternata*: portions of sporulation clumps and habits from PCA (left) and Hay (right). The figure identifies the various spore and conidiophore developments. EGS 34-016. Bars ~ 50 µm. Line drawings copyright by E.G. Simmons, 1999. Mycotaxon 70:336.

1.2.1 Alternaria alternata

As a major plant pathogen, *A. alternata* is responsible for multiple plant diseases. Firstly, *Alternaria* leaf spot disease, also called *Alternaria* leaf blight (ALS). *Alternaria* leaf spot disease can occur on a wide variety of hosts, including soybeans, sunflowers, *Aloe vera*, potatoes, and many more. ALS causes necrotic lesions to form on the

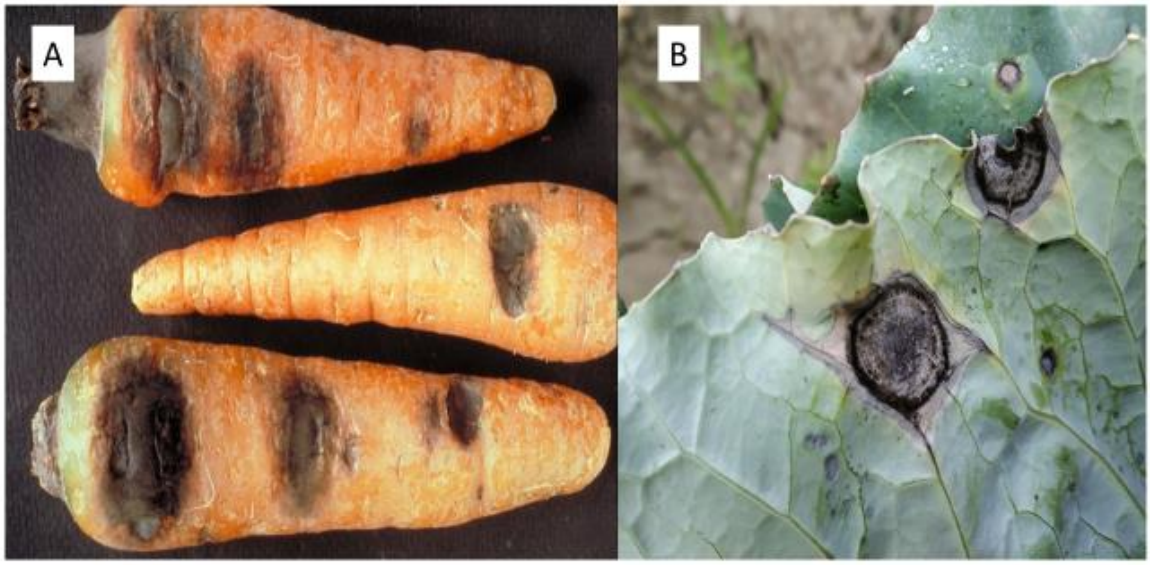

Figure 4: A: Cabbage leaf showing symptoms of the Alternaria leaf spot disease (Kohler F, Pellegrin F, Jackson G, McKenzie E (1997) Diseases of cultivated crops in Pacific Island countries. South Pacific Commission. Pirie Printers Pty Limited, Canberra, Australia)). B: Carrots showing Symptoms of the black rot disease caused by an infection with A. alternata. Thirunarayanan Perumal, Banaras Hindu University, Bugwood.org.

leaves, which can even lead to holes developing from the lesions, depending on the dryness. Even though *Alternaria* leaf spot disease doesn't necessarily directly reduce harvest yields, a heavy infestation can negatively influence plant health, which in turn can result in lower yields (Kokaeva & Elansky, 2022; Troncoso-Rojas & Tiznado-Hernández, 2014b; Zheng & Wu, 2013). While *Alternaria* leaf spot disease, as the name suggests, only occurs on leaves (Fig. 4 A), *Alternaria* black spot disease can also develop on the plant's stem (Fig.4 B) (Troncoso-Rojas & Tiznado-Hernández, 2014a). Another plant disease caused by *A. alternata* is black rot disease, which is similar to *Alternaria* leaf spot disease, except that it manifests in fruits, directly affecting yield. Aside from the plant diseases *A. alternata* causes in its hosts, the mycotoxins synthesized by this species also play a considerable role as contaminants (Isshiki et al., 2001; Troncoso-Rojas & Tiznado-Hernández, 2014a). With over 70 different mycotoxins, some of which have mutagenic or cytotoxic properties among others, *A. alternata* can be considered a significant toxigenic fungus with relevance to human health (Dall'Asta et al., 2014).

1.3 Mycotoxins

Mycotoxins, which are toxins synthesized by fungi, are capable of disturbing cells or cellular processes (Wallace Hayes, 1980). Furthermore, as secondary metabolites, mycotoxins exhibit a wide range of structural differences (Bräse et al., 2009). It is estimated that over 1,000 mycotoxins have already been described, with the number constantly rising (Bräse & Meister, 2013). Some of the most common mycotoxins in the food sector include aflatoxins, fumonisins, deoxynivalenol, zearalenone, ochratoxins, as well as *Alternaria* toxins (Tola & and Kebede, 2016). *Fusarium* species synthesize fumonisins, deoxynivalenol, and zearalenone, while *Aspergillus* species synthesize aflatoxins and ochratoxins, and *Alternaria* species synthesize alternariol and alternariol monomethyl ether (Audenaert et al., 2013; Caldwell et al., 1970; Cendoya et al., 2018). There are several possible ways mycotoxins can end up in food or animal feed. Apart from directly ingesting contaminated food due to contamination that is not visible, such as when an apple is moldy on the inside without showing symptoms on the outside, there are other ways to consume mycotoxins. One good example of this is the so-called “carry-over” effect. Cows consume contaminated feed, thereby ingesting mycotoxins such as aflatoxins, which accumulate in metabolized forms in the milk and are later consumed by humans, exposing them to aflatoxins in the process (Fink-Gremmels, 2008). Furthermore, processed foods pose a health risk since consumers cannot determine how contaminated the raw fruits and vegetables were before processing. Even if the source material for processed food is relatively free from mycotoxins, the process chains that include transport and storage can often lead to a significant increase in mycotoxin spread and degree of contamination (Bautista-Baños et al., 2013; Dawlal et al., 2012). Whilst some mycotoxins are unstable under certain conditions, like the ones that are thermolabile and are thereby degradable by heat (Jackson et al., 1996), some mycotoxins, such as the *Alternaria*

toxins, are relatively stable and hence unlikely to be degraded while being processed (H. B. Lee et al., 2015). Beyond the scope of mycotoxin degradation, the concentrations of mycotoxins can be altered by the fungus's surrounding environment (Priesterjahn et al., 2020; Schmidt-Heydt et al., 2008). This means that the amounts and kinds of mycotoxins synthesized by the fungus will change depending on the host and the environment the host is in. Factors such as light intensity, wavelength of light, absence of light, water activity, oxidative stress, heat, cold, and changes in pH value can strongly impact the chemotype of fungi (Etcheverry et al., 1994; Fanelli et al., 2016; Schmidt-Heydt et al., 2015). This impact is likely rooted in the genetic regulation of mycotoxins, which are often synthesized by whole gene clusters as part of the fungal stress responses (Kolawole et al., 2021; Ponts, 2015). In the case of mycotoxins like citrinin, which is linked to the fungal stress response since it acts as a scavenger for reactive oxygen species, reactions to external stress are feasible (Heider et al., 2006; Schmidt-Heydt et al., 2015). Yet, in many other cases, even though the mycotoxin synthesis can be linked to external stresses, the function of many mycotoxins still remains unclear (Geisen et al., 2017). The most prominent mycotoxins with yet unknown functions are aflatoxins, which, incidentally, are the most potent mycotoxins, some of them possessing carcinogenic and mutagenic properties (Massey et al., 1995; Wong & Hsieh, 1976). The major mycotoxins synthesized by *A. alternata*, which are addressed in this work, are alternariol (AOH), alternariol monomethyl ether (AME), alternariol sulfate (AOH-S), altenuene (ALN) , altenusin (ALS), tenuazonic acid (TeA), and altertoxin-I (ATX-I).

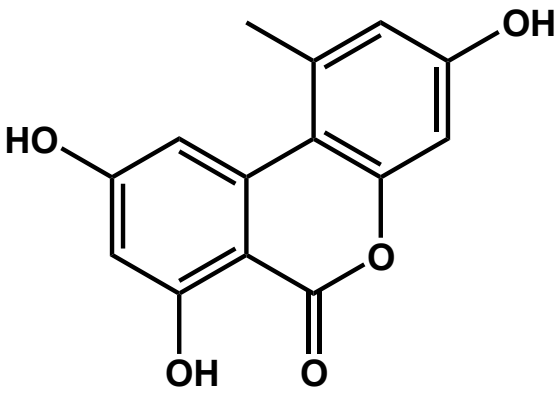

1.3.1 Alternariol

AOH is a benzochromenone and therefore a member of the phenol group. Structurally, AOH comprises two phenolic rings with hydroxy groups at positions 3,7, and 9 (Fig. 5). AOH is synthesized through a polyketide pathway in which one acetyl-CoA and six malonyl-CoA molecules are combined via PKS-I (Saha et al., 2012). While the toxicity of AOH has not been thoroughly investigated at this point, it has been demonstrated

Figure 5: Chemical structure of the mycotoxin alternariol.

to interact with DNA topoisomerases I and II. While AOH inhibits the catalytic activity of both topoisomerases, it also stabilizes the covalent topoisomerase-DNA intermediates, suggesting that AOH acts as a topoisomerase poison (Fehr et al., 2009). Furthermore, AOH was found to reduce proliferation in Caco-2 cells, resulting in an accumulation of cells in the G2/M phase. Since the S-phase requires topoisomerase activity, the reduced proliferation is likely a result of topoisomerase inhibition (Fernández-Blanco et al., 2016). In macrophages, after exposure to AOH, the level of γH2AX increases rapidly, indicating the presence of double-strand breaks. Another result of AOHs' ability to inhibit topoisomerases is the induction of polyploidy and abnormal nuclei, which were observed after prolonged treatment of RAW264.7 cells. This is likely due to insufficient decatenation and incomplete condensation of the DNA, resulting from the inhibition of topoisomerase IIα. Among the other consequences of

AOH's ability to inhibit DNA topoisomerases, both autophagy and macrophage senescence were induced after exposure to AOH. Beyond that, after prolonged exposure to AOH, macrophage morphology changed from round to star-shaped with increased galactosidase activity (Solhaug et al., 2013) (Solhaug et al., 2015).

Hence, it cannot be excluded that AOH exposure may cause a decreased immune response. Furthermore, AOH was found to induce reactive oxygen species (ROS) in multiple cellular models (Fernández-Blanco et al., 2014; Solhaug et al., 2012; Tiessen et al., 2013). This finding was supported by the report that AOH undergoes aromatic hydroxylation by CP450 as part of phase 1 metabolism, which generates both reactive catechols and hydroquinones (Burkhardt et al., 2011; Pfeiffer et al., 2007). Catechols and hydroquinones are known to undergo redox cycling through which ROS are generated (Weinshilboum, 1986). Following the cellular toxicity, AOH is also suggested to be an endocrine disruptor. In a cell-free system, it was confirmed that AOH acts as a weak estrogen agonist. Interestingly, those estrogenic properties were present at lower concentrations where AOH does not possess genotoxic properties (Lehmann et al., 2006).

1.3.2 Alternariol monomethyl ether

Alternariol monomethyl ether is AOH in which the hydroxy group at position nine is converted into the corresponding methyl ether (Fig. 6). The methyltransferase omtI

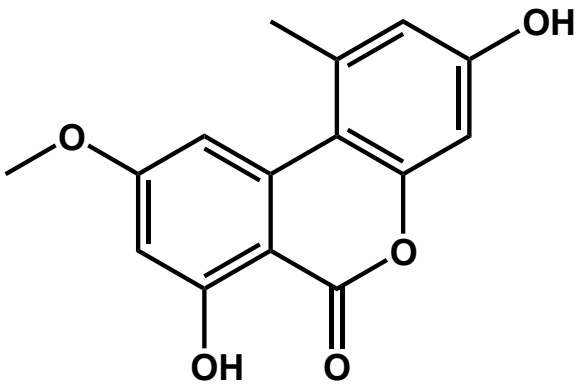

leads to the conversion of AOHs' hydroxy group to the corresponding methyl ether. AME was shown to be genotoxic in vivo when tested on Sprague-Dawley rats (Tang et al., 2022).

1.3.3 Alternariol sulfate

Alternariol sulfate (Fig. 7) is a derivative of AOH that is formed by the sulfation of AOH,

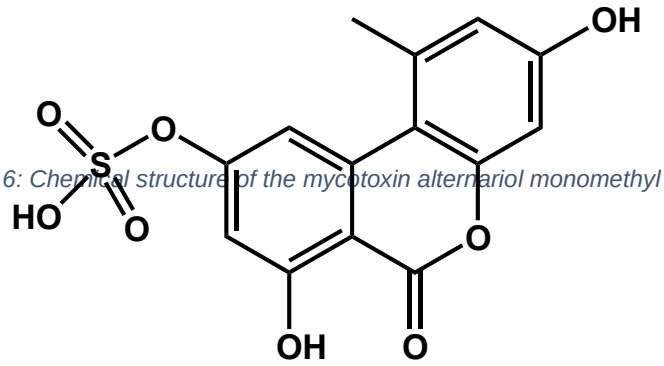

Figure 6: Chemical structure of the mycotoxin alternariol monomethyl ether

which is likely to be catalyzed by a sulfotransferase (SULT). Interestingly, when plants are exposed to xenobiotics like mycotoxins, their phase II metabolism is utilized to either conjugate the xenobiotic with a specific sugar or sulfate it, allowing for the storage of the derived xenobiotic in their cell wall or its excretion (Xu et al., 2005).

Yet, in the case of AOH-S, it was demonstrated that it was present even in the absence

Figure 7: Chemical structure of the mycotoxin alternariol sulfate

of a plant, indicating that the fungus itself must catalyze the sulfation (Soukup et al., 2016). But to do so, the organism needs a SULT, which has not yet been identified in *A. alternata*. A later chapter will investigate this in more detail. To date, research on AOH-S is scarce.

1.3.4 Altenuene

Altenuene is another derivative of AOH shown in Fig. 8. Altenuene is likely synthesized from ALT through Dox I. ALT is reported to exhibit both cytotoxic and antibacterial

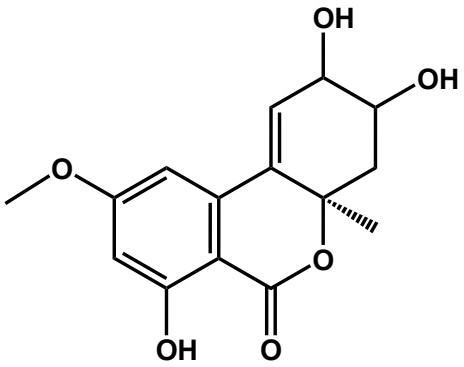

effects (Wang et al., 2014). Moreover, ALT can be used as an acetylcholinesterase inhibitor, an agent used in Alzheimer's therapy (Bhagat et al., 2016).

1.3.5 Altenusin

Altenusin is another AOH derivative formed by *A. alternata*. ALN is a carboxy biphenyl that is a biphenyl-2-carboxylic acid, which is substituted by a hydroxy group at positions 3, 4, and 5, and a methoxy group at position 5, as well as a methyl group at position 2

Figure 8: Chemical structure of the mycotoxin altenuene

(NCBI, 2025)(Fig. 9). This process is catalyzed by the monooxygenase MOXI (H.

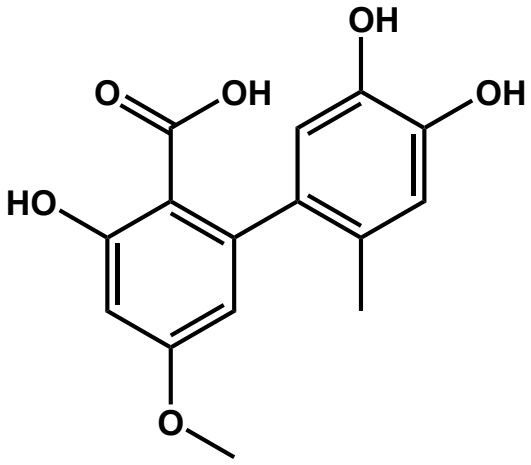

Wang et al., 2022). Like the other AOH derivatives, ALN is also a polyphenol and a member of the catechols. ALN is reported to exhibit cytotoxic activities (Takahashi et al., 2024).

1.3.6 Tenuazonic Acid

Tenuazonic acid is a tetrameric acid and the most abundantly synthesized mycotoxin for *A. alternata* (Antony et al., 1991) (Robeson & Jalal, 1991). Its chemical structure is shown in Fig. 10. TeA is reported to inhibit photosynthetic activity by inhibiting the photosystem II in plants (Chen et al., 2008). Fluorescence studies with chlorophyll showed that the electron flow from Q_A to Q_B in the acceptor side of photosystem II was

Figure 9: Chemical structure of the mycotoxin altenusin

blocked (Liu et al., 2014). Beyond its phytotoxicity, TeA was found to be toxic in animal systems as well, causing hemorrhages in chicken and dogs, precancerous changes in esophageal mucosa, dysplastic transformation and proteinbiosynthesis inhibition in mouse cells as well as causing suppression of weight gain, reduced feed efficiency, lesions and edema in chickens (Griffin & Chu, 1983) (Steyn & Rabie, 1976) (Yekeler et al., 2001). Furthermore, TeA possesses moderate entomotoxic properties (Salimova et al., 2021). At a cellular level, TeA inhibits the incorporation of amino acids into proteins in vitro and in vivo. It can inhibit the release of newly formed microsomal proteins, thereby inhibiting protein synthesis (Shigeura & Gordon, 1963). Two genes are known to be involved in the genetic regulation of the TeA biosynthesis in *A. alternata*. Firstly, there is *AaTAS1*, the gene responsible for TeA biosynthesis.

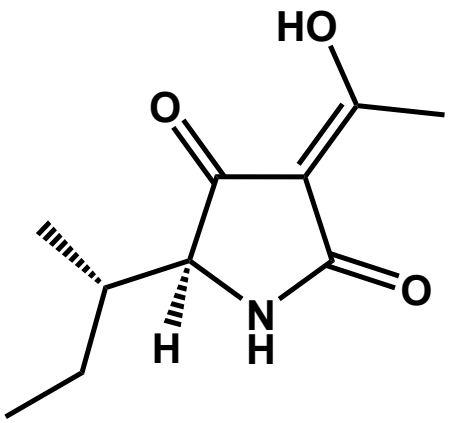

Figure 10: Chemical structure of the mycotoxin tenuazonic acid

Secondly, *AaMFS1* is necessary for the transmembrane transport of TeA (F. Sun et al., 2022).

1.3.7 Altertoxin-I

Altertoxin-I is a perylenequinone that belongs to the subgroup that is made up of two fully intact benzene rings in a stacked orientation (Fig. 11) (NCBI, 2025a). Other members of this group are altertoxin-II and stemphyltoxin. ATX-I harbors cytotoxic, mutagenic, possibly carcinogenic, immunosuppressive, and antiestrogenic properties (Louro et al., 2024) (Schrader et al., 2006) (H. Wang et al., 2022).Yet, compared to ATX-II, which has an epoxy group and selectively induces double-strand breaks, the toxicity mechanism of ATX-I is still to be determined (Crudo et al., 2025).

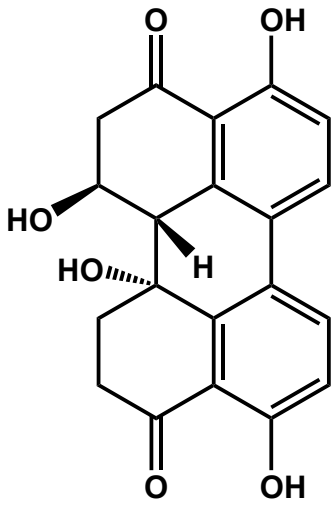

Figure 11: Chemical structure of the mycotoxin altertoxin-I

1.4 Food safety

While many mycotoxins, such as aflatoxins, citrinin, and patulin, are strictly regulated in food and animal feed, no such regulations exist for *Alternaria* toxins (Bonerba et al., 2010; López Sáncheza et al., 2017; Van Egmond & Jonker, 2004). Furthermore, if this endeavor were to be undertaken, the issue would arise that the food industry primarily

uses MS methods to identify contaminants (Songsermsakul & Razzazi-Fazeli, 2008). However, many *Alternaria* toxins, such as the aforementioned AOH-S,

are mycotoxin derivatives, as illustrated by the few examples shown in Fig. 12. Given the significant number of these derivatives, potential attempts at regulation can be hindered. Additionally, the impact of derivatization on the toxicity of most *Alternaria* toxin derivatives remains unknown, which can lead to significant miscalculations when evaluating health concerns based on toxin concentrations (Berthiller et al., 2013).

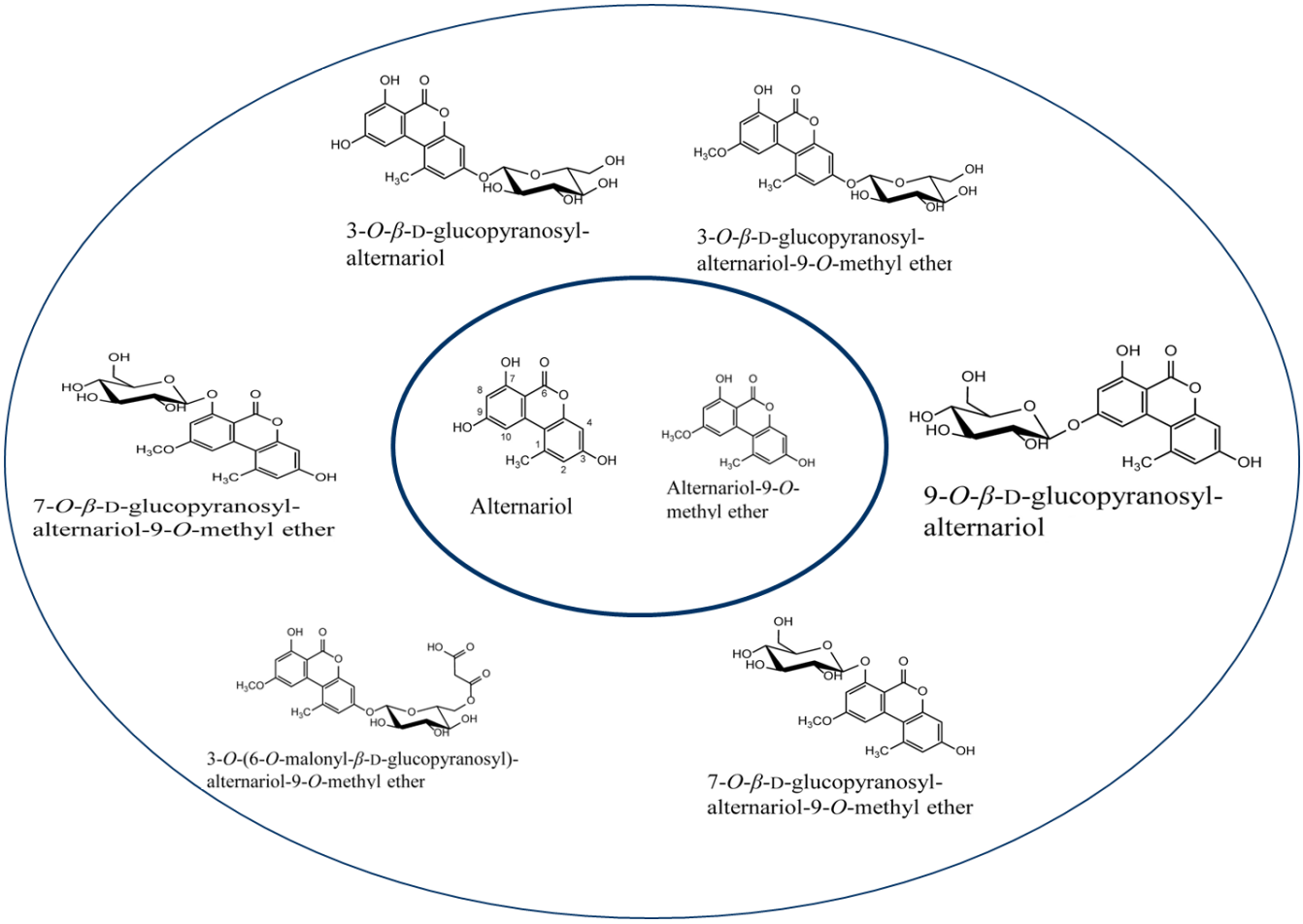

Figure 12: The inner ring shows the chemical structures of AOH and AME while the outer ring shows the chemical structures of a small number of possible derivatives which can be formed with the base of AOH or AME.

1.4.1 Mycotoxin occurrence and relevance for food safety and consumer health

To date, there are no federal limits for *Alternaria* toxins in Germany or the European Union. So, in 2011, the European Food Safety Authority (EFSA) deemed it necessary to collect more data on toxicity and occurrence (Chain, 2011). Thereafter, in 2016, when some more data was generated, it led to the conclusion that TeA might be a relevant mycotoxin due to it having the highest mean levels in measured samples. Furthermore, the data suggested higher consumer exposure than estimated. Hence, it was recommended that analytical methods be improved and more analytical data on relevant food commodities be generated (Angel et al., 2016). Finally, in 2022, the European Commission gave a monitoring recommendation for AOH, AME, and TeA, shown in Table 1. Thus, indicative levels for certain foods were recommended for the monitored *Alternaria* toxins.

Table 1: Monitoring recommendation given by the European Commission based on data available in the EFSA database

FOOD	ALTERNARIOL (AOH) (µg/kg)	ALTERNARIOL MONOMETHYL ETHER (AME) (µg/kg)	TENUAZONIC ACID (TEA) (µg/kg)
Processed tomato products	10	5	500
Paprika powder	–	–	10
Sesame seeds	30	30	100
Sunflower seeds	30	30	1000
Sunflower oil	10	10	100
Tree nuts	–	–	100
Dried figs	–	–	1000
Cereal-based foods for infants and young children	2	2	500

1.4.2 Mycotoxin prevention strategies

Several different strategies are employed to prevent mycotoxin contamination in food and animal feed. In an industrial setting, the produce is washed, and visible contaminants are removed (Pearson et al., 2009). Depending on the produce, peels that have the potential to harbor contaminants are removed. Another strategy is to homogenize the produce to distribute the mycotoxins evenly, thereby lowering the average concentration per batch. Some toxins like aflatoxins, ochratoxins, or fumonisins are derivatized or even degraded at higher temperatures (Raters & Matissek, 2008) (Jackson et al., 1996). An example is AFB1, which is reduced by 41,9 % after a heat treatment of 150 °C for 30 minutes (J. Lee et al., 2015). Other Measures that can have more implications for food or feed that can be taken to reduce mycotoxin concentrations, are irradiation with UV-, or microwaves, mycotoxin binding agents like activated charcoal which binds patulin, cold plasma that can destroy some mycotoxins or enzymatic degradation for example by hydrolases (He et al., 2021) (Gavahian & Cullen, 2020; Sands et al., 1976) (Fang et al., 2023; Qin et al., 2021). Additionally, strong acids can destroy toxins, like aflatoxins, while strong bases can destabilize toxins such as ochratoxin. Finally, oxidizing or reducing agents can also degrade or derivatize mycotoxins (McKenzie et al., 1997) (Doyle et al., 1982).

1.5 Objective of this thesis

At the beginning of this work, *Alternaria* strains were to be isolated from several different apples, grapes, tomatoes, and wheat in order to achieve a more representative picture of *Alternaria* contamination and toxigenicity of different strains. Thereafter, an improved system for *A. alternata* identification was to be established, evaluated, and especially compared to the systems used in the past.

In which chemotyping and spore morphology played more significant roles (Emory G Simmons, 2007). To date, regulations and thresholds regarding *Alternaria* toxins are not in place. Hence, data is necessary to evaluate how many *Alternaria* toxins are synthesized on average and which factors affect toxin biosynthesis. Therefore, all strains are supposed to be exposed to various physical stress factors to investigate how toxin synthesis changes in response to specific stress factors.

The resulting data is supposed to be used to develop prevention and avoidance strategies for mycotoxin contamination. Beyond the scope of general mycotoxin contamination, this work also focuses on identifying and functionally characterizing putative SULTs, which are enzymes necessary for conjugating AOH to AOH-S. Furthermore, since mycotoxins like AOH and TeA are known virulence factors for plant infection, a system was to be implemented through which the severity of an apple infection, the resulting lesion size, and penetration depth of mycotoxins can be evaluated and potentially correlated to improve consumption recommendations for fruits with a focus on apples (Kumari & Tirkey, 2019).

2 Materials and Methods

2.1 Material

2.1.1 Organisms

Table 2: List of organisms used in this thesis

Species	Identifier	Source
Alternaria alternata	APBO	Isolated in this study, (Karlsruhe)
Alternaria alternata	APBR	Isolated in this study, (Karlsruhe)
Alternaria alternata	APCY	Isolated in this study, (Karlsruhe)
Alternaria alternata	APKA	Isolated in this study, (Karlsruhe)
Alternaria alternata	APSA	Isolated in this study, (Karlsruhe)
Alternaria alternata	APSA2	Isolated in this study, (Karlsruhe)
Alternaria alternata	APTO	Isolated in this study, (Karlsruhe)
Alternaria alternata	KPN1	Isolated in this study, (Karlsruhe)
Alternaria alternata	RS071	Provided by Remco Stam (CAU), (Peru)
Alternaria alternata	RS102	Provided by Remco Stam (CAU), (Peru)
Alternaria alternata	CS042	Provided by Remco Stam (CAU), (Peru)
Alternaria alternata	CS046	Provided by Remco Stam (CAU), (Peru)
Alternaria alternata	CS057	Provided by Remco Stam (CAU), (Peru)
Alternaria alternata	CS330	Provided by Remco Stam (CAU), (Chile)
Alternaria alternata	CS339	Provided by Remco Stam (CAU), (Chile)
Alternaria alternata	CS403	Provided by Remco Stam (CAU), (Chile)
Alternaria alternata	RS002	Provided by Remco Stam (CAU), (Peru)
Alternaria alternata	RS007	Provided by Remco Stam (CAU), (Peru)
Alternaria alternata	RS026	Provided by Remco Stam (CAU), (Peru)
Alternaria alternata	RS040	Provided by Remco Stam (CAU), (Peru)
Alternaria alternata	RS052	Provided by Remco Stam (CAU), (Peru)
Alternaria alternata	CS007	Provided by Remco Stam (CAU), (Chile)
Alternaria alternata	CS013	Provided by Remco Stam (CAU), (Chile)

Alternaria alternata	CS017	Provided by Remco Stam (CAU), (Chile)
Alternaria alternata	CS139	Provided by Remco Stam (CAU), (Chile)
Alternaria alternata	CS371	Provided by Remco Stam (CAU), (Chile)
Alternaria alternata	CS330	Provided by Remco Stam (CAU), (Chile)
Alternaria alternata	CS339	Provided by Remco Stam (CAU), (Chile)
Alternaria alternata	CS403	Provided by Remco Stam (CAU), (Chile)
Alternaria alternata	CS311	Provided by Remco Stam (CAU), (Chile)
Alternaria alternata	CS313	Provided by Remco Stam (CAU), (Chile)
Alternaria alternata	CS314	Provided by Remco Stam (CAU), (Chile)
Alternaria alternata	DSM12633	Purchased at DSMZ
Alternaria brassicicola	DSM62008	Purchased at DSMZ
Alternaria carotiincultae	DSM62029	Purchased at DSMZ
Alternaria citri	DSM62023	Purchased at DSMZ
Alternaria tenuissima	DSM63360	Purchased at DSMZ
Escherichia coli	DH-5-alpha	Purchased at New England Biolabs

2.1.2 Oligonucleotides

Table 3: Oligonucleotides used in this thesis

Oligonucleotide	Sequence (5´-3´)	Tm
Gdp1	CAACGGCTTCGGTCGCATTG	62°C
Gdp2	GCCAAGCAGTTGGTTGTGC	62°C
RPB2-5F2	GGGGNGANCAGAAGAAGGC	57°C
fRPB2-7cR	CCCATNGCTTGTNNNCCCAT	53°C
ALTa-1-F	ATGCAGTTCACCACCATCGC	60°C
ALTa-1-R	ACGAGGGTGAYGTAGCGTC	59°C
Endo-PG3	TACCATGGTTCTTTCCGA	51°C
Endo-PG2b	GAGAATTCRCARTCRTCYTGRTT	49°C
ITS1	TCCGTAGGTGAACCTGCGG	62°C
ITS4	TCCTCCGCTTATTGATATGC	53°C
SULT1-F	CGTTGGTGTAGGTTGGTGGTG	60°C
SULT1-R	TCCTCCTGGTGGTTACAATGGA	59°C
SULT2-F	GCAATGGCCGACCGT	58°C
SULT2-R	TCACCATGCCTGCGC	58°C
SULT3-F	CGCCCGCTTATTAGCCTAAT	56°C
SULT3-R	GATATATGACATGACCACGGC	54°C
SULT5-F	CCATGCCTGCGCCAATGCCT	67°C
SULT5-R	ATGTTGGGATATGAAGGTGT	52°C

SULT6-F	ATGTCTACGCAGAGGCTGAT	57°C
SULT6-R	CAATTCCCCTGTGTCCATGT	57°C
SULT9-F	ACGCTTCAAAAACAGAGGAA	53°C
SULT9-R	ATGGGCAATCAACCCTC	54°C
SULT15-F	ATGTTGGGATATGAAGGTGTACAT	54°C
SULT15-R	TCACCATGCCTGCGC	58°C
SULT1-QRT-F	TCGTGGGGAACCAGTCACAG	62°C
SULT1-QRT-R	CTAGCCTATCCTCCGGCAC	59°C
SULT2-QRT-F	GGCGAGGTTTGCCAAGAATG	59°C
SULT2-QRT-R	CCGTAGCCCATTGTACACCA	59°C
SULT3-QRT-F	CTGGCTGTGTATTTGCGTCG	59°C
SULT3-QRT-R	TCGCCACGTATCAAGACACC	59°C
SULT6-QRT-F	GTACCCAAAGACCGCTTGCT	60°C
SULT6-QRT-R	AATGCGTGGTGGGGTATGGT	61°C
SULT15-RTQ-F	TCTTCGTAGCCAGCTTCGTCA	60°C
SULT15-RTQ-R	GTCACCCCAAATTCTCCATTCCAT	59°C
SULT17-RTQ-F	GCGGCCCCATCCCATAATA	59°C
SULT17-RTQ-F	GAGACAAGTCGGGGTTGGA	59°C
SULT17-RTQ-R	ATAGTTTCCGGGTGGCGTTT	59°C
CRISPY_fw_2.0/3.0	GGTCATAGCTGTTTCCGCTGA	59°C
CRISPY_re_TtrpCkurz/PtrpC	CTTCAATATCAGTTAACGTCGAGCCAAGAGCGGATTCC	66°C
CRISPY_fw_PtrpC	GACGTTAACTGATATTGAAGGAG	52°C
CRISPY_re_TtrpClang/Vect	GTCTCGGCTGAGGTCTTAATTCTAGAAAGAAGGATTACCTCTAAAC	65°C
Proto-SULT1-fwd1	GTCCGTGAGGACGAAACGAGTAAGCTCGTCAAGAAGACTAGCCTATCCTCGTTTTAGAGCTAGAAATAGCAAGTTAAA	72°C
hh-SULT1-rev1	GACGAGCTTACTCGTTTCGTCCTCACGGACTCATCAGAAGAAGCGGTGATGTCTGCTCAAGCG	76°C
Proto-SULT1-fwd2	GTCCGTGAGGACGAAACGAGTAAGCTCGTCGCCGGTACACTGCTTGTATAGTTTTAGAGCTAGAAATAGCAAGTTAAA	73°C
hh-SULT1-rev2	GACGAGCTTACTCGTTTCGTCCTCACGGACTCATCAGGCCGGTATCGATGCTTGGGTAGAATAGG	76°C
Proto-SULT2-fwd1	GTCCGTGAGGACGAAACGAGTAAGCTCGTCGTGGTATGACAGTATGGAAGGTTTTAGAGCTAGAAATAGCAAGTTAAA	72°C
hh-SULT2-rev1	GACGAGCTTACTCGTTTCGTCCTCACGGACTCATCAGGTGGTACGGTGATGTCTGCTCAAGCG	77°C
Proto-SULT2-fwd2	GTCCGTGAGGACGAAACGAGTAAGCTCGTCGCAATGTGAAGGACA	73°C

	TGCGAGTTTTAGAGCTAGAAATA GCAAGTTAAA	
hh-SULT2-rev2	GACGAGCTTACTCGTTTCGTCCT CACGGACTCATCAGGCAATGATC GATGCTTGGGTAGAATAGG	74°C
SULT15-proto-fw-1	GTCCGTGAGGACGAAACGAGTA AGCTCGTCTCCAACTATCGACGC GGCGTGTTTTAGAGCTAGAAATA GCAAGTTAAA	74°C
SULT15-HH-rev1	GACGAGCTTACTCGTTTCGTCCT CACGGACTCATCAGTCCAACCGG TGATGTCTGCTCAAGCG	77°C
SULT15-proto-fw-2	GTCCGTGAGGACGAAACGAGTA AGCTCGTCGACAGCATGCAATAT GCTAGGTTTTAGAGCTAGAAATA GCAAGTTAAA	72°C
SULT15-HH-rev2	GACGAGCTTACTCGTTTCGTCCT CACGGACTCATCAGGACAGCATC GATGCTTGGGTAGAATAGG	75°C
crispy_seq_fw	CGTCAGTCCAACATTTGTTGC	56°C
crispy_seq_doko_rev	GGCTGGTGACGGAATTTTCAT	57°C

2.1.3 Plasmids

Table 4: Plasmids used in this thesis

Plasmid	Content	Reference
pFC330	tef1(p)::cas9::tef1(t); AfpyrG; ampR; AMA1	Nodvig et al. (2015)
pFC332	tef1(p)::cas9::tef1(t); hph; ampR; AMA1	Nodvig et al. (2015)
pFC334	tef1(p)::cas9::tef1(t); gpdA(p)::sgRNA-AnyA::trpC(t);Afpyr4; ampR; AMA1	Nodvig et al. (2015)
pJET1.2 blunt	Klonierungsvektor, Bestandteil des CloneJET PCR Cloning Kits	
pAA1	tef1(p)::cas9::tef1(t); gpdA(p)::Aasult1-sgRNAcassette1:: Aasult1-sgRNAcassette2:: gpdA(t); hph; ampR; AMA1	This study
pAA2	tef1(p)::cas9::tef1(t); gpdA(p)::Aasult2-sgRNAcassette1::	This study

	Aasult2-sgRNAcassette2:: gpdA(t); hph; ampR; AMA1	
pAA3	tef1(p)::cas9::tef1(t); gpdA(p)::Aasult15-sgRNAcassette1:: Aasult15-sgRNAcassette2:: gpdA(t); hph; ampR; AMA1	This study

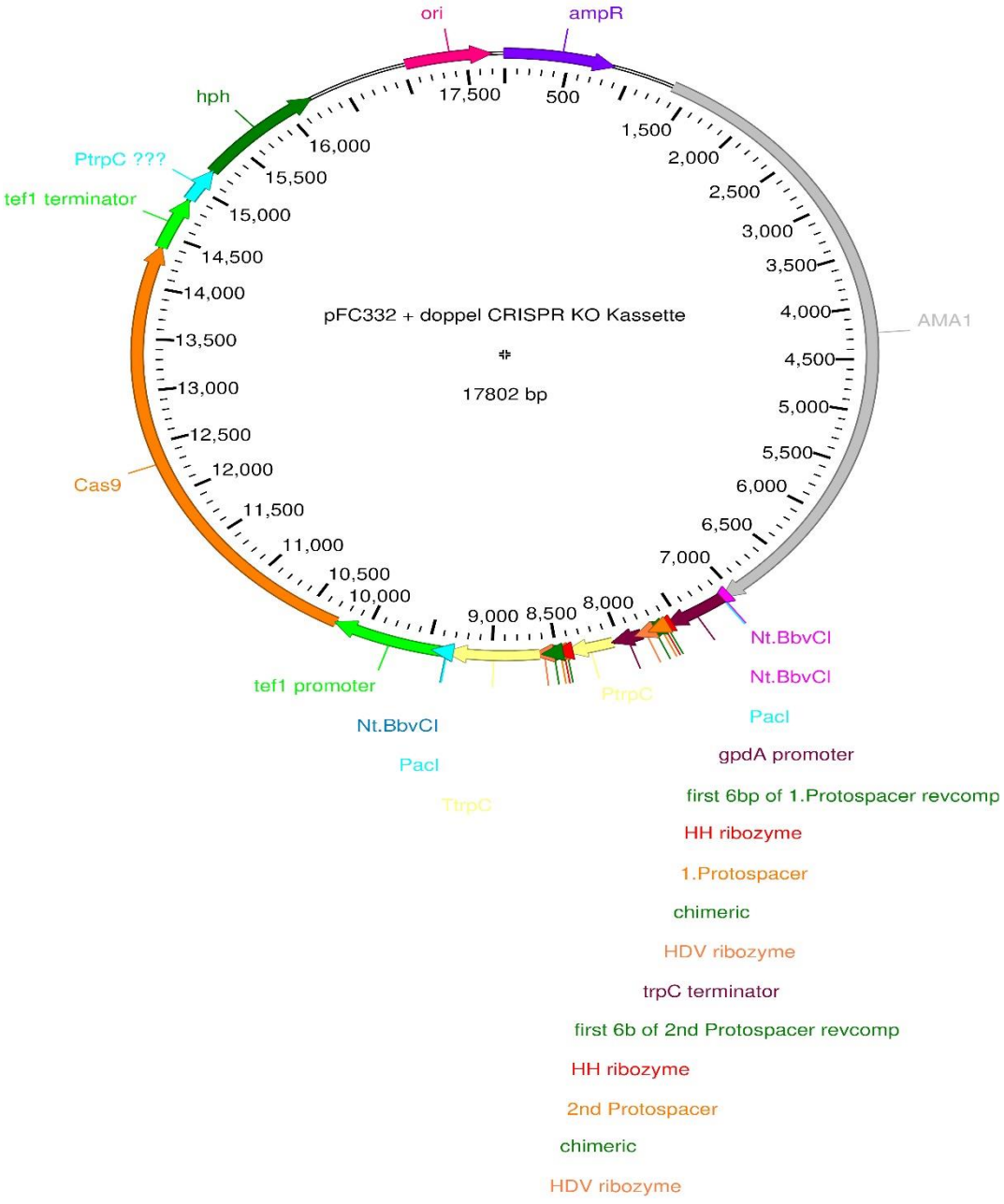

Figure12: Plasmid construct on the bass of which the knockout plasmids were built

2.1.4 Devices and chemicals

Table 5: Devices used in this study

Device	Specification	Manufacturer
Analytical scale	BP 2215-OCE	Sartorius, Göttingen, Germany
Analytical scale	Entris	Sartorius, Göttingen, Germany
Centrifuge	Heraeus, megafuge 8	Thermo Fisher Scientific GmbH, Bremen, Germany
Centrifuge	Heraeus, Pico 17	Thermo Fisher Scientific GmbH, Bremen, Germany
Electrophoresis power supply	GPS 200/400	LKB Pharmacia, Uppsala, Sweden
Fluorometer	Qubit 3.0	Thermo Fisher Scientific GmbH, Bremen, Germany
Fridge, freezer		Liebherr
Gel imaging system	ChemiDoc XRS+ system	Bio-Rad, Feldkirchen, Germany
High-speed benchtop homogenizer	FastPrep®-24 5G	MP Biochemicals Germany GmbH, Eschwege, Germany
High-throughput sequencer	MiSeq	Illumina, San Diego, US
HPLC system	HPLC: Hitachi Chromaster HPLC system Column: ZORBAX Eclipse XDB C18 Column (150 mm × 4.6 mm, 5 µm particle size)	HPLC: VWR International GmbH, Darmstadt, Germany Column: Agilent Technologies, Waldbronn, Germany
Incubator	IP110	Memmert, Schwabach, Germany
Long-read sequencer	MinION Mk1C	Oxford Nanopore Technologies, Oxford, United Kingdom
Magnetic stirrer with heating function	RCT classic	IKA, Staufen im Breisgau, Germany
Magnetic stand-96		Thermo Fisher Scientific GmbH, Bremen, Germany

Microbiological safety cabinet	safeflow 1.8, Bioair	Euroclone, Milan, Italy
PCR Plate Spinner		VWR International GmbH, Darmstadt, Germany
pH meter	765	Knick Elektronische Messgeräte GmbH und Co. KG, Berlin, Germany
Rotary shaker	VXR basic Vibrax®	IKA, Staufen im Breisgau, Germany
Thermal cycler	Gene Touch	Bioer, Hangzhou, China
Thermal cycler (for PCR)	iCycler	Bio-Rad, Feldkirchen, Germany
Thermal cycler (for qPCR)	iQ5	Bio-Rad, Feldkirchen, Germany
Spectrophotometer	NanoDrop 1000	Thermo Fisher Scientific GmbH, Bremen, Germany
Thin-layer chromatography chambers	ADC	CAMAG, Muttenz, Switzerland
Thin-layer chromatography visualizer	TLC Visualizer	CAMAG, Muttenz, Switzerland
Thoma cell counting chamber		Paul Marienfeld GmbH & Co. KG, Lauda-Königshofen, Germany
Vacuum centrifuge	SpeedVac Savant	Thermo Fisher Scientific GmbH, Bremen, Germany
Vortex Mixer	7-2020	neoLab Migge GmbH, Heidelberg, Germany

Table 6: List of chemicals used in this study

Chemical	Manufacturer
2-mercaptoethanol (≥ 99 %)	Carl Roth, Karlsruhe, Germany
2-propanol	Carl Roth, Karlsruhe, Germany
Acetonitrile HiPerSolv Chromanorm® (≥ 99.9 %)	VWR International GmbH, Darmstadt, Germany
Agar-Agar Kobe I	Carl Roth, Karlsruhe, Germany

Agarose	Serva, Heidelberg, Germany
Ammonium acetate	Sigma-Aldrich Chemie GmbH, Taufkirchen, Germany
DNA Ladder 1 kb, peqgreen	VWR International GmbH, Darmstadt, Germany
DNA Ladder 100 bp, peqgreen	VWR International GmbH, Darmstadt, Germany
Ethanol absolute EMSURE (≥ 99.9 %)	Merck KGaA, Darmstadt, Germany
Ethyl acetate, Rotipuran (≥ 99.5 %)	Carl Roth, Karlsruhe, Germany
Gel loading dye (6×) purple	New England BioLabs GmbH, Frankfurt, Germany
Glucose	Carl Roth, Karlsruhe, Germany
Glycerin Solvagreen (≥ 98 %)	Carl Roth, Karlsruhe, Germany
Hydrochloric acid (37 %, fuming)	Carl Roth, Karlsruhe, Germany
iQ SYBR Green Supermix	Bio-Rad, Feldkirchen, Germany
Malt extract	Carl Roth, Karlsruhe, Germany
Methanol Rotipuran (≥ 99.9 %)	Carl Roth, Karlsruhe, Germany
Potato dextrose agar	VWR International GmbH, Darmstadt, Germany
RNase inhibitor, recombinant, 2.000 units	New England BioLabs GmbH, Frankfurt, Germany
Saccharose (> 99.5 %)	Carl Roth, Karlsruhe, Germany
Sodium acetate	Carl Roth, Karlsruhe, Germany
Sodium chloride	Carl Roth, Karlsruhe, Germany
Toluol Rotipuran (≥ 99.5 %)	Carl Roth, Karlsruhe, Germany
Tris-HCl (pH 8.5) with 0.1 % Tween-20	Teknova, Hollister, CA, US
Tween-80	Serva, Heidelberg, Germany
Yeast extract, microgranulated	Carl Roth, Karlsruhe, Germany

Table 7: List of media used in this thesis

Culture media	Components	Amount/volume per liter deionized water	Final pH value
Malt extract glucose agar (MG)	malt extract glucose agar	17 g 5 g 16 g	7.0
Potato dextrose agar (PDA)	Potato dextrose agar agar	39 g 10 g	5.6
Yeast extract sucrose agar (YES)	yeast extract saccharose agar	20 g 150 g 20 g	6.0–6.5
PDA, aw = 0.99	Potato dextrose agar agar glycerol	39 g 10 g 108 mL	
PDA, aw = 0.98	Potato dextrose agar agar glycerol	39 g 10 g 131 mL	
PDA, aw = 0.95	Potato dextrose agar agar glycerol	39 g 10 g 199 mL	
PDA, aw = 0.93	Potato dextrose agar agar glycerol	39 g 10 g 245 mL	
PDA, aw = 0.90	Potato dextrose agar agar glycerol	39 g 10 g 313 mL	
Yeast extract sucrose agar (YES)	yeast extract saccharose agar	20 g 150 g 20 g	6.0–6.5
Eagle essential medium	L-arginine hydrochloride L-cystine 2HCl L-glutamine L-histidine hydrochloride-H2O L-isoleucine L-leucine L-lysine hydrochloride L-methionine L-phenylalanine L-threonine L-tryptophan	0.126 g 0.031 g 0.292 g 0.042 g 0.052 g 0.052 g 0.073 g 0.015 g 0.032 g 0.048 g 0.010 g	

	L-tyrosine disodium salt dihydrate L-valine Choline chloride D-calcium pantothenate Folic acid Niacinamide Pyridoxal hydrochloride Riboflavin Thiamine hydrochloride i-Inositol Calcium chloride (CaCl2, anhyd.) Magnesium sulfate (MgSO4, anhyd.) Potassium chloride (KCl) Sodium bicarbonate (NaHCO3) Sodium chloride (NaCl) Sodium phosphate monobasic D-Glucose (dextrose) Phenol red	0.052 g 0.046 g 0.01 g 0.01 g 0.001 g 0.001 g 0.001 g 0.0001 g 0.001 g 0.002 g 0.200 g 0.097 g 0.400 g 2.200g 6.800 g 0.140 g 1 g 0.010 g	

Table 8: Chemical solutions used in this study

Solutions	Components	Amount per liter	Notes
NaCl-Tween	sodium chloride tween-80 agar deionized water	 9 g 1 g 1 g 1 L	Autoclaving for 15 min at 121 °C at 2 bar
Sodium acetate (3 M, pH 5.0)	sodium acetate deionized water	246.09 g fill up to 1 L	Adjusting the pH value to 5.0 using HCl (37 %)
Tris-Borate-EDTA (TBE) buffer (10 ×)	Tris boric acid EDTA deionized water	107.8 g 55 g 7.4 g fill up to 1 L	
Tris (1 M, pH 8.0)	Tris deionized water	121.14 g fill up to 1 L	Adjusting the pH value to 8.0 using HCl (37 %

Table 9: List of kits used in this thesis

Kit	Manufacturer
DNeasy Plant Mini Kit	Qiagen, Hilden, Germany
iQ SYBR Green Supermix	Bio-Rad, Feldkirchen, Germany
MinElute PCR Purification Kit	Qiagen, Hilden, Germany
Min Elute Gel Extraction Kit	Qiagen, Hilden, Germany
NucleoSpin Plant II Kit	Macherey-Nagel, Düren, Germany
Omniscript RT Kit	Qiagen, Hilden, Germany
QIAquick® PCR Purification Kit	Qiagen, Hilden, Germany
Qubit™ dsDNA BR Assay Kit	Thermo Fisher Scientific GmbH, Bremen, Germany
Rapid Sequencing Kit	Oxford Nanopore Technologies, Oxford, United Kingdom
RNAse-Free DNase Set	Qiagen, Hilden, Germany
RNeasy Plant Mini Kit	Qiagen, Hilden, Germany
NucleoSpin Plant II Kit	Macherey-Nagel, Düren, Germany
Omniscript RT Kit	Qiagen, Hilden, Germany
QIAquick® PCR Purification Kit	Qiagen, Hilden, Germany
Qiaprep Spin Miniprep Kit	Qiagen, Hilden, Germany
Qubit™ dsDNA BR Assay Kit	Thermo Fisher Scientific GmbH, Bremen, Germany
Rapid Sequencing Kit	Oxford Nanopore Technologies, Oxford, United Kingdom
RNAse-Free DNase Set	Qiagen, Hilden, Germany
RNeasy Plant Mini Kit	Qiagen, Hilden, Germany

Table 10: List of software used in this thesis

Software	Manufacturer
antiSMASH version 6.0.1	(Medema et al., 2011)
Basic Local Alignment Search Tool (BLAST)	National Center for Biotechnology Information (NCBI), Bethesda, US (Altschul et al., 1990)
ChemDraw version 20.1	PerkinElmer, Inc., Waltham, US
DNASTAR Lasergene version 17: Gene Vision Pro version 17.3.0 MegAlign Pro version 17.3.0 SeqBuilder Pro version 17.3.0 SeqMan Pro version 17.3.0	DNASTAR, Inc., Madison, US
iQ5 version 2.0	Bio-Rad, Feldkirchen, Germany
NanoDrop 1000 version 3.7.0	Thermo Fisher Scientific GmbH, Bremen, Germany
winCATS version 1.4.4.6337	CAMAG, Muttenz, Switzerland
Protein **H**omology/AnalogY **R**ecognition **E**ngine V 2.2	Structural Bioinformatics Group, Imperial College, London
TMHMM - 2.0	Department of Health Technology Ørsteds Plads, Building 345C DK-2800 Kgs. Lyngby Denmark
MEGA11	https://www.megasoftware.net/

2.2 Methods

2.2.1 *Alternaria* isolate acquisition and cultivation

The local *A. alternata* strains used in this study were isolated in Adeyemo & Schmidt-Heydt (2024). Fruits and vegetables from different sources were collected to isolate local *A. alternata* strains. Table 2 shows strain names and sources from which the strains were obtained. Those fruits and vegetables were cut into small pieces of the parts that are most likely to carry spores, like the apple stem pit. Those pieces were placed on DCBR medium containing chloramphenicol to prevent bacterial growth. Then, 1 mL of Tween-NaCl80 was poured over the pieces to flush spores from the sample surface onto the DCBR plate. Once colonies were visible on the DCBR plate, those that fit the *Alternaria* phenotype were isolated using the three-stroke technique. Thereafter, the strains were observed under a light microscope at 400x magnification to verify their genus. Once their genus was verified through spore morphology, multiple molecular markers were used to identify the strains at the species level. Beyond that, several strains, which are designated as strains from Peru and Chile, were kindly provided by Prof. Dr. Remco Stam and Tamara Schmey in the framework of a joint research cooperation (CAU Kiel).

Table 11: List of Additional strains isolated in this study

Grape Isolates	Carrot Isolates	Wheat Isolates
TRGR	KASC	WEBI
TRDU	KAGR	
	KAPR	
	KP1A	
	KF1	
	KP1BD	

2.2.1.1 *Strain cultivation*

Initially, *A. alternata* strains were incubated on PDA for 7 days, then spores were scrubbed from the plates and mixed with Tween NaCl80, and finally diluted to a 10^5 spores per mL spore suspension. Unless stated otherwise, *Alternaria* strains were inoculated with 50 µL of a 10^5-spore suspension and then incubated at 28°C in darkness on potato dextrose Agar for 10 days.

2.2.1.2 *Strain cultivation with incurred stress*

To induce the desired stresses on the tested samples, the incubation media had to be modified. PDA was used as a basis for the different stress media. The compounds added to the PDA to incur certain stress factors are listed in Tab. 12. Beyond the chemical stress factors, light irradiation was used as a stress factor. Hence, the samples were incubated in a so-called “light box” (Schmidt-Heydt et al., 2011). The light box was subdivided into six chambers.

Table 12: Supplement to medium for the corresponding stress to be incurred

Stress is to be incurred	Compound supplemented
Low oxidative stress	5mM H2O2
High oxidative stress	8mM H2O2
Low water activity	15% glycerol
pH 4	Set up with 10% HCl until a pH of 4 was reached.
pH 8	Set up with 10 %NaOH until pH eight was reached.

2.3 Molecular biology methods

2.3.1.1 *DNA extraction (DNeasy Plant Mini Kit)*

DNA extraction was performed using the DNeasy Plant Mini Kit according to the manufacturer's guidelines. Spores and mycelium were scraped from a 7-day-old PDA plate and transferred to a 50mm petri dish with MG broth. After 2 days of incubation, the biofilm that has developed on the surface is removed from the petri dish using a spatula. Then the Sample is immediately frozen in liquid nitrogen. Thereafter, the sample was ground into a fine powder using a mortar and pestle while keeping the sample frozen by regularly adding liquid nitrogen. The grounded powder was transferred to a 1.5 mL reaction tube, and then 600 µL buffer AP1 and 4 µL RNase A were added. Afterwards, the samples were vortexed vigorously and subsequently incubated at 65 °C for 10 min to achieve cell lysis. Then, stop the lysis and precipitate polysaccharides, proteins, and detergents. The samples were incubated on ice for 5 minutes. After centrifugation at 20.000 × g for 5 min, the lysate was transferred to a QIAshredder spin column and centrifuged again for 2 min at 17.000 × g. The resulting

flow-through was pipetted into a new tube and mixed with 1.5 volumes of washing buffer AW1. Then, the mixture was transferred onto a DNeasy Mini spin column, which was then centrifuged for 1 min at 6.000 × g to bind the DNA to the column. Afterwards, the flow-through was discarded, and the DNA was washed by adding 500 µL of buffer AW2 to the column, followed by a 1-minute centrifugation at 6.000 × g. The flow-through was discarded again, and the washing step was repeated with another 500 µL of buffer AW2, followed by centrifugation for 2 min at 20.000 × g. To elute the DNA, 50 µL ddH2O was pipetted onto the column, which was then placed into a new 1.5 mL tube. Lastly, the samples were incubated for 5 minutes at room temperature before being centrifuged for 1 minute at 6000 × g.

2.3.1.2 *Polymerase Chain Reaction (PCR)*

To amplify the target marker genes for sequencing, a specific PCR protocol had to be used for every molecular marker. The components were mixed according to the manufacturer's manual and were pipetted into a PCR tube, mixed, and then placed into a PCR cycler. The program used is shown in Table 13, with the specific annealing Temperature shown in Table 3

Table 13: Components and amounts used in PCRs

Reaction step	Temperature	Time	Number of cycles
Initialization	95	03:00	1
Denaturation	95	00:30	40
Annealing	Primer specific	00:40	
Extension	72	1:30	
Final Extension	72	3:00	1
Final hold	4	∞	∞

2.3.1.3 *Gel electrophoresis*

To verify the quality of the extracted DNA and the efficiency of the PCR amplification, nucleotide sequences were separated by length on a 1 % agarose gel using gel electrophoresis. Agarose was dissolved in a Tris-Borate-EDTA (TBE) buffer by heating it in the microwave. The DNA was detected using peqGreen (1 µL/20 mL TBE buffer), which was added to the dissolved agarose. Afterwards, a five µL sample and one µL of 6 × DNA loading buffer were mixed and then loaded into the wells of the hardened gel. Furthermore, 5 µL of a DNA ladder (1 kb or 100 bp) was loaded for comparison of fragment sizes. The separation was achieved using a gel electrophoresis apparatus at a voltage of 100 V. The DNA was visualized under UV light using the ChemiDoc XRS+ Imaging system and Image Lab v. 5.2.1 software.

2.3.1.4 *Extraction of DNA fragments from a gel (MinElute Gel Extraction Kit)*

After electrophoresis, the gel is placed on a UV table, where the DNA fragment is excised from the agarose gel using a clean scalpel. A gel slice of approximately 100 mg is weighed and placed into a reaction tube, and three volumes of QG Buffer are added to one volume of gel. Then, the tube is incubated at 50°C for 10 minutes, with vortexing every 3 minutes, until the gel dissolves. After the gel is completely dissolved, and if the mixture is not yellow, 10 µL of 3 M sodium acetate (pH 5.0) is added to adjust the pH value. Afterwards, one gel volume of isopropanol is added to the sample, after which it is mixed by inverting. Then, the sample is applied to the MinElute column and centrifuged for 1 minute at 13.000 rpm. The flow-through is discarded. Thereafter, 500 µL BG buffer QG is added to the MinElute column and centrifuged for 1 minute at 13.000 rpm. The flow-through is then discarded.

Next, 750 µL of buffer PE was added to the MinElute column and centrifuged for 1 minute at 13.000 rpm. Afterward, the flow-through was discarded. To remove residual alcohol from buffer PE, the tube is centrifuged again for 1 minute at 13.000 rpm. Then, the MinElute column is placed into a 1.5 mL reaction tube, and 10 µL of water is dispensed directly onto the membrane for elution. The column is incubated for 1 minute at room temperature and then centrifuged at 13.000 rpm for 1 minute.

2.3.1.5 *PCR product purification (MinElute PCR purification Kit)*

PCR products were purified using the MinElute PCR Purification Kit for shorter products (70 bp – 4 kb) or the QIAquick PCR Purification Kit for longer products (100 bp – 10 kb). Using both kits, 40 µL of PCR product was mixed with 200 µL buffer PB containing pH indicator (4 µL/mL). If the pH was not in the recommended range, 10 µL sodium acetate (3 M, pH 5.0) was added. Then, the DNA fragments were bound to the membrane of a QIAquick column by centrifuging the sample for 1 min at 20.000 × g. The sample was then washed by pipetting 750 µL of PE buffer onto the column and centrifuging once more for 1 min at 20.000 × g. After discarding the flow-through, the columns were dried by centrifuging again for 1 min. 30 µL of nuclease-free water was added to the column and then incubated for 1 minute at room temperature. Finally, the column is placed into a 1.5 mL reaction tube and centrifuged for 1 minute at 20.000 × g.

2.3.1.6 *Sanger sequencing of purified PCR products*

Purified PCR products, which were used to identify fungal strains or to generate phylogenetic trees, were Sanger sequenced using the Tubeseq supreme service of Eurofins Genomics (Cologne, Germany). The purified PCR products were sequenced

in both the forward and reverse directions, and the resulting sequences were assembled using APE (a plasmid editor). The consensus sequence was used for further analysis.

2.3.1.7 *Phylogenetic analysis*

For each strain to be analyzed, the marker sequences acquired through Sanger sequencing were aligned using ClustalW (Multiple sequence alignment) with MEGA11(Tamura et al., 2021). Afterwards, the sequences were manually trimmed to a common length ranging between 400 and 500 bp, depending on each respective marker, and then concatenated. Thereafter, a Maximum likelihood analysis was carried out, which was done with 1000 bootstrap replications. The trees were built using the GTR (General Time Reversible) and gamma-distributed rates (Siciliano et al., 2018).

2.3.1.8 *Plasmid preparation (QIAprep Spin Miniprep Kit)*

The bacterial strain carrying the desired plasmid is incubated overnight at 37 °C in liquid LB medium with the appropriate selection markers, while shaking at 150 RPM. Two milliliters of the culture are then transferred to a reaction tube and centrifuged at 13.000 rpm. Afterwards, the supernatant is removed, and the Pellet is resuspended in 250 µL P1 buffer. Then, cell lysis is initiated by adding 250 µL buffer P2, inverting the sample 4-6 times, and incubating for 5 minutes at room temperature. Thereafter, 350 µL Buffer N3 is added and immediately mixed thoroughly by inverting the tube 4-6 times. Then, the sample is centrifuged for 10 minutes at 13.000 rpm. The supernatant is applied to a Qiaspin column and then centrifuged for 1 minute at 13.000 rpm. Afterward, the flow-through is discarded. Afterwards, the Qiaspin column

is washed by adding 500 µL of Buffer PB and centrifuged again at 13.000 × g; the flow-through is then discarded. Now, 750 µL of PE Buffer is added, and the sample is centrifuged once again at 13.000 rpm to wash the Qiaprep spin column. The flow-through is discarded, and the samples are centrifuged again to remove residual wash buffer. Lastly, the Qiaprep column is placed into a clean 1.5 mL reaction tube, and 30 µL ddH_2O is pipetted onto the column to elute the DNA. After incubation for 1 minute at room temperature, the samples are centrifuged for 1 minute at 13.000 rpm one last time.

2.3.1.9 *Restriction digestion*

Restriction digestions were performed at a final volume of 10 µL according to the manufacturer's guide. The digestions were incubated for 60 minutes at 37 °C.

2.3.1.10 *CRISPR/Cas9 plasmid construction for gene deletions.*

For the design of the deletion constructs, two protospacer sequences were chosen for each gene to produce two different sgRNAs from the respective constructs concurrently. The strategy is based on Gao et al. (2022). To insert two different protospacer sequences into the linearized vector pFC332, two chimeric PCR fragments, obtained by fusing two small PCR fragments, were combined in a Gibson reaction (New England Biolabs, Frankfurt, Germany). To insert the first protospacer, two small PCR fragments (f1 and f2) were amplified using pFC334 as the template. The second protospacer was inserted by amplifying another small PCR (f3 and f4), using pAK4 as the template. The two chimeric fragments F1 and F2 were obtained by combining f1 with f2 and f3 with f4 in a fusion-PCR step. 1 µL of 50 ng of the

linearized vector pFC332 with 3-fold molar excess of both inserts (F1&F2), so 3 µL of 50ng fragment, as well as 3 µL deionized H_20 and 10 µL Gibson Assembly Master Mix (2x) are put into a reaction tube on ice. Then, the sample is incubated at 50 °C for 60 minutes and stored on ice for subsequent transformation.

Table 14: PCR program to amplify necessary DNA fragments

CRISPY_Low	Steps	Temperature [°C]	Time [s]	Repeats	Back to step
	1	98	180	1	
	2	98	20	5	
	3	61	20	5	
	4	72	15	5	2
	5	98	20	5	
	6	59	20	5	
	7	72	15	5	5
	8	98	20	25	
	9	57	20	25	
	10	72	15	25	8
	11	72	180	1	
	12	4	∞	1	

Table 15: PCR program to fuse DNA fragments

CRISPY_FUSE	Steps	Temperature [°C]	Time [s]	Repeats	Back to step
	1	98	480	1	
	2	98	20	30	
	3	63	20	30	
	4	72	25	30	2
	5	72	120	1	
	6	4	∞	1	

2.3.1.11 *Protoplast transformation*

A. alternata Fungal spores were harvested from a PDA plate and inoculated into 100 mL liquid RLM for overnight cultivation at 28 °C and 180 rpm. The mycelium was harvested by filtering through Kimtech paper, washed with 0.7 M NaCl, and digested in a Kitalase (Wako Chemicals) suspension (100 mg in 15 mL 0.7 M NaCl) for one hour with slight shaking at 120 rpm at 30 °C. Protoplast quality and quantity were checked through microscopy. Protoplasts were separated from cell fragments by filtering through two layers of Kimtech paper and precipitated at 560 g for 10 min at room temperature. The Kitalase solution was discarded, and the protoplasts were washed once with ice-cold 0.7 M NaCl and resuspended in 100 µL STC (1 M sorbitol, 50 mM $CaCl_2$, 50 mM Tris-HCl, pH 8). 5 µg of plasmid DNA were added to the protoplasts, followed by a 10 min incubation on ice. DNA uptake was induced with a heat shock at 42 °C for 5 min and, after a 5 min incubation step on ice, 800 µL 40 % PEG (40 % polyethylene glycol [PEG] 4000, 50 mM Tris-HCl [pH 8], 50 mM $CaCl_2$) was added to the protoplasts, followed by 15 min incubation at room temperature. The suspension was mixed with 30 mL of warm soft agar (34 % sucrose, 0.5 % yeast extract, 0.5 %

casein hydrolysate, 0.75 % agar) and split into two petri dishes. After overnight incubation at 28 °C, the transformation plates were overlaid with 15 mL of soft agar containing hygromycin (80 µg /mL).

2.3.1.12 *RNA extraction (RNeasy Mini Kit)*

To extract the RNA of *A. alternata* strains, the target strains were grown on PDA for 10 days. Thereafter, the mycelium and spores were scraped from the plate into a new Petri dish filled with 10 mL of MG broth. After 24 hours of incubation at 28 °C, the fungal biofilm is harvested with a clean spatula, and the sample is placed into an RNase-free reaction tube, which is then frozen in liquid nitrogen. Samples are ground with a mortar and pestle while frozen in liquid nitrogen and then transferred into new RNase-free reaction tubes. RNase-free pipette tips were used to ensure the protocol was completed without contamination. 600 µL RLT lysis buffer was added to the samples and mixed carefully. Then, the samples were centrifuged for 3 min at 20.000 x g. The supernatant is transferred to a new reaction tube and mixed with 1 volume of 70 % ethanol. 700 µL of the sample is pipetted onto a RNeasy Mini spin column and then centrifuged for 30 s at 8000 × g; thereafter, the flow-through is discarded. Next, an on-column DNase digestion was performed using the RNAse-Free DNase Set. For each sample, 70 µL of RDD buffer was gently mixed with 10 µL of DNase I stock solution (1.500 Kunitz units dissolved in 550 µL of RNase-free water) and pipetted directly onto the RNeasy spin column membrane. DNA digestion was achieved by incubating the samples for 15 min at 25 °C. Then, the washing step was repeated with 350 µL RW1 buffer and a centrifugation for 1 min at 9.600 × g. After discarding the flow-through, the columns were washed twice with 500 µL RPE buffer by centrifuging at 9.600 × g. The first centrifugation is done for 1 min, and the second time for 2 min. The columns were

placed into new collection tubes to avoid buffer residuals and centrifuged again for 1 min at 17.000 × g. Thereafter, the RNA was eluted with 100 µL RNase-free water, which was pipetted directly onto the columns and then centrifuged for 1 min at 9.600 × g. Next, the concentration and quality of the extracted RNA were checked using the NanoDrop 1000 spectrophotometer. The RNA purity was indicated by a ratio of absorbance (260 nm/280 nm) of 2.0. After extracting the RNA, it was transcribed into complementary cDNA using the Omniscript RT Kit. The reaction mixture was used according to the manufacturer's manual. The volume of the template RNA was determined by the RNA concentration measured using the NanoDrop 1000 spectrophotometer, to obtain an input of 50 ng to 2 µg of RNA. An RNase inhibitor was used to prevent possible RNase contaminations, which was diluted 1:2 with 1 × RT buffer. Reverse transcription was performed at 37 °C for 60 minutes. Then, the cDNA was stored at -20 °C until usage for gene expression analysis by qPCR, whereas the remaining RNA was stored at -80 °C.

2.3.1.13 *Quantitative PCR (qPCR)*

First, the master mix without template was prepared in a 1.5 mL micro-reaction tube, mixed by vortexing, and briefly centrifuged. Then, the mixture was transferred into the wells of an iQ 96-well plate. Thereafter, the cDNA was mixed into the master mix by pipetting up and down. Samples were measured in triplicate. A non-template control, containing nuclease-free water instead of cDNA, was included in every run. The 96-well plate was covered with a seal and briefly centrifuged. The cycling program for amplifying the target genes is shown in Tab. 16.

Table 16: PCR cycler program for qPCR

Reaction step	Temperature	Time	Number of cycles
Initialization	50	02:00	1
Initial denaturation	95	10:00	1
Denaturation	95	00:20	40
Annealing	50-60	00:40	
Extension	72	01:00	
Meld curve	55 to95 in 0.5°C steps	0:30	81
Final hold	8	∞	∞

Data analysis was performed using the iQ5 v. 2.0 software. Differences in gene expression were calculated using the 2–ΔΔCT method (Livak & Schmittgen, 2001), based on the CT values obtained from quantitative PCR (qPCR). This method involved measuring the gene expression of a reference gene, in addition to the target genes.

2.3.2 Detection of secondary metabolites

2.3.2.1 *Extraction of mycotoxins*

In order to extract the target mycotoxins AOH, AME, ATX-I, TeA, ALS, ALT, and AOH-S, a modified version of the approach described by Müller et al. (2016) was employed. Here, four agar blocks were taken from each plate of a triplicate set of plates. Two of those four blocks were taken at the outer edges of the colonies and two at the center. All four blocks were then placed into a reaction tube. Two metal beads were added to each reaction tube, and the samples were homogenized using a FastPrep-24 5G bead

beater (MP Biomedicals, Eschwege) at 4 m/s. Thereafter, 800 µL of an acetonitrile: water: acetic acid (v: v: v) (79:20:1) was added to the reaction tube. Then the homogenization step was repeated. Afterwards, the reaction tube was incubated in an ultrasonic bath for 15 minutes and shaken for 1 hour. Both steps were repeated one more time. Following the incubation, the samples were centrifuged at 10.000 RPM for 5 minutes. Next, 500 µL each of the supernatants was transferred to a new reaction tube and evaporated to dryness in a vacuum concentrator. Then, depending on how the secondary metabolites were to be analyzed, the pellet was either dissolved in 150 µL of methanol, vortexed vigorously, and finally filtered with a 0.2 µm PTFE filter (Phenomenex) when HPLC analysis was to be performed. If thin-layer chromatography (TLC) were to be performed, the dried pellet would be dissolved in 100 µL of solvent, and no further filtration would be performed.

2.3.2.2 *High Performance Liquid Chromatography*

In this work, *Alternaria* toxins were quantified by HPLC. Hence, an Agilent Zorbax Extend C18 (150 x 4.6 mm, 5 µm) column was used at a column furnace temperature of 20 °C with a flow rate of 0.6 mL/min and an injection volume of 5 µL. Solvent A consisted of 5 mM ammonium formate, pH 9 (Aldrich Chemistry), and solvent B of methanol HiPerSolv Chromanorm (VWR). The gradient started with 10 % solvent B and 90 % solvent A, then rose to 100 % solvent B by 5 minutes and remained constant until 10 minutes. Afterwards, the gradient returned to 10 % solvent B and 90 % solvent A, and remained there until 21 minutes had passed. were reached. Measurements were performed in 4 different UV channels for the different mycotoxins, namely altenusin at 293 nm, altenuene at 241 nm, alternariol, alternariol sulfate, altertoxin-I, and alternariol monomethyl ether at 261 nm, and tenuazonic acid at 280 nm.

2.3.2.3 *Thin-layer chromatography*

The TLC was performed on a HPTLC Silica gel 60 20 × 10 cm glass plate (Merck, Gernsheim) using the Camag Automatic TLC Sampler 4 (Camag, Muttenz). While N2 was used as the propellant, methanol was used as the rinsing solution. 30 µl of the standard mix containing (5 µl AOH (cfm Oskar Tropitzsch GmbH, Marktredwitz), five µl ATX-I (cfm Oskar Tropitzsch GmbH, Marktredwitz), and 20 µl TeA (Bioviotica, Dransfeld) filled up to 60 µl with methanol) was applied to the TLC plate. Samples, all of which were extracted in triplicate beforehand, were pooled, and 25 µl of the pooled samples were applied to the TLC plate. The band's spray width was set to 6 mm. After applying the mycotoxin extracts to the TLC plate, they were placed into the Camag ADC2 automatic developing chamber (Camag, Muttenz). To saturate the chamber, 25 mL of the mobile phase, consisting of Toluol /ethyl acetate/formic acid (60:35:5, v/v/v), was used. For development, 10 mL of the mobile phase was used. The development progressed until the running front reached about 3 cm from the upper edge of the TLC plate. Once dried, the Camag TLC Visualizer (Camag, Muttenz) was used to irradiate the TLC plates at 366 nm and 254 nm wavelengths, and the plates were analyzed using the WinCATS (Camag, Muttenz, Version 1.4.10.001) program.

2.3.3 Toxicity tests

2.3.3.1 *Sample preparation*

Alternariol (AOH) was acquired from AdipoGen (Fuellinsdorf, Switzerland) and alternariol sulfate (AOHS) from ASCA (Berlin, Germany). Both substances were dissolved in DMSO (Sigma-Aldrich, Steinheim, Germany) and stored at -20°C for the duration of the experiments. Working solutions were prepared fresh daily and diluted

with cell culture medium, with all solutions prepared so that the final DMSO concentration was 1%.

2.3.3.2 *Caco-2 cell culture*

The human colon adenocarcinoma cell line CaCo-2 was obtained from the German Collection of Microorganisms and Cell Cultures (DMSZ, Braunschweig, Germany). The cells were cultured in EMEM (enriched with 10 % FCS, 1 % L-Glutamine, 1 % NEAA, and 1% P/S) at 37 °C and 5 % CO_2. The cell culture medium (EMEM) was purchased from PAN-Biotech (Aidenbach, Germany). L-Glutamine and Penicillin/Streptomycin (P/S) were from Lonza (Verviers, Belgium), non-essential amino acids (NEAA) from Thermo Fisher Scientific (Schwerte, Germany), and fetal calf serum (FCS) from Biowest (Nuaillé, France)

2.3.3.3 *Comet Assay*

Preheated 6-Well plates are flushed twice with PBS and are then incubated for 2 hours at 37°C. The supernatant is drained, and 500 µL Trypsin is added to the cells. Then, the plate is incubated at 38.5 °C for four minutes. The detachment process is stopped by adding 2 mL EMEM + FKS, after which the cells are resuspended and transferred into a 15 mL reaction tube. The tube is centrifuged at 1000 RPM for 6 minutes. The supernatant is poured into a beaker. Another 1ml of EMEM+ FKS is added for resuspension. Cells are then counted to determine the vitality and the total cell count. Cells are then centrifuged again at 2000 RPM for 5 minutes, and the supernatant is again poured into a beaker. The cell pellet is mixed with 85 µL and (0.7 %) and agarose covered with a cover glass until it is solid. Afterwards, the cover glass is removed, and

85 µL of 0.7 % LMA is added. Thereafter, the Electrophoresis is performed for 40 min at 25 V and 300 mA. Then the gel is neutralized with neutralization buffer and finally stained for evaluation.

2.3.3.4 *WST- Assay*

To determine cytotoxicity using the WST-Assay, cells were cultured for 6 days in 96-well plates (Corning® No. 3599) at a density of 1,500 cells per well, with medium changes three times a week. On day 6, CaCo-2 cells were treated with various concentrations of AOH and AOHS, as well as with EMEM (without FCS) as a negative control. Incubation with the test media lasted 24 hours. Afterward, the test media were removed, and a two-hour incubation with a 5 % solution of WST-1 reagent (Roche, Mannheim, Germany) was performed at 37 °C. Subsequently, the color intensity, which is proportional to the number of metabolically active cells, was determined at 450 nm using a plate photometer (Tecan, Safire II).

3 Results

3.1 *Alternaria alternata* identification and comparison

The genus *Alternaria* possesses a high rate of variation, which makes correctly assigning fungal strains to a specific species quite challenging. Beyond that, even the correct identification using molecular markers can be error-prone, depending on the markers. Hence, we used the established morphological means of identification as well as their chemotype and compared those to the use of varying numbers of molecular markers in order to find the system best suited for *A. alternaria* identification (Emory G Simmons, 2007).

3.1.1 Morphology

3.1.1.1 *Spore and conidia morphology*

While observing the spore morphology of the local isolates shown in Fig. 13, it became apparent that all of these isolates possess the typical septed, club-shaped morphology paired with a brown color caused by the enclosure of melanin in the spores. In comparison, the commercial strains from the DSMZ, shown in Fig. 14, which included various *Alternaria* species, exhibited higher morphological variation. Two of the five observed spore types were easily distinguishable from the others. One of those peculiar strains was DSM12633 (*A. alternata*), which we found to have a phenotype similar to the previously described one, yet with septa that are more bulging. The other salient strain was DSM620013 (*A. citri*), which has a nearly globular morphology and is significantly larger compared to the other spores. Yet, apart from spore shape and size, other morphological features, such as conidia chain length, branching, spore color, and septation, were also observed. Fig. 15 shows conidia chains from the local isolates, and Fig. 16 shows conidia chains of the commercial DSMZ strains.

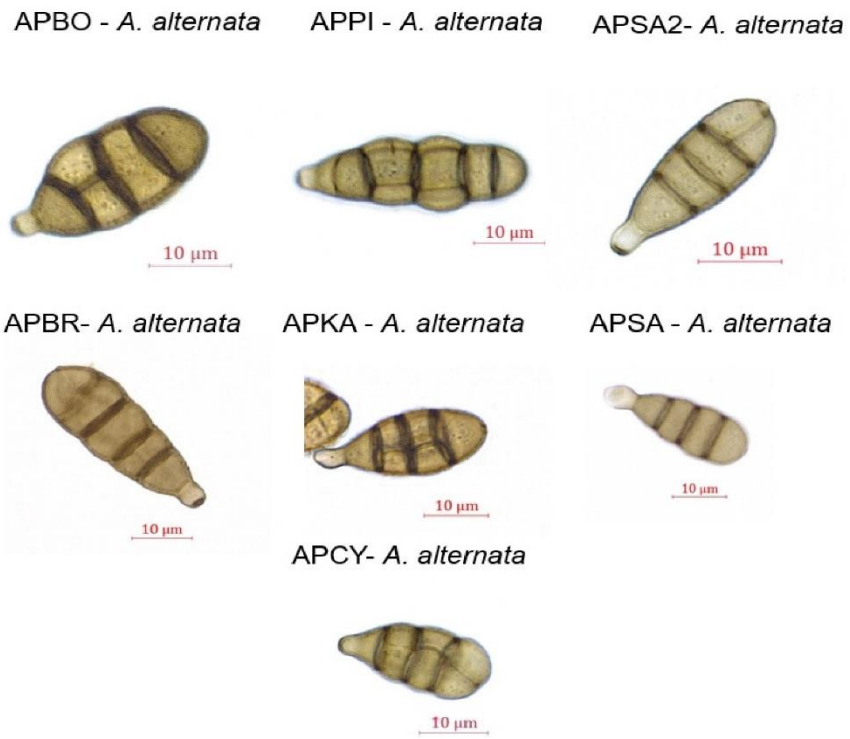

Figure 13: Morphological features of representative spores from *Alternaria* isolates isolated in this study.

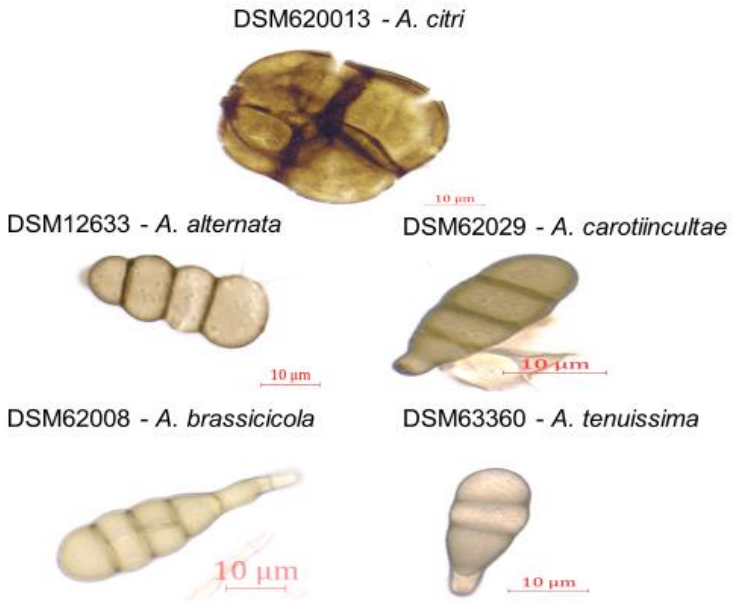

Figure 14: Morphological features of representative spores from commercial *Alternaria* strains bought at DSMZ

If those features are considered, out of the local and the commercial strains, DSM62008, DSM63360, APKA, and APCY stood out the most. In terms of spore color, only isolate APSA had a somewhat darker color compared to all other strains. Branching was not observed in any of the strains.

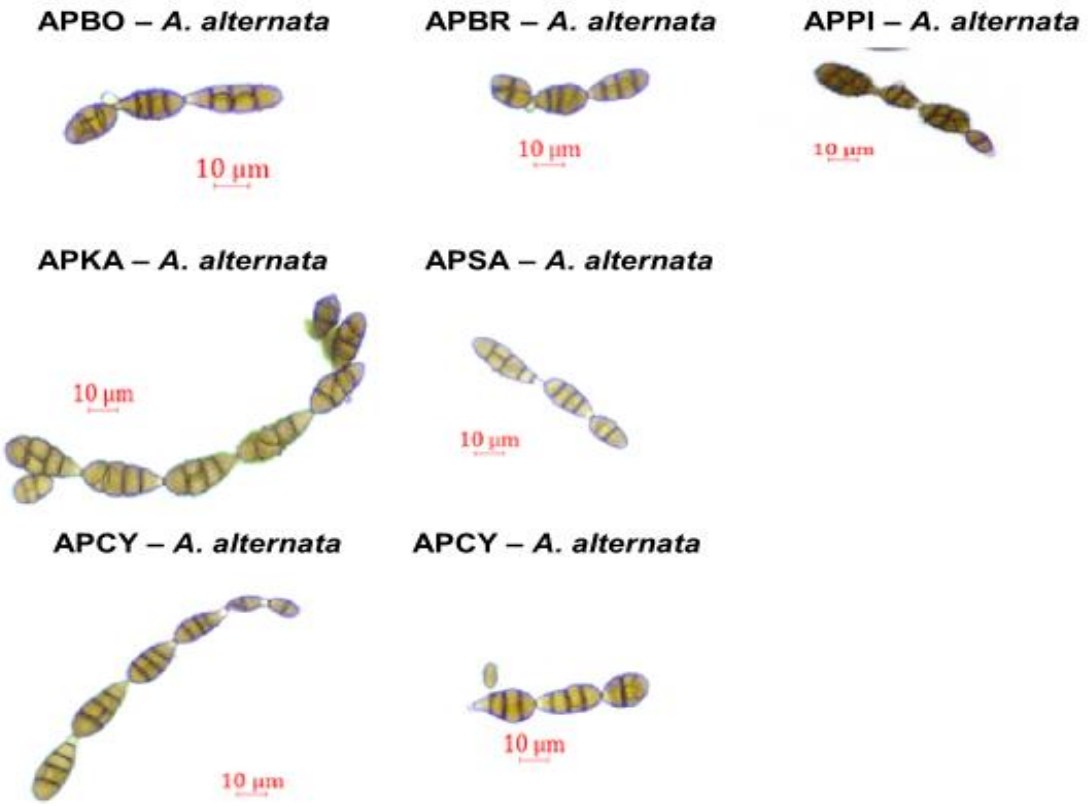

Figure 15: Representative chains of conidia from *Alternaria* isolates, isolated in this study

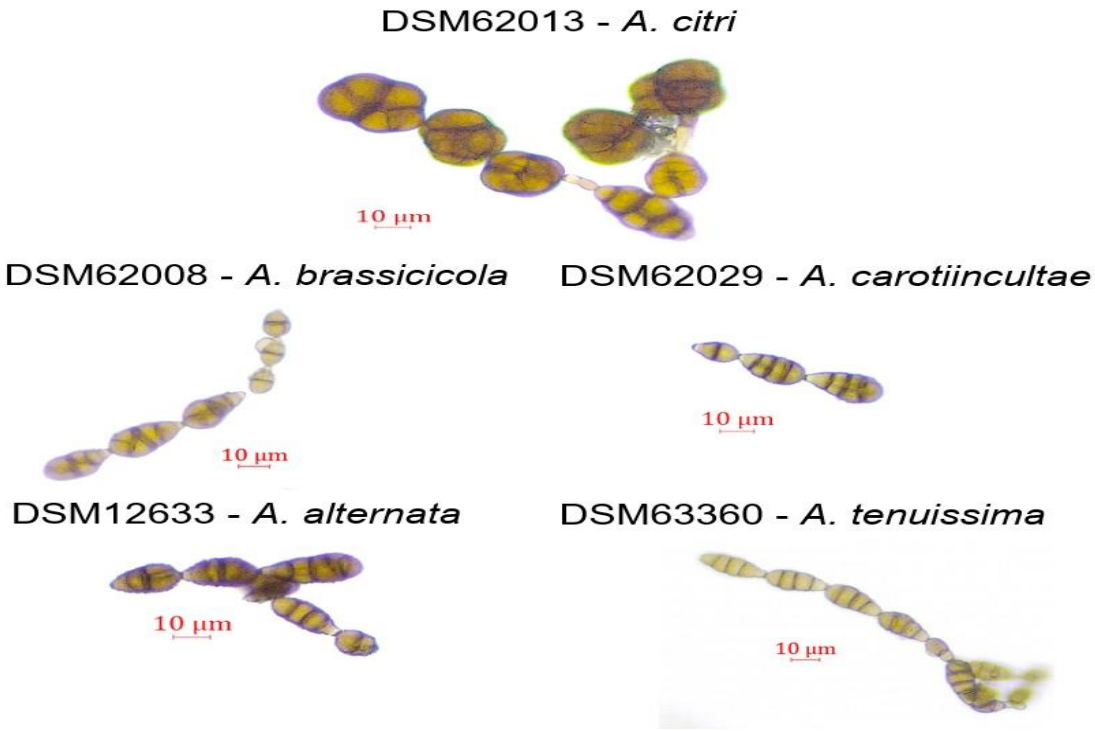

Figure 16: Representative chains of conidia from commercial *Alternaria* strains bought at DSMZ.

3.1.1.2 *Colony phenotype*

To substantiate the inaptitude of an *Alternaria* characterization via morphology, the local strains were incubated on three different growth media. Fig. 17 shows that there can be drastic differences in the appearance of the fungal isolate caused by a different growth substrate. This behavior was particularly evident in APBO, APPI, and APSA. Those isolates altered their phenotype from a mostly smooth, black surface when inoculated on Potato Dextrose Agar (PDA) to a brown, wavy phenotype when inoculated on Yeast Extract Sucrose (YES). Furthermore, it can be stated that all isolates exhibited different phenotypes when incubated on PDA compared to incubation on YES medium, even if some changes are less apparent than those mentioned above.

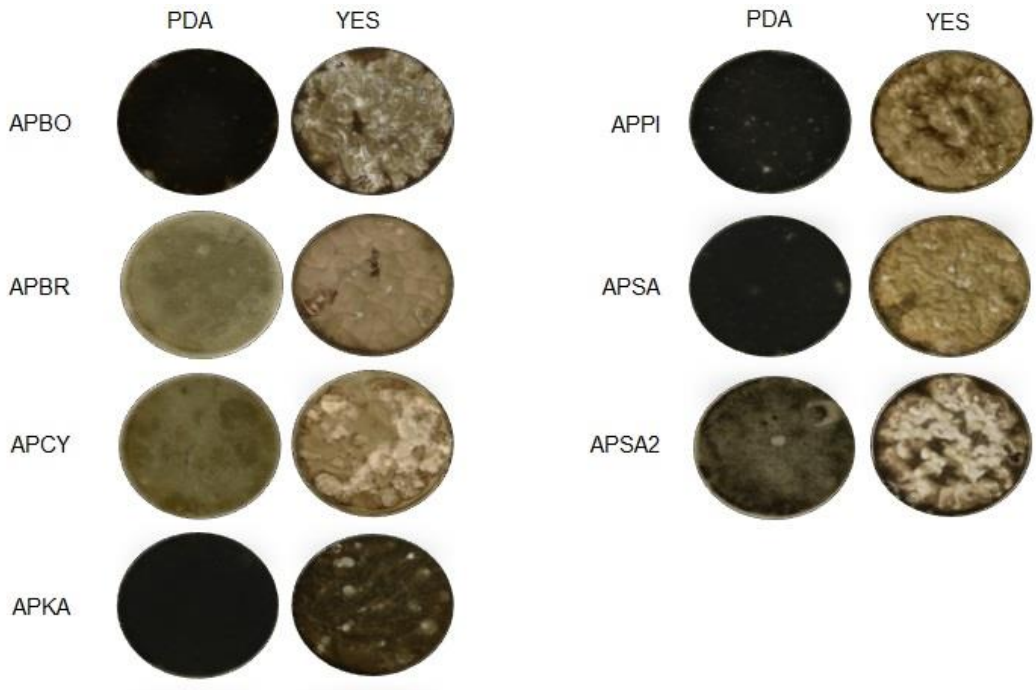

Figure 17: Phenotype of *Alternaria* strains isolated in this work. The isolated strains were incubated for seven days on PDA and YES agar plates respectively

The corresponding change in phenotype between different growth media was further substantiated by the phenotypes of the commercially available strains used as references, as shown in Fig. 18. Apart from DSM62008, all other commercial strains exhibited a significant change in phenotype in terms of color between PDA and YES agar.

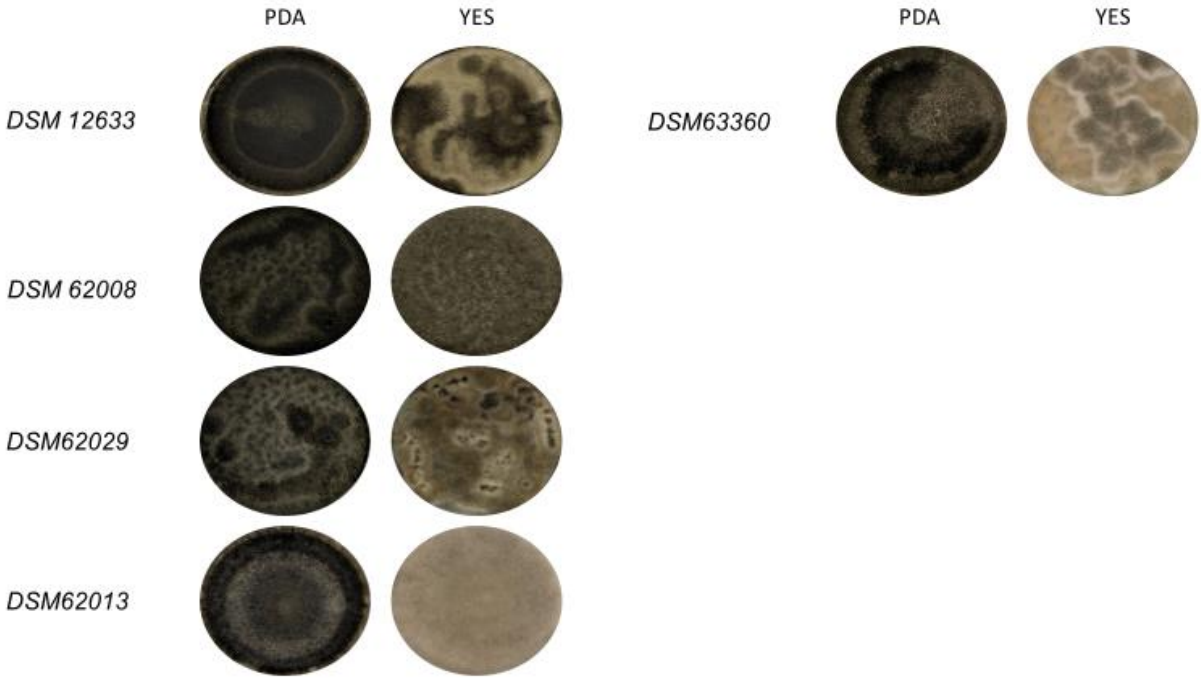

Figure 18: Phenotype of commercially available *Alternaria* strains purchased from DSMZ. The strains were incubated for seven days on PDA and YES agar plates respectively.

3.1.1.3 *Chemotyping*

To compare the chemotype variation of the different *Alternaria* species and the differences in chemotypes within the species *A. alternata*, thin-layer chromatography (TLC) analyses were performed. The reference toxin standards of AOH, ATX-I, and TeA, along with toxin extracts of all commercial strains we purchased as references from DSMZ, were applied to the TLC plate shown in Fig. 19. Fig. 19 shows that strain DSM12633 produced only one yellowish band, which is possibly an altertoxin or an altertoxin derivative.

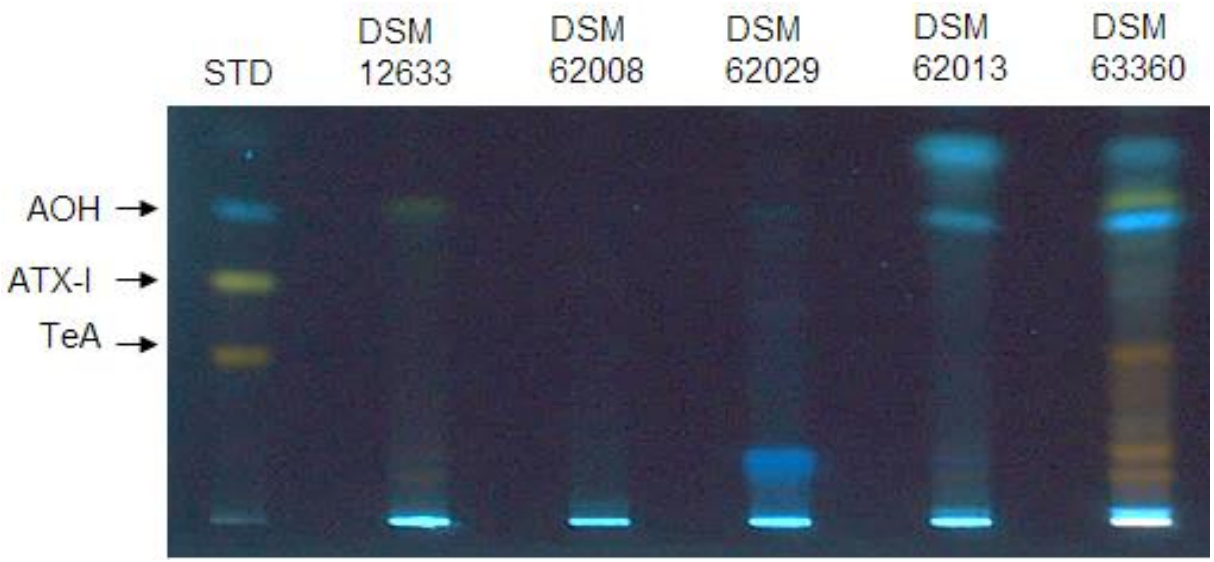

Figure 19: Thin layer chromatography of toxin extracts isolated from commercially available *Alternaria* strains incubated on PDA. Standards applied are alternariol (AOH), altertoxin-I(ATX-I) and tenuazonic acid (TeA). The plate was developed with (Toluol: ethyl acetate: formic acid - 60:35:5). The image was captured at 366nm.

This is suggested because it is known that ATX-II has a shorter retention time compared to AOH on a TLC plate and exhibits a similar fluorescence color to ATX-I (Gao et al., 2022). DSM62029 harbored a single band emitting light, which seemed to be part of the higher region of the blue light spectrum. In contrast to the previously mentioned strains, DSM63360 exhibited bands corresponding to all three applied standards, as well as additional bands in close proximity to those of AOH and ATX-I, which are likely to be AOH and ATX derivatives. Lastly, DSM62013 can be seen on the lane, left of the rightmost lane, showing two visible bands. The first one can be assigned to AOH, while the second one emitted light on a similar wavelength to AOH but less intensely and with a longer retention time. Thirdly, a band which emitted light at a high intensity again, with a wavelength in close proximity to the one emitted by AOH, which is located at the top of the picture. Both bands surrounding the AOH band are likely to be AOH derivatives (Wenderoth et al., 2017). Fig. 20, however, presents a more consistent picture, with all isolated strains exhibiting a well-visible AOH band. Yet, upon closer investigation, discrepancies between the isolates became evident.

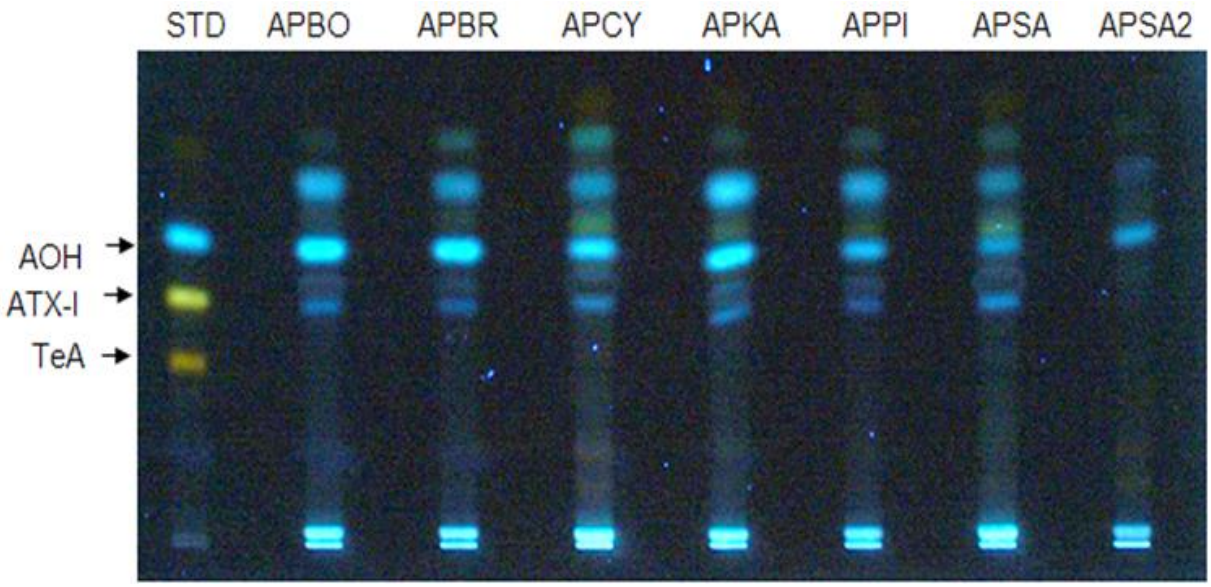

Figure 20: Thin layer chromatography of toxin extracts isolated from strains isolated in this study incubated on PDA. Standards applied are alternariol AOH, ATX-I and TeA. The plate was developed with (toluol: ethyl acetate: formic acid) Image was captured at 366nm

While APCY, APKA, APPI, and APSA seemed to produce ATX-II, all other strains did not. Only APCY had brownish/orange bands in the lower part of its lane. Another striking difference observed in isolate APSA2 was the presence of a visible AOH band and a second, less intense blue band, which also emitted blue light. This band originates from a substance with a shorter retention time than AOH, while lacking the other visible bands present in the other strains. The final visible difference, apart from the presence or absence of the bands, was the fluorescence intensity, which is positively proportional to the amounts produced. Lastly, Fig. 21 shows the strains isolated in this study, yet incubated on YES-agar instead of PDA. Multiple discrepancies are evident compared to the incubation on PDA. When Taking a closer look at particular bands, it can be observed that sample APSA2, which, when grown on PDA, only produced AOH, switches to solely producing ATX-I when incubated on YES agar.

Moreover, APBO, when grown on PDA, possesses a band that can be assigned to AOH and two additional bands that are likely AOH derivatives. However, when grown on YES-agar, only a weak AOH band remains. It can be concluded that although the chemotyping method is very valuable as additional information for the identification of a fungal species, especially if an initial health risk assessment is necessary, it cannot be used as the sole means of identification due to the high variability of fungal metabolite biosynthesis, which can be highly variable depending on the growth phase, pre-culture, substrate, external influencing factors.

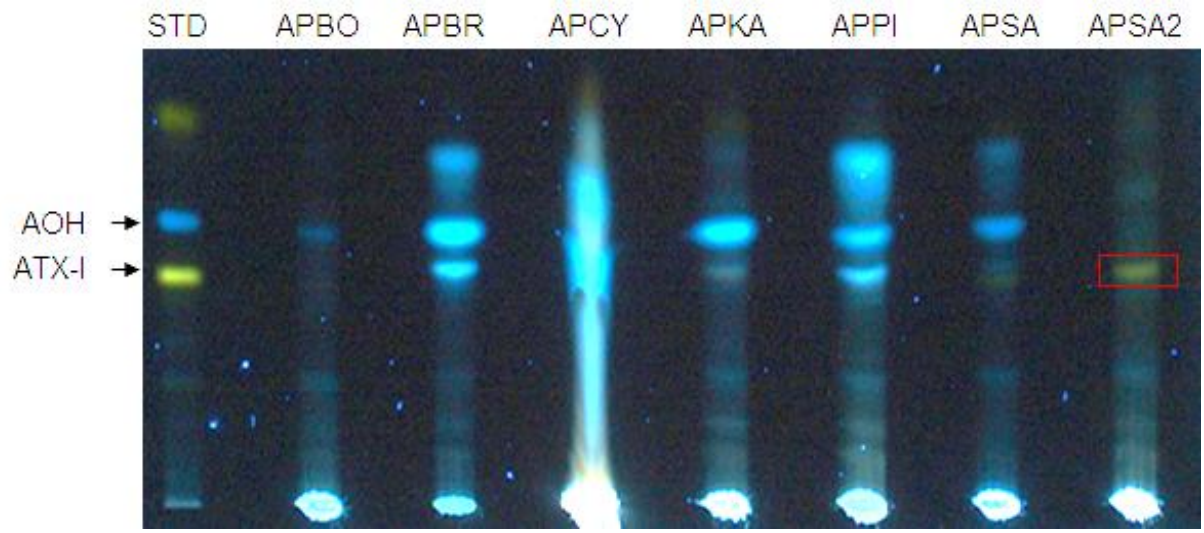

Figure21: Thin layer chromatography of toxin extracts isolated from strains isolated in this study incubated on PDA. Standards applied are alternariol (AOH), altertoxin-I(ATX-I). The plate was developed with (Toluol: ethyl acetate: formic acid - 60:35:5). Image was captured at 366nm.

3.1.2 Molecular markers

3.1.2.1 *Single molecular markers*

Firstly, the ability of different markers to distinguish between the strains used in this study was to be evaluated. Hence, we performed alignments with single molecular markers and examined the resulting trees. By comparing the phylogenetic trees shown in Fig. 22, it became apparent that even though some subsegments of the shown trees look similar to each other, in total, all of them differed at least to a certain degree. Hence, even if multiple of them are used, redundancy should not be an issue.

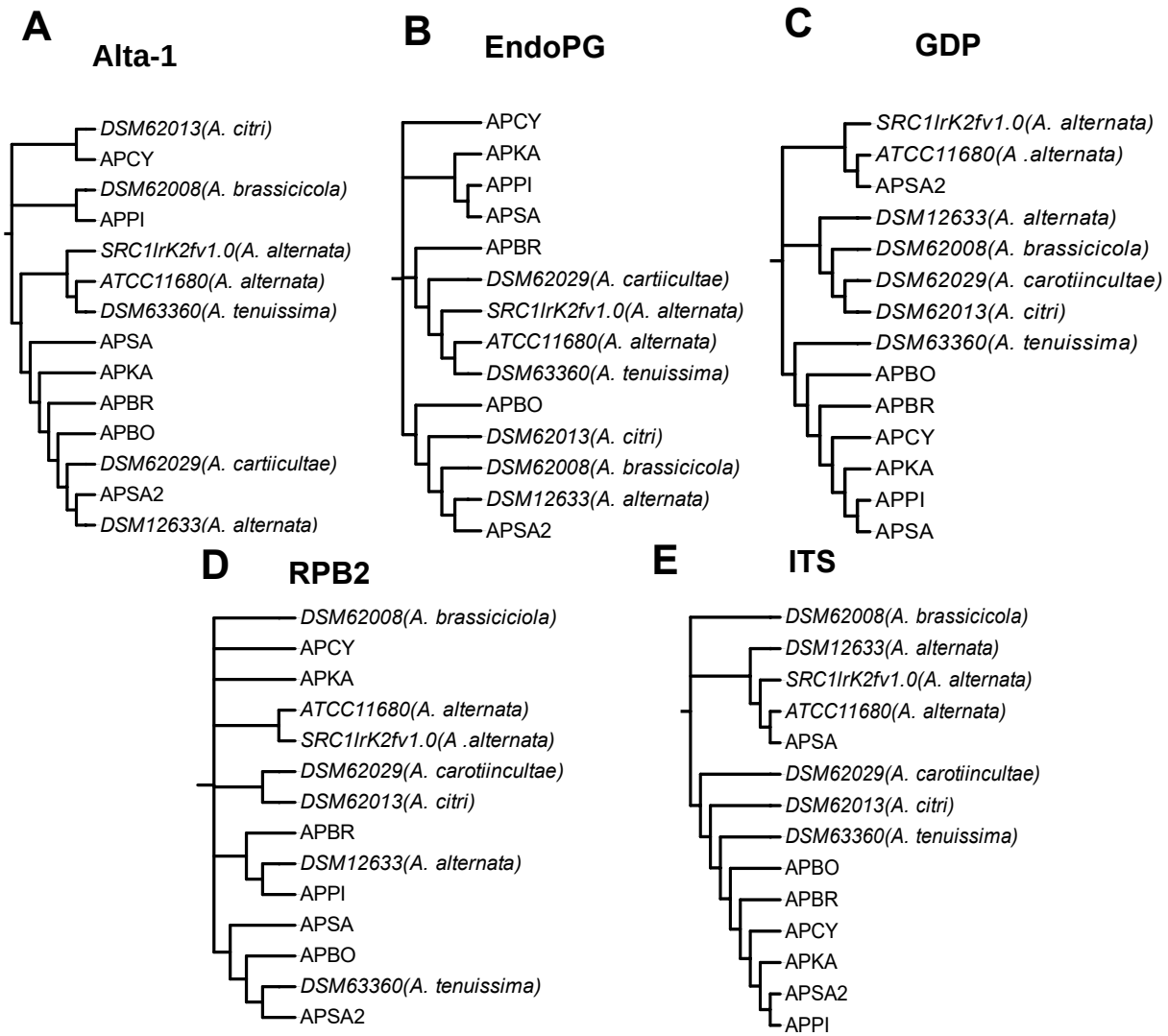

Figure 22: Phylogenetic trees of single molecular markers. **A** Phylogenetic tree built with MEGA11 on the basis of an Alta-1 sequence alignment. **B** Phylogenetic tree built with MEGA11 on the basis of an EndoPG sequence alignment **C** Phylogenetic tree built with MEGA11 on the basis of an GDP sequence alignment. **D** Phylogenetic tree built with MEGA11 on the basis of an ITS sequence alignment. **E** Phylogenetic tree built with MEGA11 on the basis of an RPB2 sequence alignment.

3.1.2.2 *Concatenation of molecular markers*

To compare the different possibilities of marker concatenation for varying numbers of markers, we constructed phylogenetic trees using three, four, and five molecular markers concatenated. The three phylogenetic trees shown in Fig. 23 share some similarities in the sense that some species consistently grouped together regardless of the number of markers used. This behavior was observed with *A. citri* consistently grouping closely with *A. carotiincultae*, as well as SRC1lrK2fv1.0 always grouping closely together with ATCC11680. The tree consistencies end with the constant close clustering of isolates: APSA, APBO, and APSA2. All other strains vary in placement within the different trees in relation to the number of markers used.

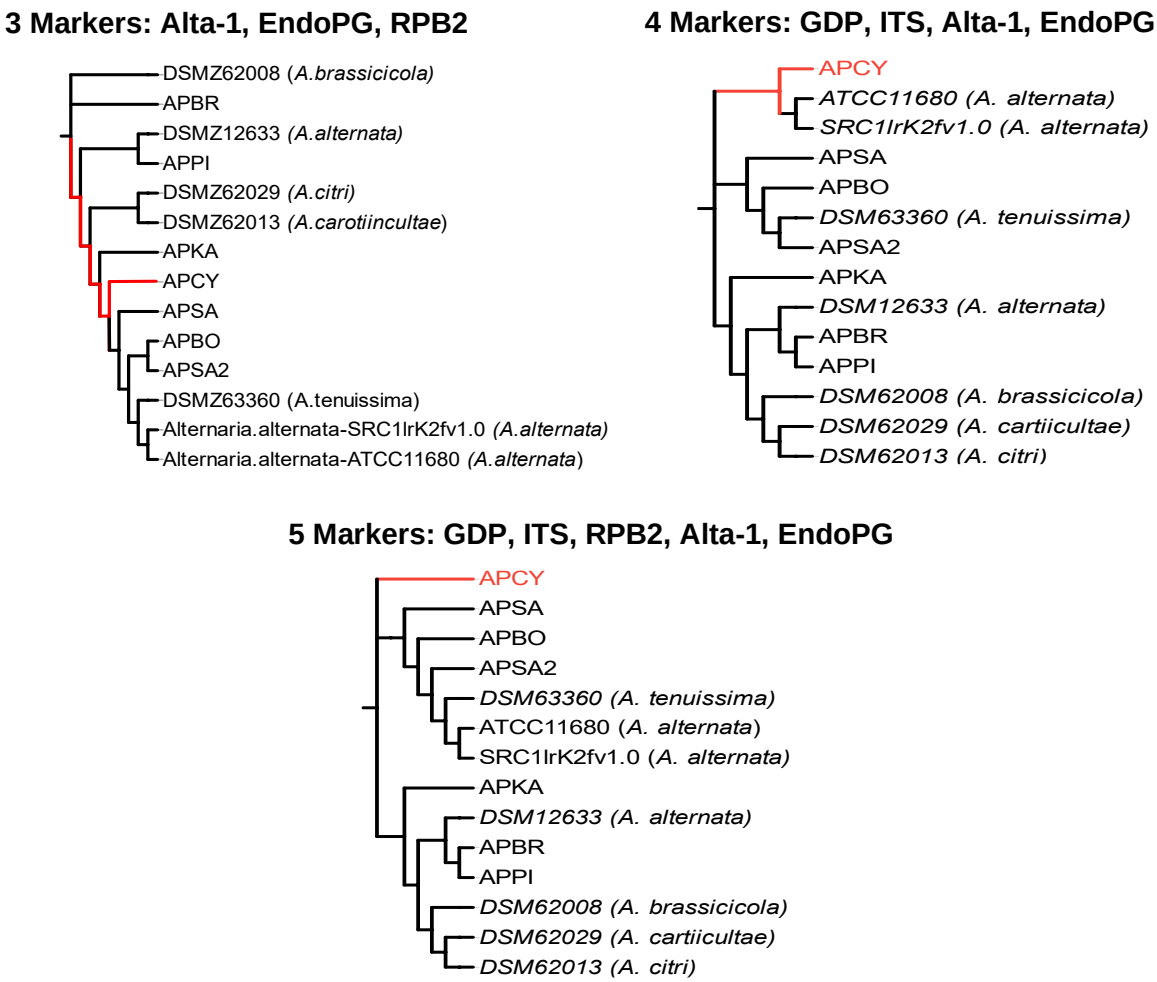

Figure 23: Phylogenetic trees built with MEGA11 on the basis of concatenation of multiple sequence alignments. **A** Phylogenic tree built from a concatenation of Alta-1, EndoPG and RPB2 sequence alignments. **B** Phylogenic tree built from a concatenation of GDP, ITS, Alta-1 and EndoPG sequence alignments. **C** Phylogenic tree built from a concatenation of GDP, ITS, Alta-1, EndoPG and RPB2 sequence alignments.

3.2 Analysis of Peruvian and Chilean strains

Analyzing a bandwidth of different strains of the same species from varying geographical locations opens the opportunity for comparison. Discrepancies in phenotype and chemotype are possibly linked to their respective unique environment. Those comparisons can help to further evaluate the toxigenic potential of the species as well as possibly deliver clues for an adaptation mechanism for the respective native environment of the fungal strain. Hence, we analyzed and compared phenotypes and chemotypes of the Peruvian and Chilean strains to be able to draw comparisons.

3.2.1 Colony phenotypes

The colony phenotype of all strains incubated on PDA was mostly dark brownish in color, with some exceptions, which tended to be dark green (Fig. 24), (Fig. 25). Furthermore, some strains, such as CS314 or CS339, exhibited visible fringes in their growth pattern. Yet, compared to the colony phenotypes that resulted from incubation on PDA, the phenotypes on MG were more consistent. After incubation on MG, all but three strains showed a similar dark brown phenotype without any fringes or a strong presence of aerial hyphae. Exceptions were CS339 and CS314, which possessed aerial hyphae in their center, and CS313, which also showed aerial hyphae and fringes. In contrast to MG, which led to relatively consistent colony phenotypes, there was YES. Incubation on YES led to a rather diverse range of colony phenotypes, from the aforementioned dark brown phenotype without fringes to predominantly light green phenotypes, with major fractions exhibiting white and circular patterns. The comparison of different *A. alternata* strains on various media revealed the species' diversity and how its differences result in distinct responses to its environment.

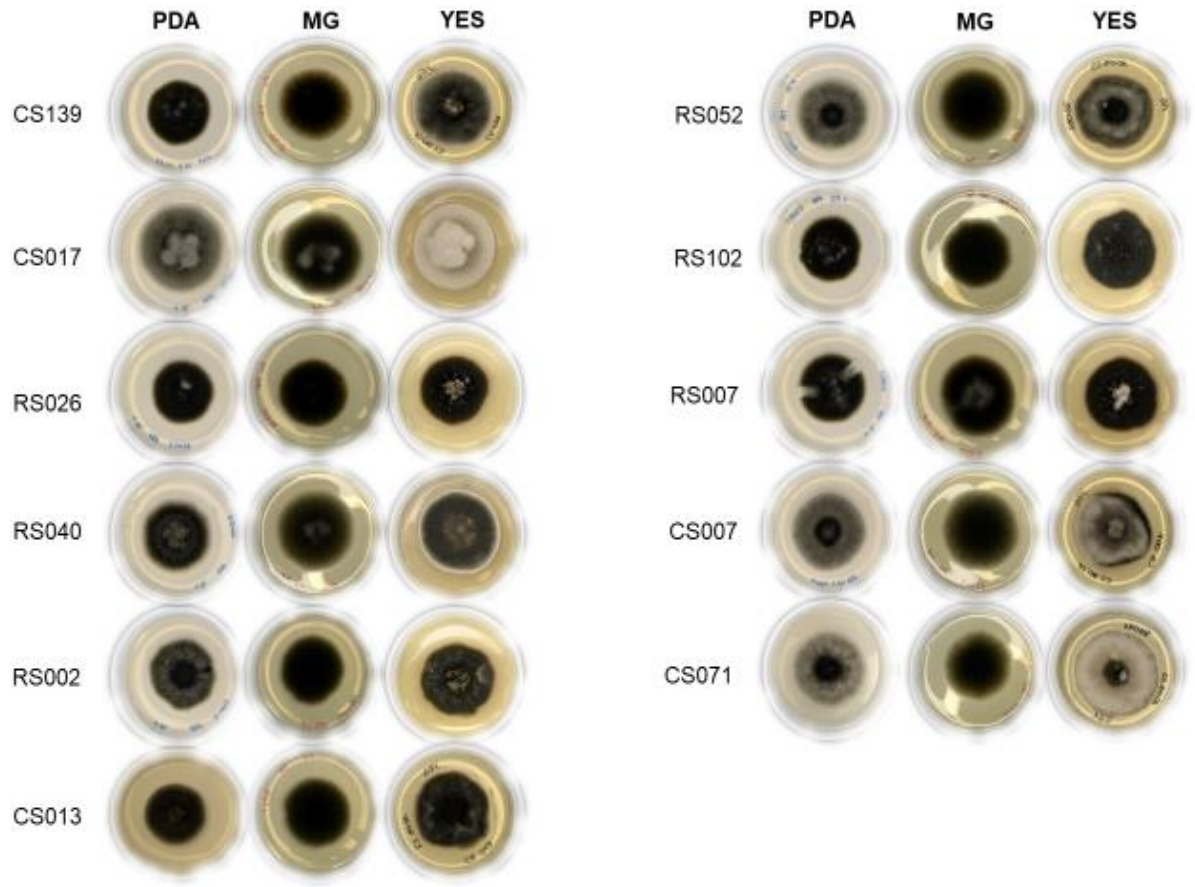

Figure 24: Colony phenotypes of strains CS139, CS017, RS026, RS040, RS002, CS013 RS052, RS102, RS007, CS007 and CS071 after 10 days of incubation on PDA, MG and YES in the dark at 28°C

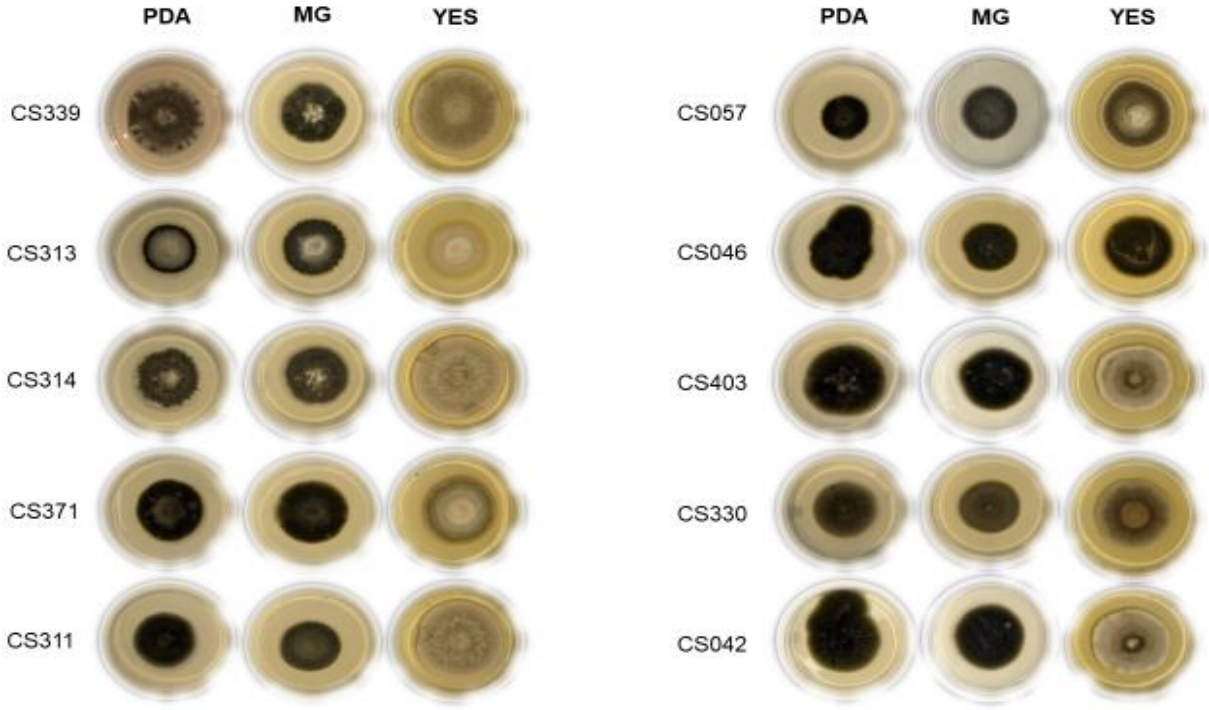

Figure 25: Colony phenotypes of strains CS339, C313, CS314, CS371, CS311, CS057, CS046, RS403, R330, and CS042 after 10 days of incubation on PDA, MG and YES in the dark at 28°C

3.2.2 Chemotype

3.2.2.1 *Untargeted metabolite fingerprint*

Untargeted metabolite fingerprinting, which can be performed using thin-layer chromatography (TLC), is a valuable method for depicting both metabolites for which standards are available and those for which no standards exist. Additionally, it can be used to investigate the appearance of entirely unknown metabolites. Hence, we used this method to determine which metabolites were synthesized by those strains under known circumstances, along with the possibility of deriving at least a rough relative quantification of some metabolites. All 21 strains isolated in Chile and Peru were applied to TLC plates after 10 days of incubation at 28°C in the dark in varying media. The strains were applied along with reference standards of AOH, ATX-I, and TeA. Fig. 26 shows the first half of the investigated strains from Peru and Chile after incubation on MG medium.

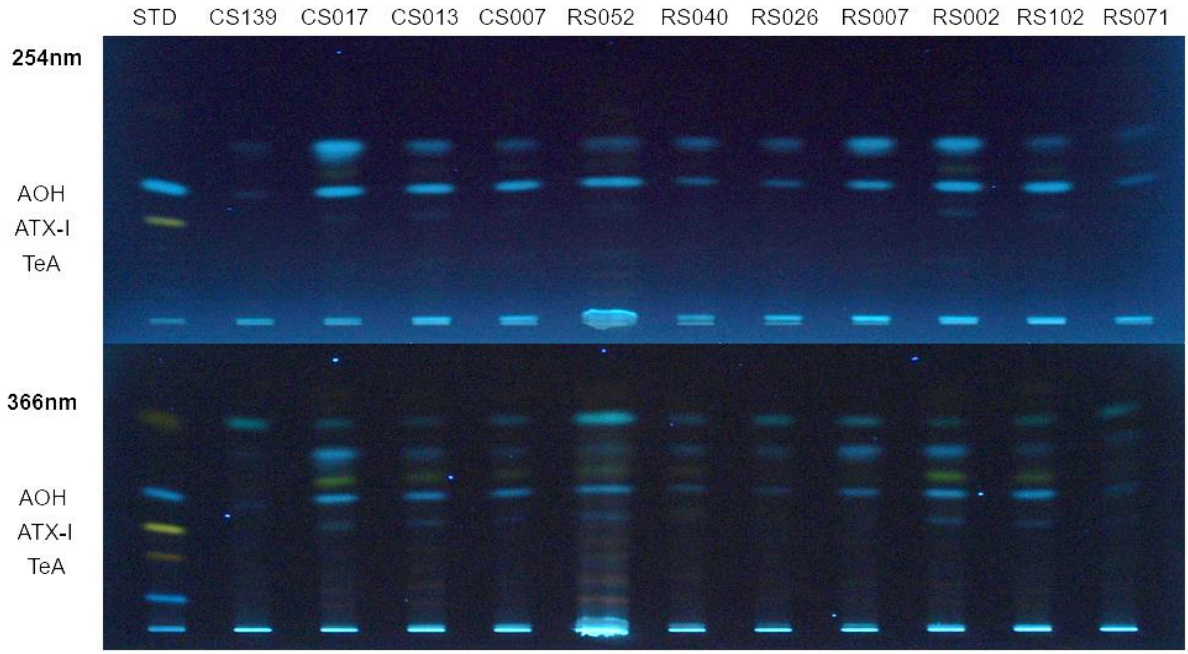

Figure 26: TLC of the first half of the *A. alternata* strains from Peru and Chile after 10 days of incubation at 28 °C in darkness on MG Medium. Along with the toxin extracts, a Standard mix was applied to the TLC plate containing AOH, ATX-I, and TeA. The same TLC plate is shown with irradiation of UV light at 254 nm and 366nm. The mobile phase consists of toluol /ethyl acetate/formic acid (60:35:5, v/v/v).

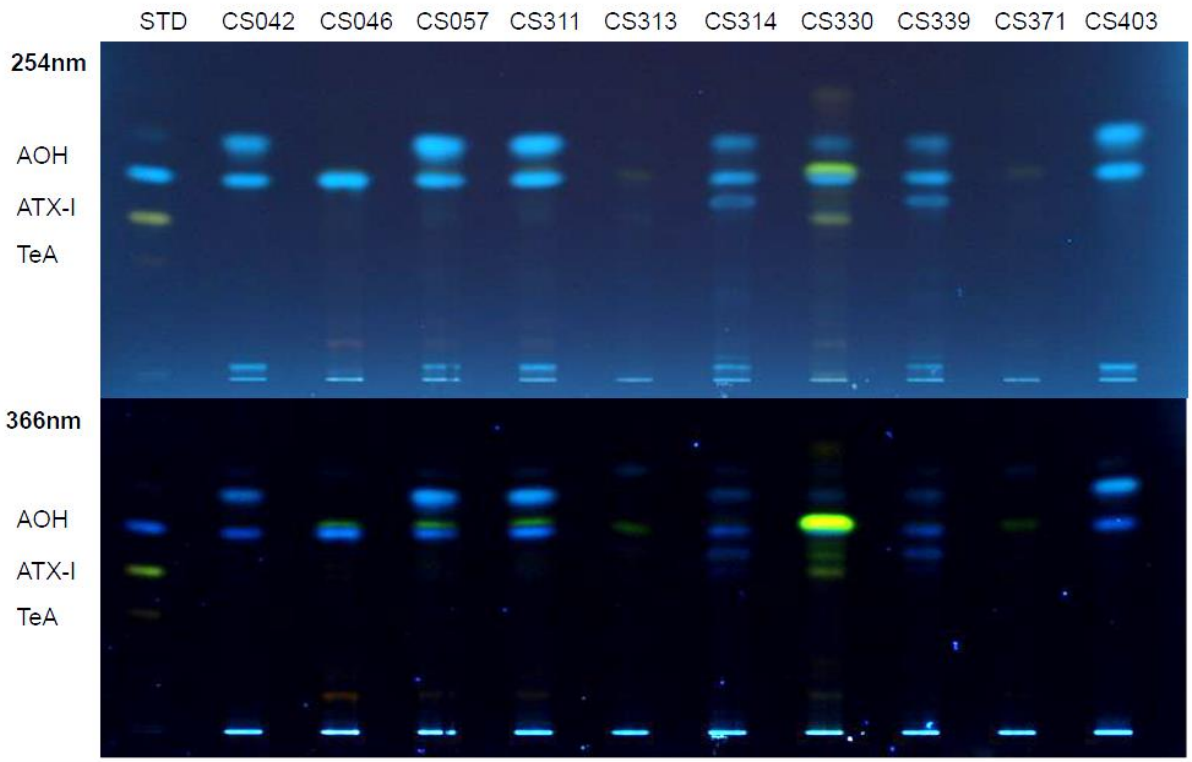

Figure 27: TLC of the second half of the *A. alternata* strains from Peru and Chile after 10 days of incubation at 28 °C in darkness on MG Medium. Along with the toxin extracts, a Standard mix was applied to the TLC plate containing AOH, ATX-I, and TeA. The same TLC plate is shown with irradiation of UV light at 254 nm and 366 nm. The mobile phase consists of toluol /ethyl acetate/formic acid (60:35:5, v/v/v).

Fig. 26 shows that apart from strains CS139 and RS071, all strains produced two bands visible at 254 nm wavelength. The one with the lower retention time corresponds to the AOH. In comparison, the one with the higher retention time is likely to be an AOH derivative due to its similar emission to AOH and the close proximity to the AOH band. Fig. 27 shows the second half of the strains after incubation on MG medium. Interestingly, while similar to Fig. 26, nearly all strains possessed the bands that can be assigned to AOH, and one of its derivatives, strains CS046, CS311, and especially CS330 showed the synthesis of a metabolite that, due to its color of emission and retention time, is likely to be ATX-II. After incubation on MG medium, we tested the incubation on PDA, which resulted in a very different band pattern than that of MG, despite having some similarities. The similarities mentioned are primarily the consistency of AOH and its derivative, with a slightly longer retention time, which is evident at 254 nm.

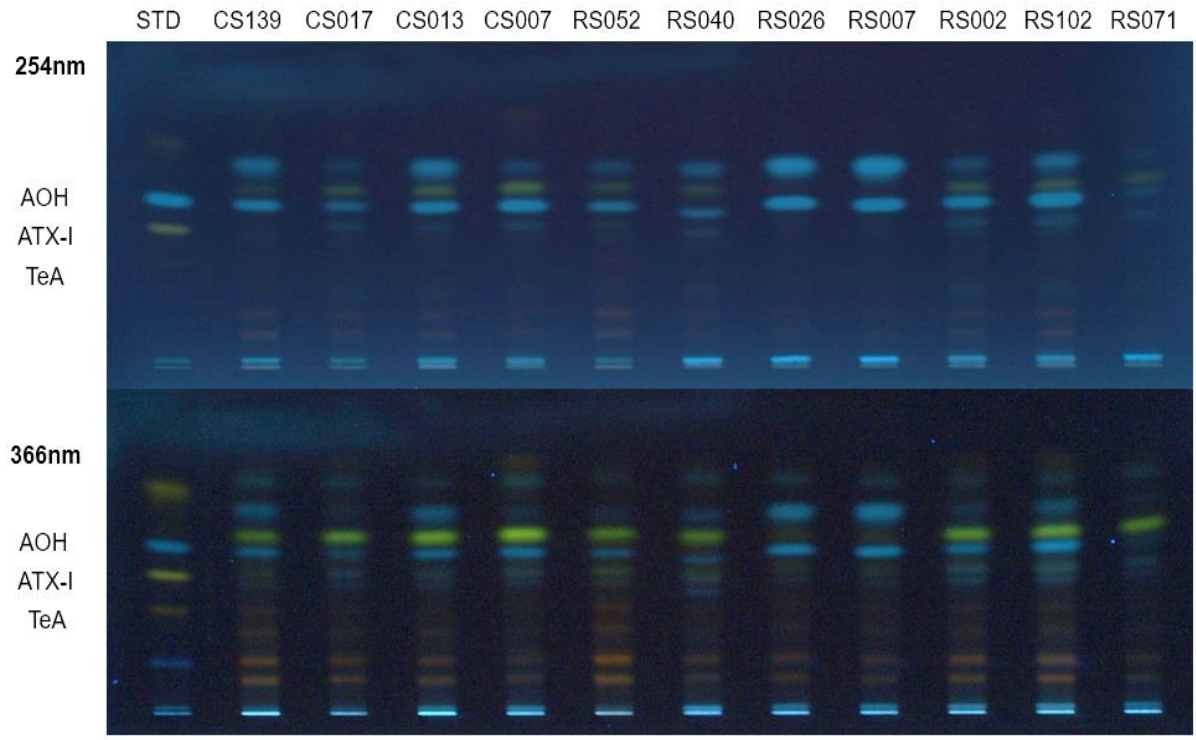

Figure 28: TLC of the first half of the *A. alternata* strains from Peru and Chile after 10 days of incubation at 28 °C in darkness on PDA Medium. Along with the toxin extracts, a standard mix was applied to the TLC plate containing AOH, ATX-I, and TeA. The same TLC plate is shown with irradiation of UV light at 254nm and 366 nm. The mobile phase consists of toluol /ethyl acetate/formic acid (60:35:5, v/v/v).

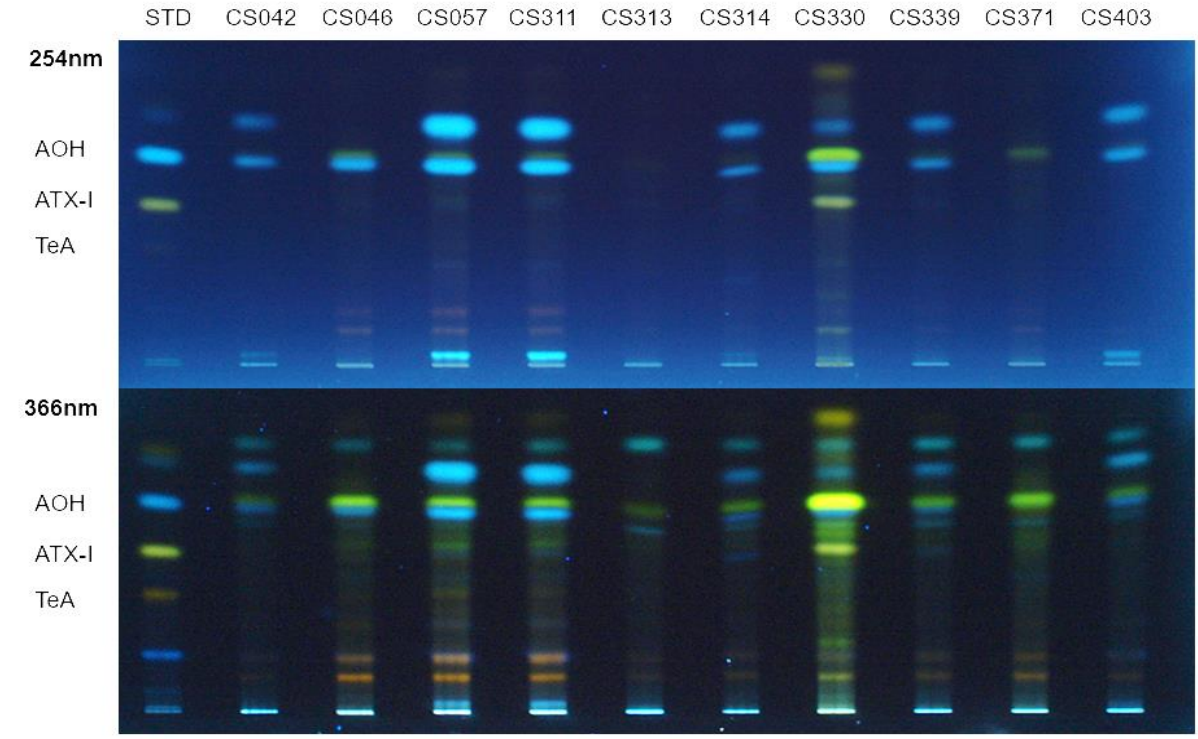

Figure 29: TLC of the second half of the *A. alternata* strains from Peru and Chile after 10 days of incubation at 2 8°C in darkness on PDA Medium. Along with the toxin extracts, a standard mix was applied to the TLC plate containing AOH, ATX-I, and TeA. The same TLC plate is shown with irradiation of UV light at 254 nm and 366 nm. The mobile phase consists of toluol /ethyl acetate/formic acid (60:35:5, v/v/v).

Another band present in most strains was a yellow band with a slightly longer retention time than AOH. Color and retention time suggest that this band is a form of altertoxin. The said band was present in all strains except RS026 and RS007, and was visible at 254 nm, with significantly more intensity at 366 nm irradiation. Beyond this unknown band, even if barely visible, most strains possessed an ATX-I band. Furthermore, even if the bands were very faint, TeA bands were visible in all strains at 366 nm wavelength. Moreover, a plethora of other faint, unknown bands were visible, especially at 366 nm. While some of them were likely derivatives of the mycotoxins used as a standard, others remain entirely unknown. The two orange bands with a very short retention time that can be seen very well in RS052 were also consistently present in all these strains at 366 nm after incubation on PDA (Fig. 28).

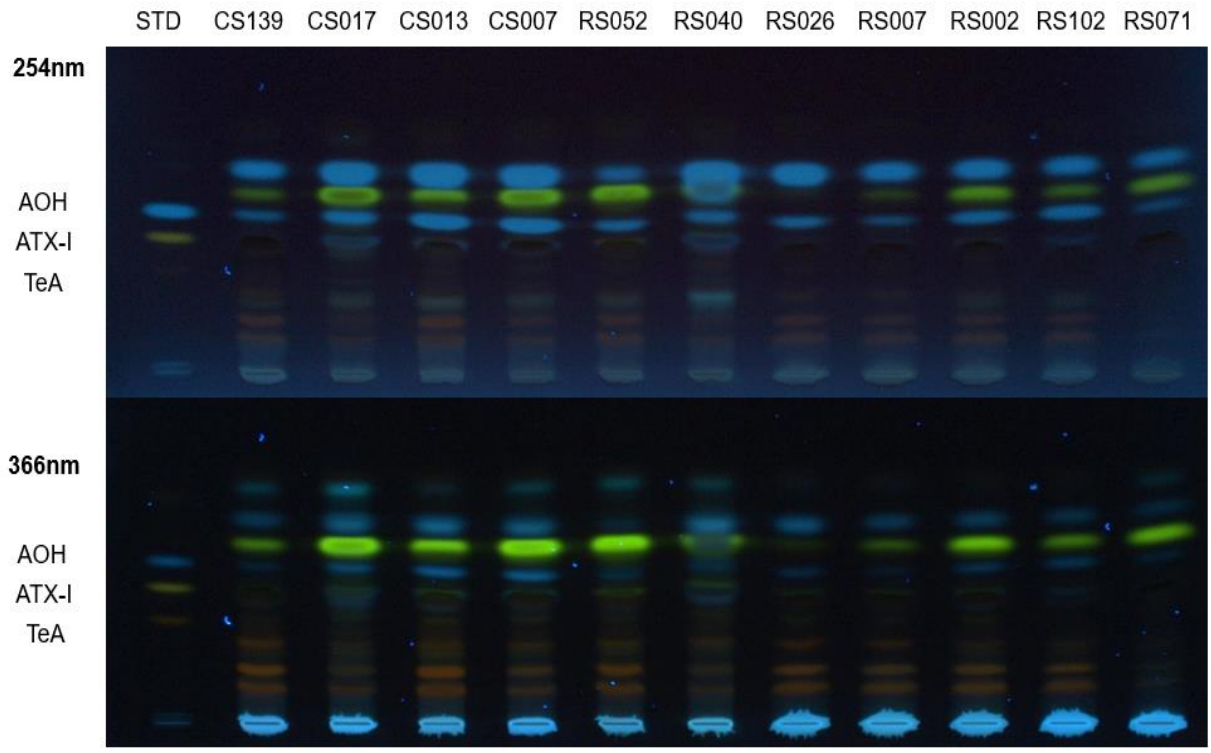

Figure 30: TLC of the first half of the *A. alternata* strains from Peru and Chile after 10 days of incubation at 28 °C in darkness on YES Medium. Along with the toxin extracts, a Standard mix was applied to the TLC plate containing AOH, ATX-I, and TeA. The same TLC plate is shown with irradiation of UV light at 254 nm and 366 nm. The mobile phase consists of toluol /ethyl acetate/formic acid (60:35:5, v/v/v).

Just like with the other bands, it is possible that those bands are derivatives of known toxins, like in this case, due to color and retention time, most likely TeA. When the TLC of the second half of the Peruvian and Chilean strains, which can be seen in Fig. 29, was observed, most strains produced similar band patterns as described for the first half of the strains when incubated on PDA. Yet, some things stand out. Firstly, two strains, namely CS313 and CS371, lacked the two very consistent bands that were AOH and its derivative. Meanwhile, CS046 possessed the AOH band but did not harbor the band of the derivative with the slightly higher retention time. Additionally, CS313 stood out due to its lack of visible bands at 254 nm, whereas CS371 exhibited only a single yellow band, likely corresponding to ATX-II. Lastly, CS330 exhibited a very striking band visible at both 254 nm and 366 nm, which was previously described as a possible altertoxin. Whilst this band was also visible in the other strains, the intensity seemed to be a manifold of the same band in the other strains. After incubation on PDA, we tested incubation on YES Agar. Hence, Fig. 30 shows the TLC with the first half of the strains isolated from Peru and Chile after incubation on YES-agar. This TLC appeared to be more homogenous than the others, especially considering the differences between 254 nm and 366 nm. All strains applied to this TLC possessed the AOH band and the AOH-derivative band in varying intensities. Moreover, all strains also exhibited the yellow band of the putative altertoxin, which has a retention time slightly higher than AOH, although it was barely noticeable in strain RS026. Similar to the TLCs shown beforehand, multiple bands from unknown metabolites can be seen. Finally, it was very apparent that bands resulting from incubation on YES agar seemed to be thicker and more intense, which can be seen as an indicator of higher amounts of metabolites applied to the TLC plate. The TLC of the second half of the strains isolated in Peru and Chile, shown in Fig. 30, was very different from the one shown in Fig. 31. At first glance, the two very consistent bands of the other TLCs are missing in

several strains, either both the AOH band and the AOH-derivative band or only the derivative band. The first group consists of CS301, CS339, and CS371, whereas the second statement only applies to CS046. Furthermore, an ATX-I band was seen in all strains except CS313. Similar to the TLC plate showing the first half of the samples after incubation on YES-agar, most strains showed a clear and very intense yellow band with a slightly higher retention time than AOH. Another fascinating observation was made, namely that, apart from the bands described in this paragraph, no other bands of potential unknown metabolites were visible, which stands in contrast to the first half of the strains isolated in the mentioned locations.

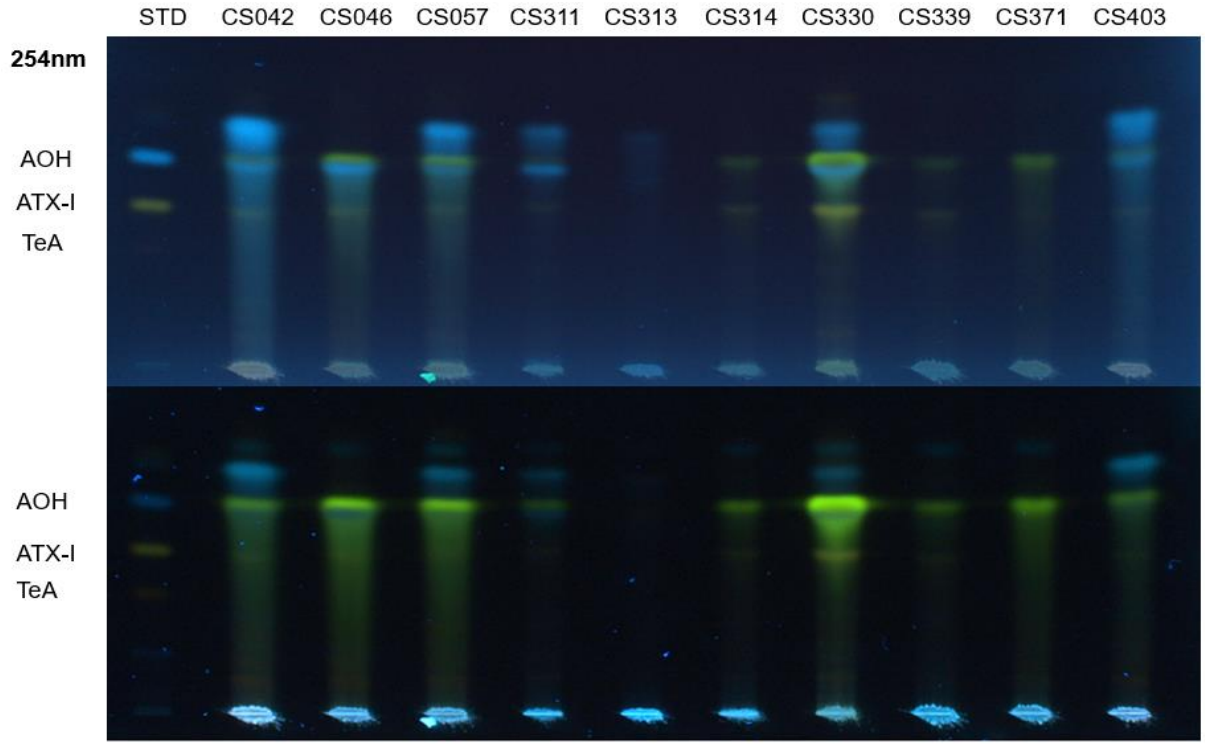

Figure 31: TLC of the second half of the *A. alternata* strains from Peru and Chile after 10 days of incubation at 28°C in darkness on YES Medium. Along with the toxin extracts, a Standard mix was applied to the TLC plate containing AOH, ATX-I, and TeA. The same TLC plate is shown with irradiation of UV light at 254 nm and 366 nm. The mobile phase consists of toluol /ethyl acetate/formic acid (60:35:5, v/v/v).

3.2.2.2 *Targeted metabolite fingerprint*

In order to compare the chemotypes of the different *A. alternata* species that were isolated, we measured the concentrations of AOH, AOH-S, AME, ALS, ALN, TeA, and ATX-I after incubation on PDA, MG, and YES. The concentrations were measured using HPLC. Starting with AOH, a severe variation in AOH synthesis was observed between the different strains and the different media for the same strain.

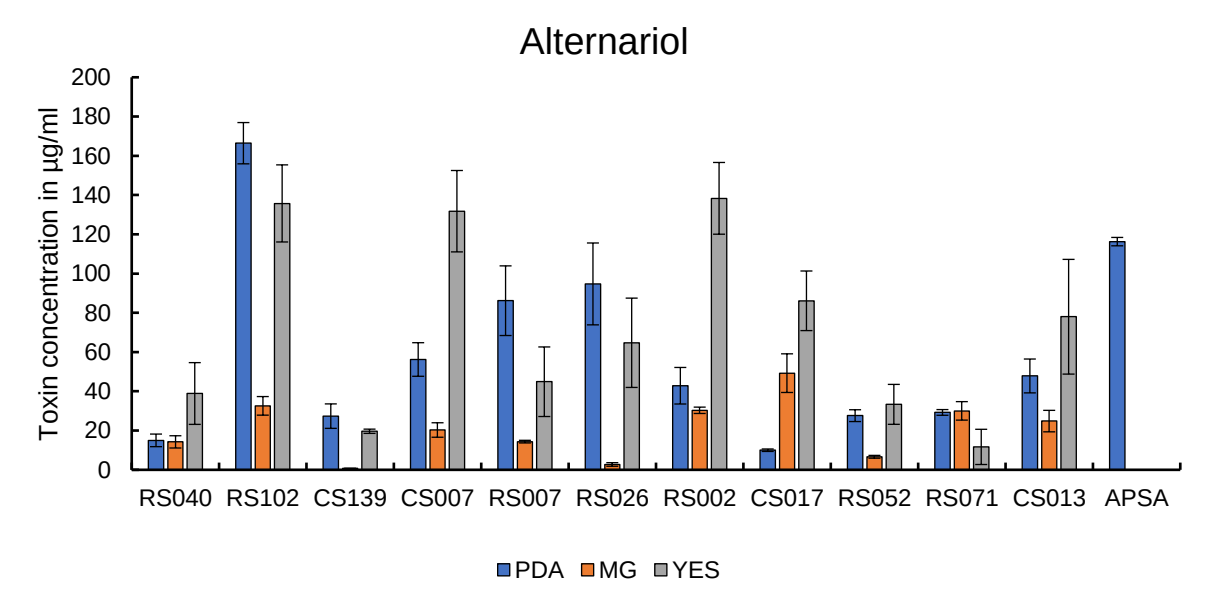

Figure 32: AOH toxin concentrations of strains RS040, RS102 CS007 RS007, RS026, RS002, CS017, RS052, RS071, and CS013 measured using HPLC after incubation in darkness for 10 days on PDA, YES and MG media. APSA is added for comparison.

When the total of all strains and media was observed, it became apparent that incubation in a particular medium led to varying concentration patterns. In the first half of the strains shown in Fig. 32, incubation on MG resulted in the lowest AOH concentrations in nearly all strains, except for RS071, for which incubation on MG and PDA yielded higher AOH concentrations than incubation on YES agar. Beyond that, apart from four exceptions, all strains reached similar concentrations as APSA after incubation on at least one medium. Meanwhile, the aforementioned exceptions reached a maximum of about 50 % of the AOH concentration as measured in APSA. Fig. 33 illustrates the contrast between the second half of the strains and the first half,

as incubation on MG yielded the highest AOH concentrations in several strains, with the exceptions being CS371 and CS046. Additionally, while some very low values of AOH were observed in the first half of the strains, AOH was measured in all strains and media. Yet, the same cannot be said about the second half of the strains, in strains CS311, CS313, CS314, CS339, and CS371, no AOH could be measured after incubation on YES medium.

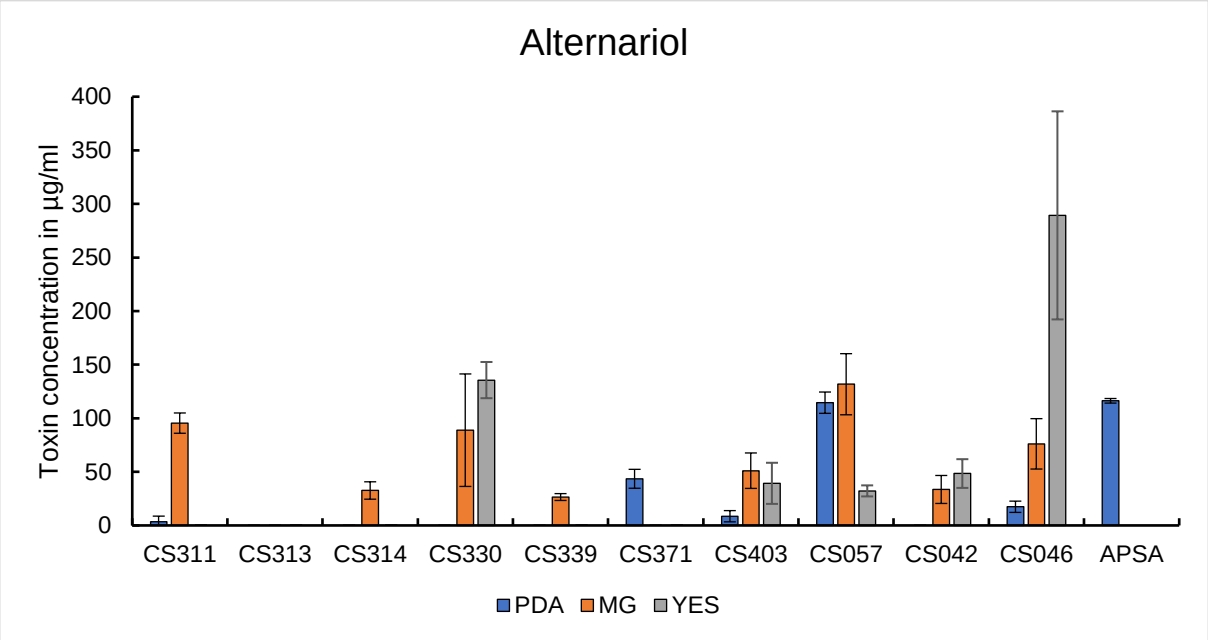

Figure 33: AOH toxin concentrations of strains CS311, CS313, CS314, CS330, CS339, CS371, CS403, CS057, CS042, CS057, CS042 and CS046 measured using HPLC after incubation in darkness for 10 days on PDA, YES and MG media. APSA is added for comparison.

Furthermore, strains CS313, CS314, and CS339 showed no measurable amounts of AOH after incubation on PDA. Lastly, the two strains that stood out the most were CS313, which didn't seem to synthesize any measurable amounts of AOH on any medium, and CS046, which is the only strain that, when incubated on YES, synthesized AOH concentrations that were nearly three times higher than our reference strain APSA. Next, AME concentrations of the first half of the strains were measured.

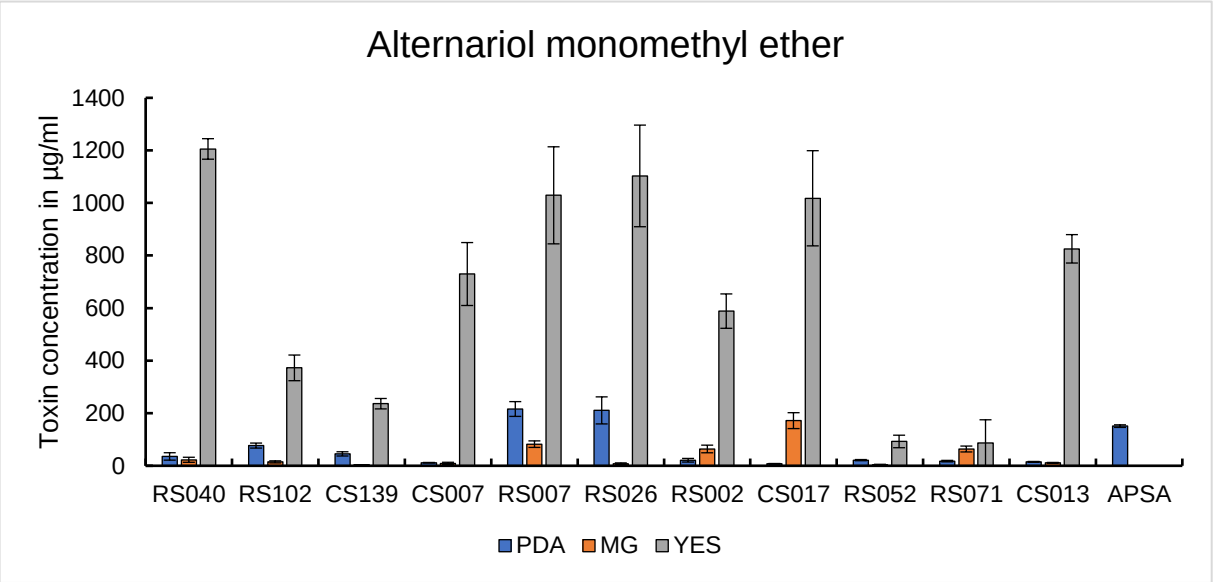

Figure 34: AME toxin concentrations of strains RS040, RS102 CS007 RS007, RS026, RS002, CS017, RS052, RS071, and CS013 measured using HPLC after incubation in darkness for 10 days on PDA, YES and MG media. APSA is added for comparison.

Fig. 34 clearly shows that several strains had tremendously higher toxin concentrations when incubated on YES than our reference strain APSA. In this instance, strains RS040, RS007, RS026, and CS017 even harbored concentrations exceeding 1000 µ/mL. Meanwhile, the concentrations measured after incubation on MG or PDA rarely exceeded the concentration of the reference strain and were usually significantly lower. In contrast to the first half of the strains, except for three strains, incubation on YES agar did not result in strikingly high concentrations of AME.

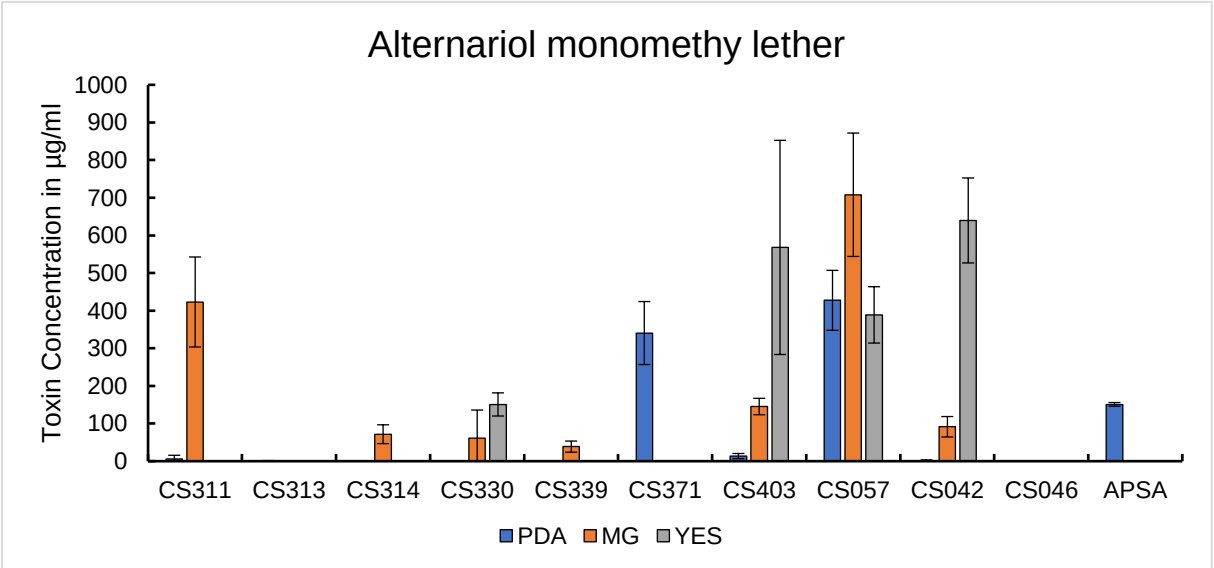

Figure 35: AME toxin concentrations of strains CS311, CS313, CS314, CS330, CS339, CS371, CS403, CS057, CS042, CS057, CS042 and CS046 measured using HPLC after incubation in darkness for 10 days on PDA, YES and MG media. APSA is added for comparison.

Only CS403, CS057, and CS042 synthesized AME in high concentrations when incubated on YES (Fig. 35).CS057 also stood out, as incubation on any tested media resulted in toxin concentrations that were two to four times higher than those of the reference strain. Then, alternariol sulfate was measured. Examining the first half of the strains, it became apparent that, with a few exceptions, incubation on YES did not result in measurable amounts of AOH-S (Fig. 36). Furthermore, PDA was the only medium that consistently yielded quantifiable amounts of AOH-S. Moreover, it could be seen that, compared to the reference strain APSA, all strains shown in Fig. 37 had considerably lower AOH-S concentrations.

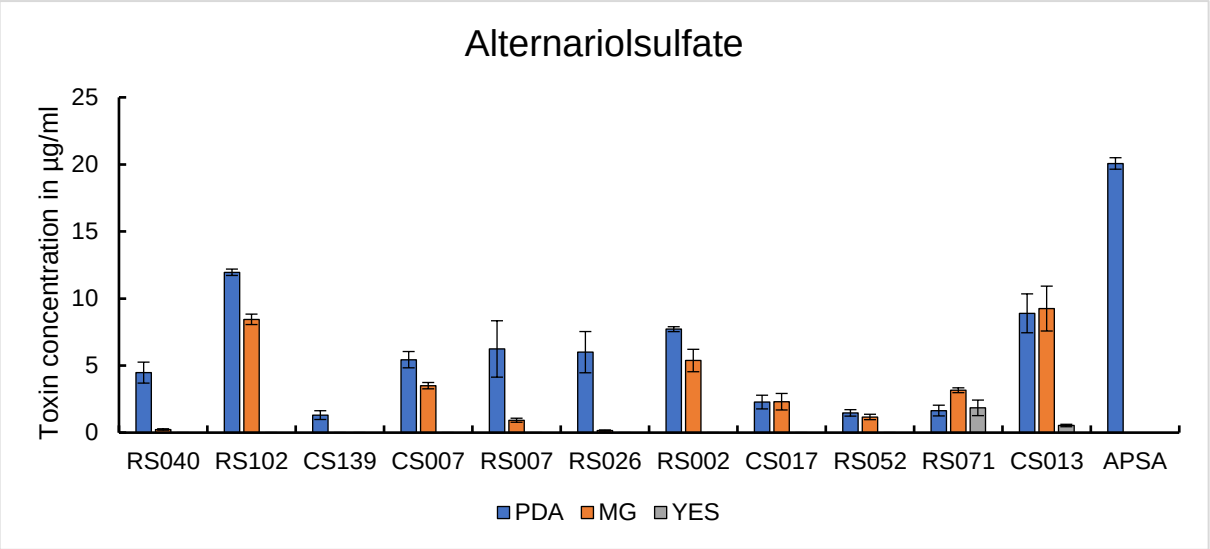

Figure 36: AOH-S toxin concentrations of strains RS040, RS102 CS007 RS007, RS026, RS002, CS017, RS052, RS071, and CS013 measured using HPLC after incubation in darkness for 10 days on PDA, YES and MG media. APSA is added for comparison.

The second half of the Peruvian and Chilean strains, as shown in Fig. 37, exhibited a distinctly different tendency from the first half. While all strains of the first half showed measurable concentrations of AOH-S after incubation in at least one medium, the second half showed several strains in which AOH-S could not be measured. Those strains include: CS313, CS314, CS330, CS339, CS403 and CS042. Yet, despite the differences between the second half and the first half, both halves have in common that none of the strains came even close to the AOH-S concentration measured in the reference strain APSA.

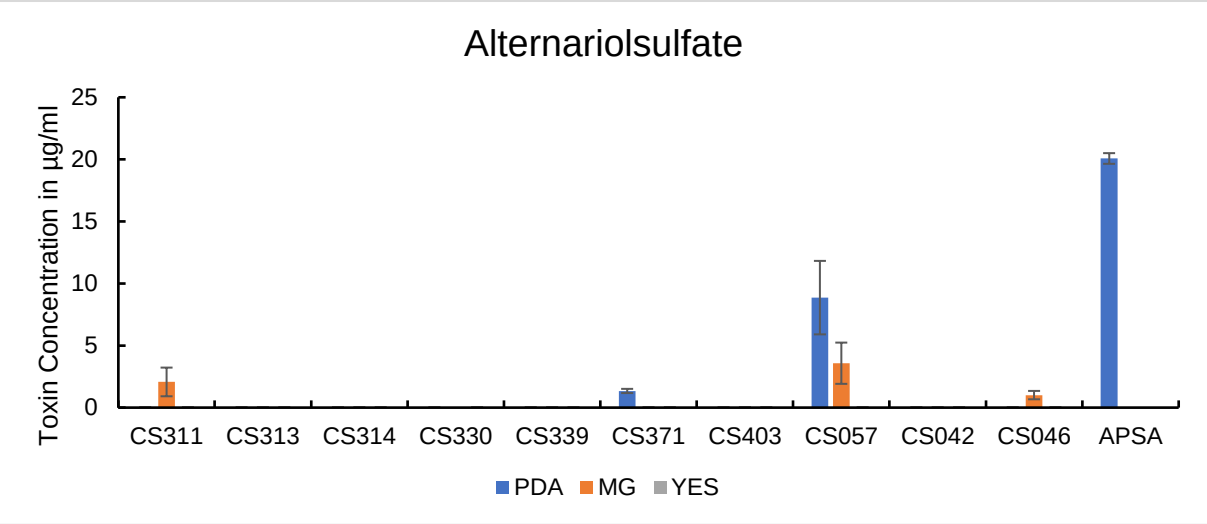

Figure 37: AOH-S toxin concentrations of strains CS311, CS313, CS314, CS330, CS339, CS371, CS403, CS057, CS042, CS057, CS042 and CS046 measured using HPLC after incubation in darkness for 10 days on PDA, YES and MG media. APSA is added for comparison.

Thereafter, ALN was measured. Here, only two strains from the first half had measurable ALN concentrations (Fig. 38). In RS102, incubation on YES medium led to ALN levels higher than those of the reference strain. Yet, even more striking, RS040 incubation on YES led to significantly higher ALN concentrations compared to the reference strain APSA. Meanwhile, apart from the two strains sticking out in the first half, the second half had the same tendency of non-measurable amounts in all strains and on all media (Fig. 39).

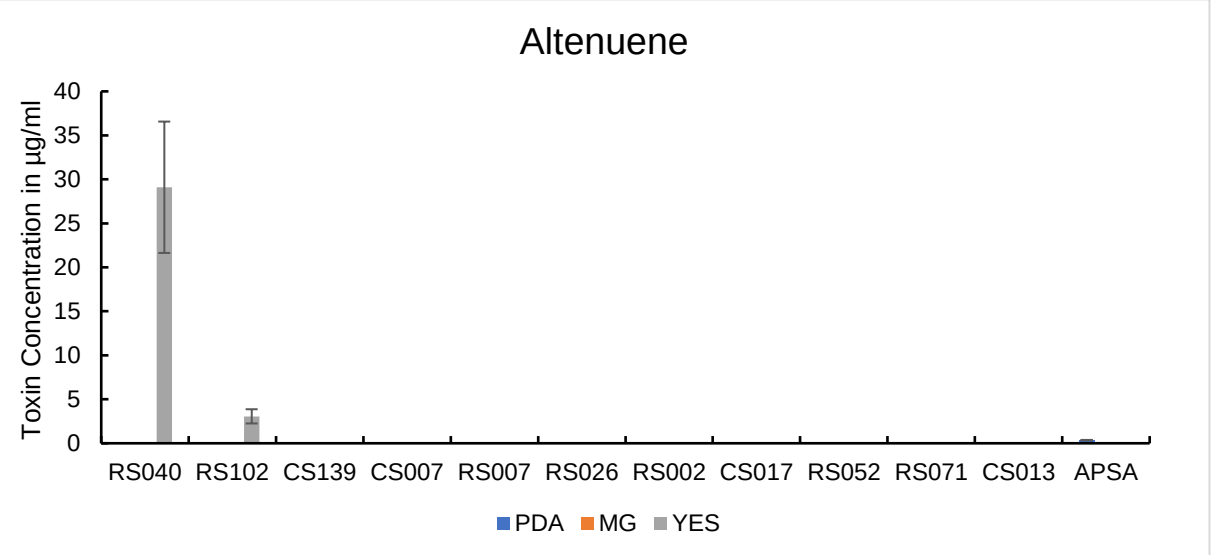

Figure 38: ALN toxin concentrations of strains CS311, CS313, CS314, CS330, CS339, CS371, CS403, CS057, CS042, CS057, CS042 and CS046 measured using HPLC after incubation in darkness for 10 days on PDA, YES and MG media. APSA is added for comparison.

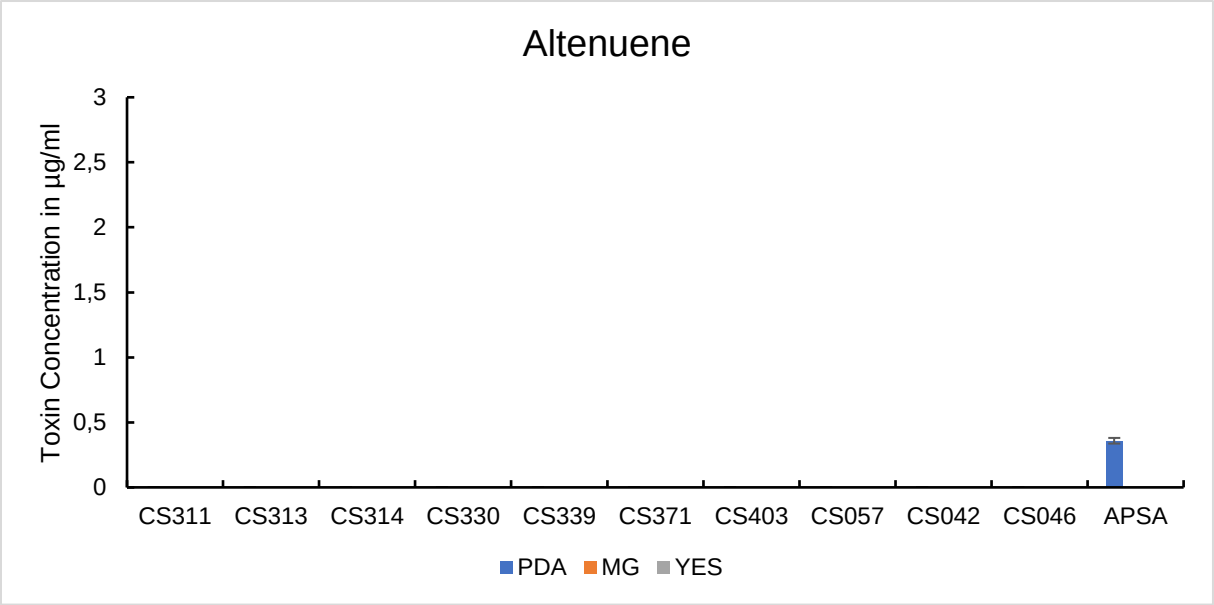

Figure 39: ALN toxin concentrations of strains CS311, CS313, CS314, CS330, CS339, CS371, CS403, CS057, CS042, CS057, CS042 and CS046 measured using HPLC after incubation in darkness for 10 days on PDA, YES and MG media. APSA is added for comparison.

The last AOH derivative measured was ALS. When the first half of the strains were observed, a highly inhomogeneous picture of toxin concentrations was visible (Fig. 40). Strains CS139, RS007, and RS026 did not synthesize measurable amounts of ALS. Apart from the aforementioned non-synthesizing strains, some strains, such as CS007, CS017, and RS052, had concentrations that were approximately the same as those of our reference strain. Yet, while incubation on PDA resulted in the highest ALS concentrations in strains with generally lower ALS concentrations, in most strains with higher concentrations, like RS040, RS071, or CS013, it was overshadowed by either MG or YES. The second half of the strains is interesting in its own regard, since the strains with measurable amounts of ALS only synthesized it after incubation on one specific medium. Interestingly, that medium was not the same, but it happened to be MG in CS314 and CS339, while being PDA in CS371. Additionally, the strains in which ALS was synthesized harbored significantly greater amounts of ALS than the reference strain APSA. All other strains of the second half synthesized amounts that resulted in concentrations below the HPLC detection threshold (Fig. 41).

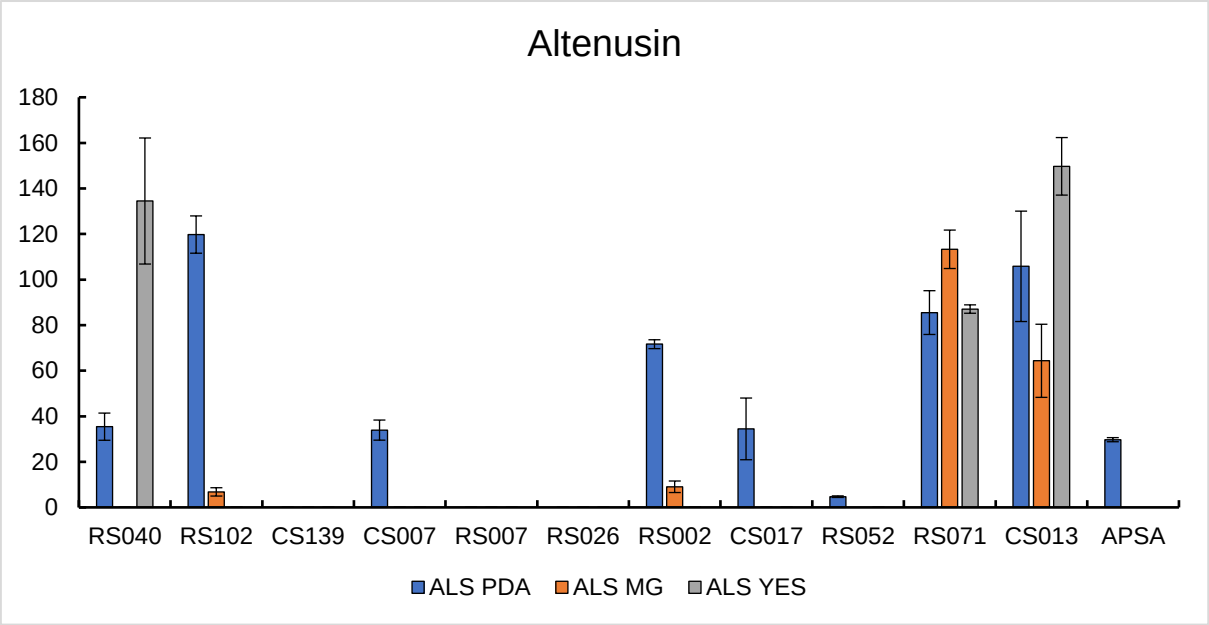

Figure 40: ALS toxin concentrations of strains RS040, RS102 CS007 RS007, RS026, RS002, CS017, RS052, RS071, and CS013 measured using HPLC after incubation in darkness for 10 days on PDA, YES and MG media. APSA is added for comparison.

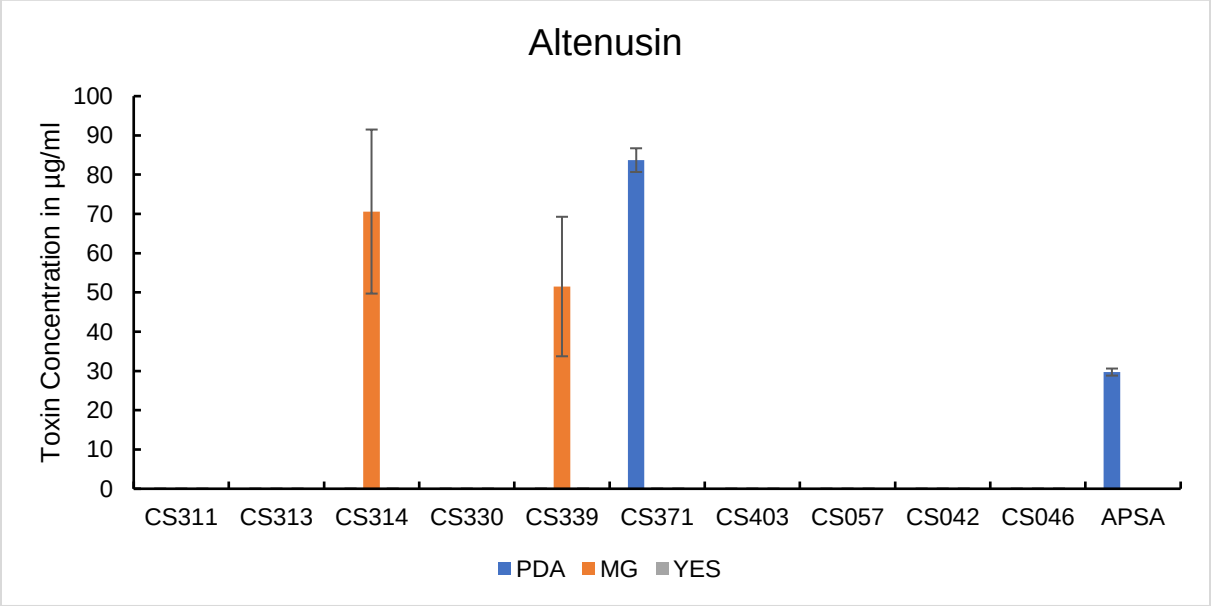

Figure 41: ALS toxin concentrations of strains CS311, CS313, CS314, CS330, CS339, CS371, CS403, CS057, CS042, CS057, CS042 and CS046 measured using HPLC after incubation in darkness for 10 days on PDA, YES and MG media. APSA is added for comparison.

After completing the analysis of AOH and its derivatives, TeA measurements followed. The first half of the strains shown in Fig. 42 made it clear that, with the exceptions of RS040, CS017, and RS071, all strains exhibited a similar pattern regarding TeA concentrations.

This pattern is characterized by incubation in PDA or MG, resulting in TeA concentrations similar to those measured in the reference strain. Furthermore, a tremendous TeA concentration exceeding 2500 µg/mL was also part of this pattern, whereas our reference strain only reached approximately 150 µg/mL. The three aforementioned exceptions possessed concentrations below three µg/mL. When the second half of the Peruvian and Chilean strains is observed, the apparent pattern in the first half was also partly discovered, at least in some strains (Fig. 43). CS330, CS371, CS057, and CS046 all harbored similarly high concentrations, which were comparable to the highest ones in the first half seen in Fig. 42. Yet, the rest of the pattern concerning TeA concentrations similar to the reference strain after incubation on MG or PDA was only present in CS046. In CS371 and CS057, incubation on PDA reached TeA levels comparable to those of the reference strain, while the TeA concentrations in Yes were significantly lower. Interestingly, CS330 showed barely any measurable TeA concentrations, apart from the aforementioned incubation in YES. Despite the high concentrations of TeA that some strains harbored,

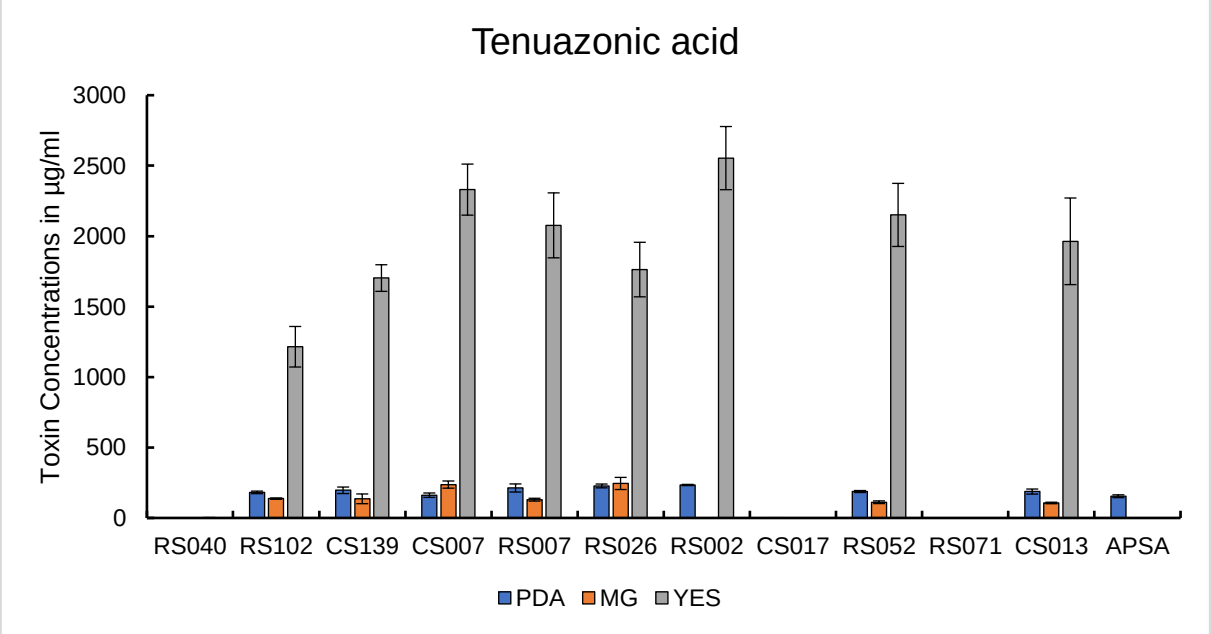

Figure 42: TeA toxin concentrations of strains RS040, RS102 CS007 RS007, RS026, RS002, CS017, RS052, RS071, and CS013 measured using HPLC after incubation in darkness for 10 days on PDA, YES and MG media. APSA is added for comparison.

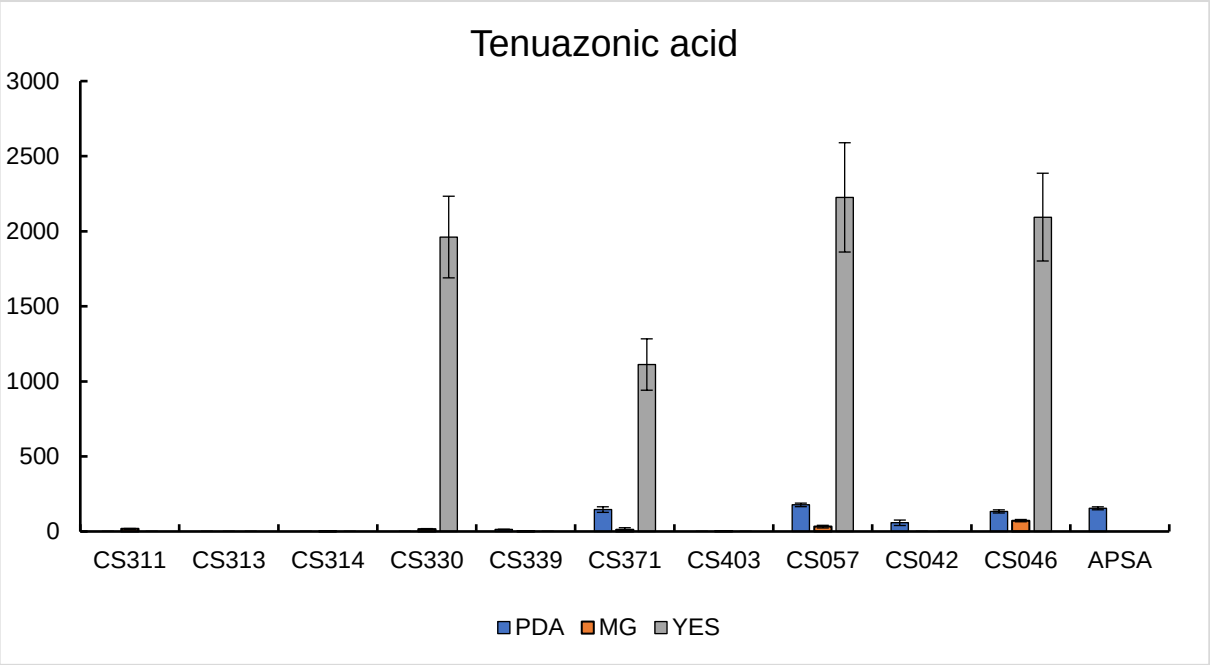

Figure 43: TeA toxin concentrations of strains CS311, CS313, CS314, CS330, CS339, CS371, CS403, CS057, CS042, CS057, CS042 and CS046 measured using HPLC after incubation in darkness for 10 days on PDA, YES and MG media. APSA is added for comparison.

especially after incubation in YES, a whole group of strains, including CS311, CS313, CS314, CS339, and CS403, either had toxin concentrations below 20 µg/mL or even below the threshold of HPLC detection. Afterwards, the toxin concentrations of ATX-I were measured.

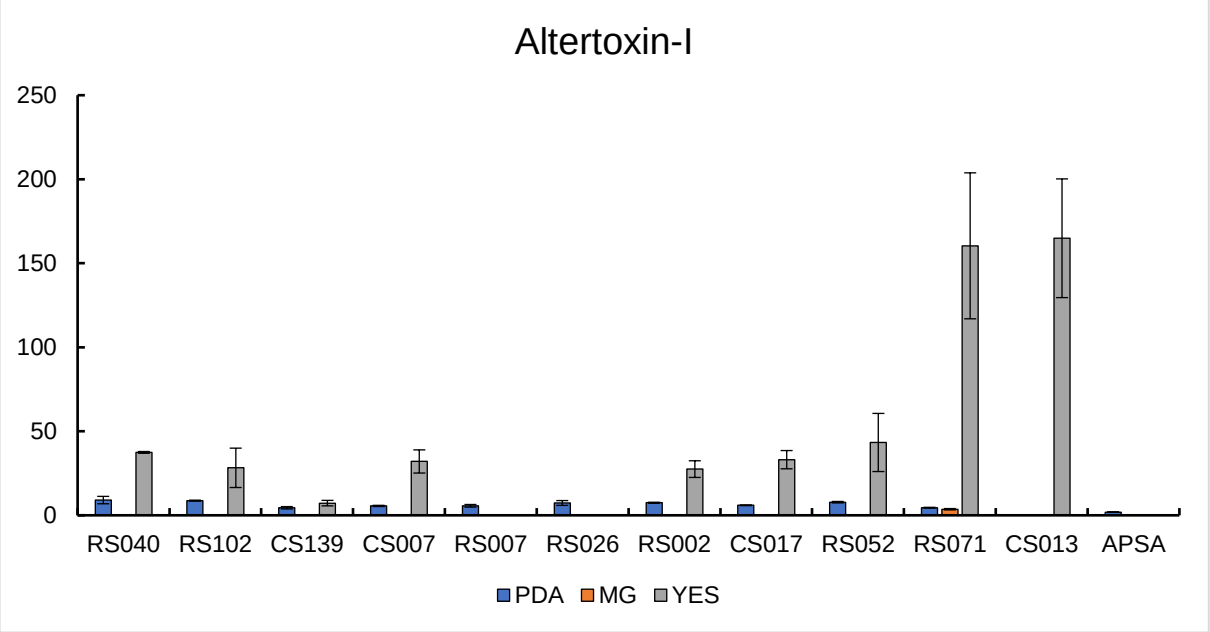

Figure 44: ATX-I toxin concentrations of strains RS040, RS102 CS007 RS007, RS026, RS002, CS017, RS052, RS071, and CS013 measured using HPLC after incubation in darkness for 10 days on PDA, YES and MG media. APSA is added for comparison.

When the first half of the strains, as seen in Fig. 44, was observed, it was clear that incubation on MG resulted in very low ATX-I concentrations or concentrations that could not be measured. Beyond that, incubation on PDA consistently resulted in lower concentrations compared to incubation on YES within these strains, yet still higher compared to the reference strain APSA. When the incubation on Yes was observed, even higher ATX-I levels were seen. Especially RS071 and CS013 stood out in this regard, as they contained concentrations of over 160 µg/mL, which is significantly higher than that of the reference strain. Yet, curiously, some strains, such as RS007 and RS026, showed no visible ATX-I concentrations after incubation on YES medium. When the second half of the Peruvian and Chilean strains, as shown in Fig. 45, is observed, the pattern that incubation on YES causes the highest ATX-I concentrations largely repeated itself. Exceptions were CS313 and CS339, in which incubation on PDA resulted in similar ATX-I concentrations.

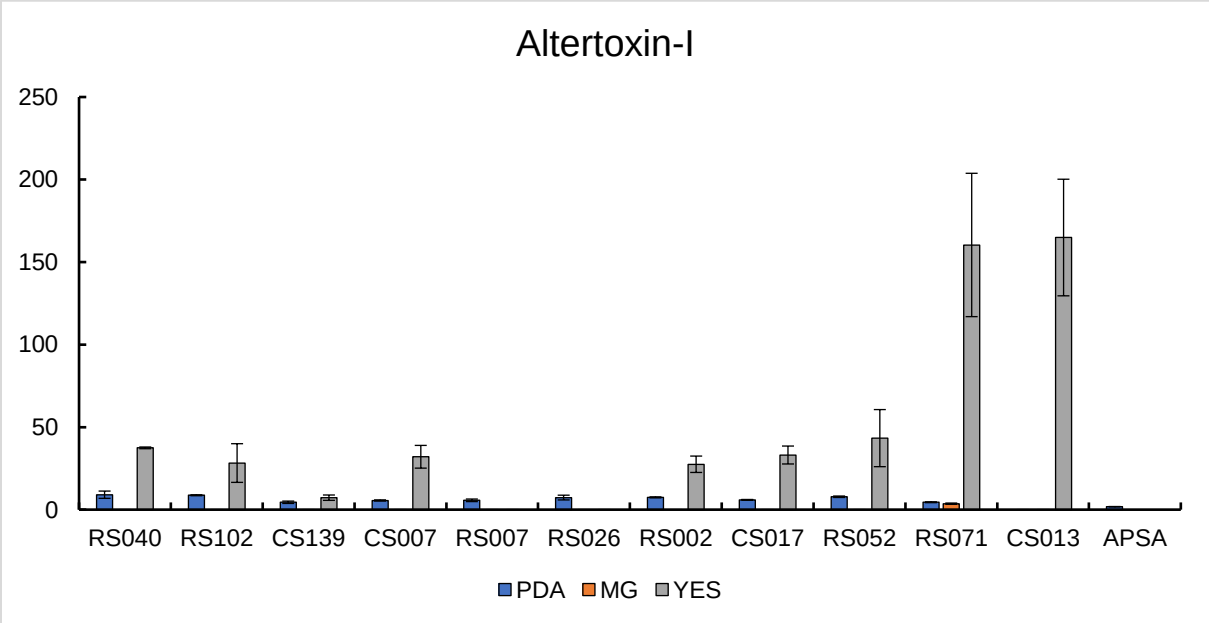

Figure 45: ATX-I toxin concentrations of strains CS311, CS313, CS314, CS330, CS339, CS371, CS403, CS057, CS042, CS057, CS042 and CS046 measured using HPLC after incubation in darkness for 10 days on PDA, YES and MG media. APSA is added for comparison.

Although multiple strains exceeded 100 µg/mL, CS046 stood out for possessing a concentration of over 200 µg/mL. Yet, CS330 again dwarfed it with a concentration of approximately 460 µg/mL. Hence, all strains exhibited concentrations far exceeding those measured in the reference strain. Yet another significant difference was observed in the second half of the strains, where, unlike the behavior in the first half, incubation on MG resulted in measurable ATX-I concentrations.

3.3 Stress tests

During the life cycle of foods, stress is omnipresent. With different stress factors having specific implications for fungi. Light is used by fungi to identify their environment in terms of what time of day it is, as well as where they are located. Examples are darkness below the earth's surface or a lack of red light due to an endophytic lifestyle. Light and darkness are often paired with different temperatures, which can be caused by a day and night cycle, making adaptations necessary. Furthermore, different pH values occur depending on the host the fungus infects, which is especially true for a fungus with a broad host range, such as *A. alternata.* Additionally, beyond the different pH values, some hosts are capable of performing an oxidative burst reaction as a means to defend themselves against the infection, which the fungus has to deal with in order to successfully infect the host. Lastly, dryness, which can be either the status quo due to geographical location or the consequence of a lack of water supply, is also a stress factor the fungus has to adapt to. Those stress factors the fungus is required to adapt to are known to impact the mycotoxin synthesis in *A. alternata*, which is why, in this work, we investigated those factors in order to derive strategies for mycotoxin prevention.

3.4 Light-induced stress

To obtain more representative results, the mycotoxin concentrations of the seven *A. alternata* isolates (APBR, APBO, APCY, APKA, APSA, APSA2, APPI) were measured (Adeyemo & Schmidt-Heydt, 2024). Concentrations of AOH, AME, AOH-S, ALS, ALN, TeA, and ATX-I were quantified in the strains mentioned above after incubation in the dark at 28 °C for 10 days, providing a negative control for the subsequent stress tests. The different *A. alternata* isolates were exposed to varying types of stress, the first stress factors tested were the different wavelengths of light. Fig. 46 B shows the relative changes in toxin concentrations caused by exposure to white light, compared to the concentrations measured in the negative control. The concentrations of both ALN and AME showed no visible differences compared to the control. However, AOH-S, TeA, and AOH showed an apparent increase, ranging from approximately 35 % to 95 %. Finally, the most substantial changes were observed in ATX-I and ALS. An increase of more than 415% was observed in ATX-I, and over 445 % in the case of ALS. Then, the changes in toxin levels caused by exposure to blue light were quantified. Fig. 46 C shows that the AOH, TeA, and ALS levels did not exhibit any significant change in response to exposure to blue light. In contrast, both AOH-S and ALN showed an increase of more than 100 %. The mycotoxin ALS showed an even greater increase of approximately 323 %. The most substantial increase was observed in ATX-I, with a nearly 630 % increase. Following up, the relative toxin concentrations after incubation in red light were assessed.

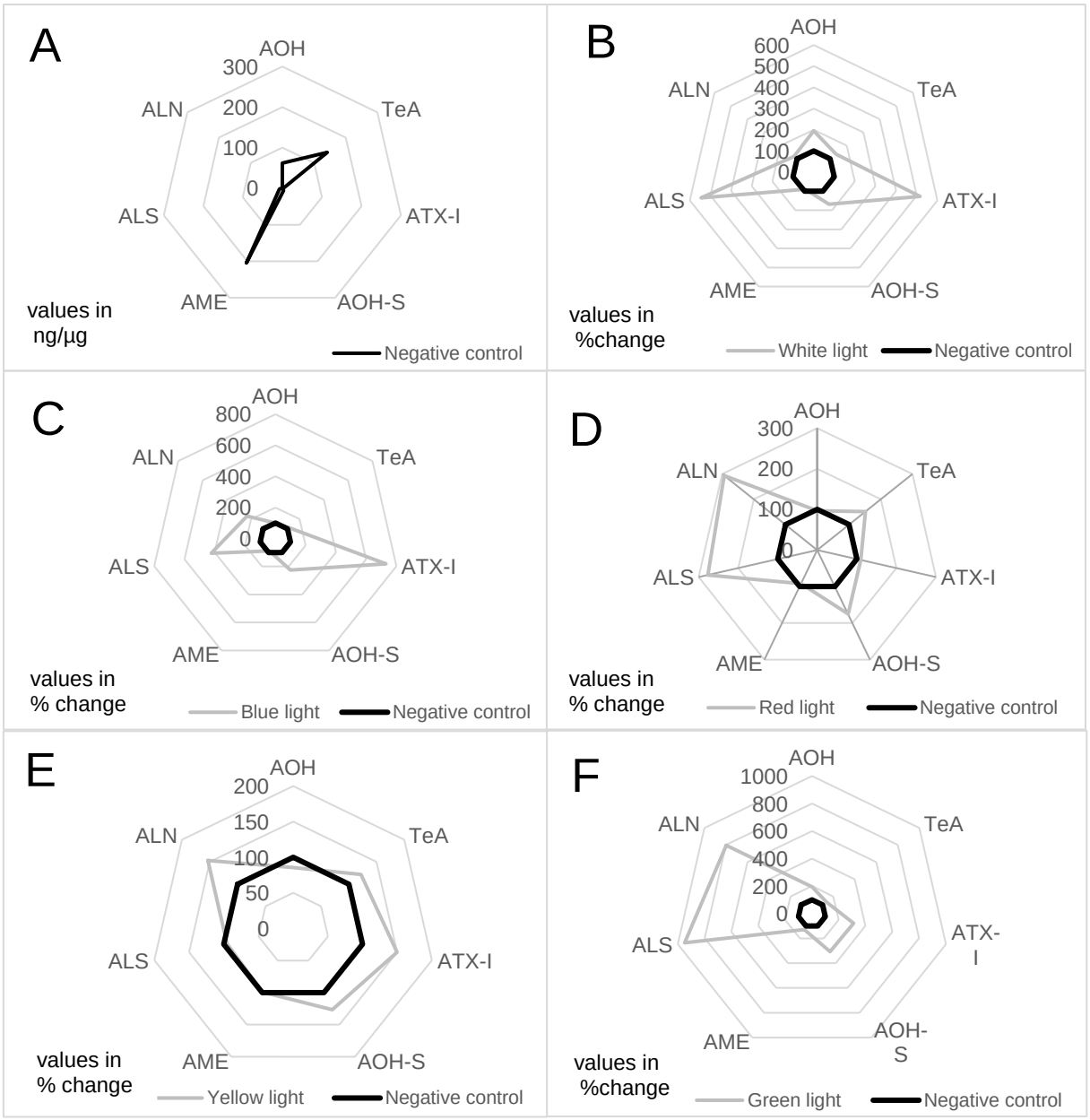

Figure 46: ***A****: Net diagram showing the mean amounts of the mycotoxins AOH, TeA, ATX-I, AOH-S, AME, ALS, and ALN measured in the strains APBR, APBO, APCY, APKA, APSA, and APSA2 after incubation in darkness.* ***B****: Net diagram showing the average relative change of the detected mycotoxins after incubation in white light compared to the negative control.* ***C:*** *Net diagram showing the average relative change of the detected mycotoxins after incubation in blue light compared to the negative control.* ***D****: Net diagram showing the average relative change of the detected mycotoxins after incubation in red light compared to the negative control.* ***E:*** *Net diagram showing the average relative change of the detected mycotoxins after incubation in yellow light compared to the negative control.* ***F:*** *Net diagram showing the average relative change of the detected mycotoxins after incubation in green light compared to the negative control.*

Fig. 46 D shows that AOH, ATX-I, and AME concentrations remained unaffected by red light exposure. Yet, TeA and AOH-S showed increases of over 50 %, while ALN and ALS exhibited even greater changes, of more than 175 %, after exposure to red light. Thereafter, the impact of yellow light on the toxin concentrations was evaluated. Fig. 46 E shows a minor decrease of approximately 15 % in AOH, with levels similar to those of the negative control in ALS and AME. TeA and AOH-S exhibited a similar increase of just over 20%, while the most significant change was observed in ATX-I and ALN, both of which showed a relative increase of approximately 50 %. Lastly, the effect of green light on toxin biosynthesis was investigated. Fig. 46 F shows that both TeA and AME experienced a slight increase of about 30 %, whereas ATX- and AOH-S experienced a significant induction of about 200 %. However, an even higher increase was observed for ALN, which was approximately 695 % higher than the negative control. Finally, ALS was the mycotoxin with the most substantial relative increase after exposure to green light, with a relative increase of approximately 848 %.

3.4.1 Non-light stress

After investigating the light impact of light, the influence of pH values higher or lower than the A. *alternata* incubation optimum was analyzed. Hence, Fig. 47 B shows how a lower pH affects the concentrations of the different *Alternaria* toxins. The most substantial decreases were observed in ALS and TeA, whose concentrations were reduced to approximately 20 % of the negative control. This was followed by AOH and ATX-I, which experienced a reduction to approximately 30 % of the negative control. Meanwhile, the most substantial decrease was observed in AOH-S, which was reduced by approximately 36 %. The only increase in concentration was observed in ALN, which increased by about 94 %. Following the lower pH,

the impact on mycotoxin synthesis after incubation at a higher pH value is evident in Fig. 47 B. The highest increase caused by the higher pH value is depicted in Fig. 47 C, which shows ALN concentrations 94% higher than the negative control.

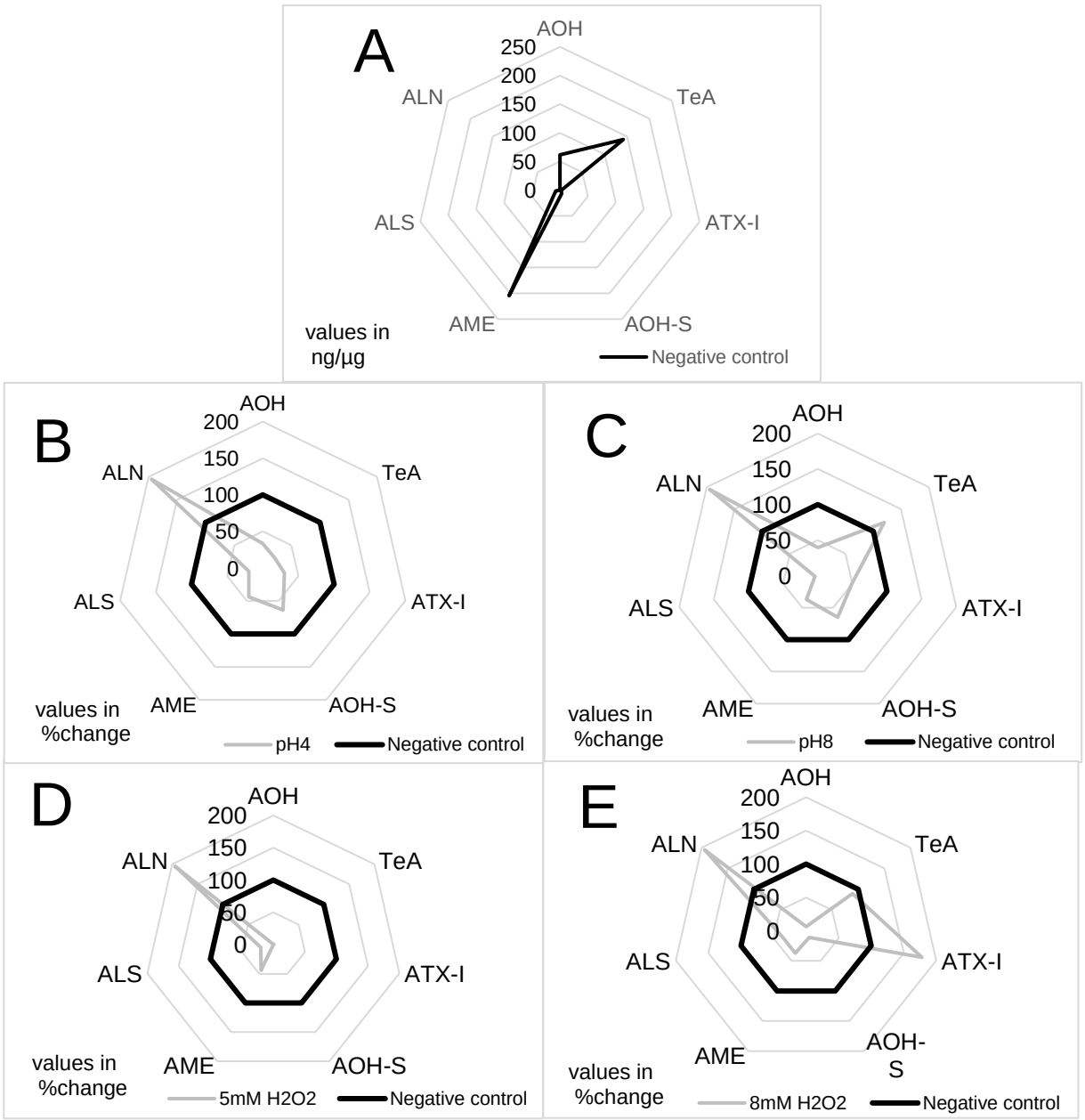

*Figure 47: **A**: Net diagram showing the mean amounts of the mycotoxins I AOH, TeA, ATX-I, AOH-S, AME, ALS, and ALN measured in the strains APBR, APBO, APCY, APKA, APSA, and APSA2 after incubation in darkness. **B**: Net diagram showing the average relative change of the detected mycotoxins after incubation at pH 4 compared to the negative control. **C**: Net diagram showing the average relative change of the detected mycotoxins after incubation at pH 8 compared to the negative control. **D**: Net diagram showing the average relative change of the detected mycotoxins after incubation in 5 mM H_2O_2 compared to the negative control. E: Net diagram showing the average relative change of the detected mycotoxins after incubation in 8 mM H_2O_2 compared to the negative control.*

Another increase in toxin quantities occurred in TeA, with a change of approximately 19 %. While AOH and TeA experienced a reduction to about 30 %, AME was reduced by only about 43 % compared to the negative control. The least substantial decrease, to approximately 63 %, was observed in AOH-S, whereas the most significant decrease was seen in ALS, which was decreased to 19 %. Afterwards, oxidative stress was investigated. First, as seen in Fig. 47 D, a minor oxidative stress was applied to the samples. This resulted in a substantial increase of approximately 94 % in ALN. In contrast, a decrease to 43 % in AME was observed, and ALS was reduced to 19 %. Meanwhile, AOH, TeA, ATX-I, and AOH-S were reduced to below 1 %. Following the oxidative stress caused by three mM H_2O_2, the oxidative stress was further intensified by using eight mM H_2O_2, as shown in Fig. 47 E. There, ATX-I increased by over 75 % compared to the negative control. Only TeA seemed to be barely affected by oxidative stress, with a reduction in concentration of about 11%. A more significant reduction followed this in ALS and AME, which were reduced to approximately 37 % of the negative control. The most substantial decreases were observed in AOH-S and AOH, which were reduced to 10 % and 6 %, respectively. Afterwards, the lower temperature of 16 °C, as shown in Fig. 48 B, was investigated. While all other toxins were reduced to below 35% of the negative control, TeA experienced an increase of about 60 %. At 33°C, as shown in Fig. 48 C, all toxin concentrations were lower than those of the negative control; however, the slightest decrease was observed in TeA, which was reduced to 87 %, and ATX-I, which was reduced to 75 %. These are followed by ALS and AOH-S, which were reduced to approximately 44 %. The AOH concentration was decreased to 15 % compared to the negative control. The two toxins that experienced the strongest reduction were AME and ALN, which were reduced to below 7 %. The final stress factor that was tested was low water activity. Adding 15 % glycerol to the samples resulted in a water activity of 0.9. Fig. 48 D shows that, apart from TeA, which

was not influenced by the low water activity, all other toxin concentrations were lowered. While ALS and ALN still possessed 60 % of the negative controls' toxin concentration, AOH-S was reduced to 25 %. Meanwhile, ATX-I was reduced to 14 %. AOH and AME were decreased to below 10 % of the negative control.

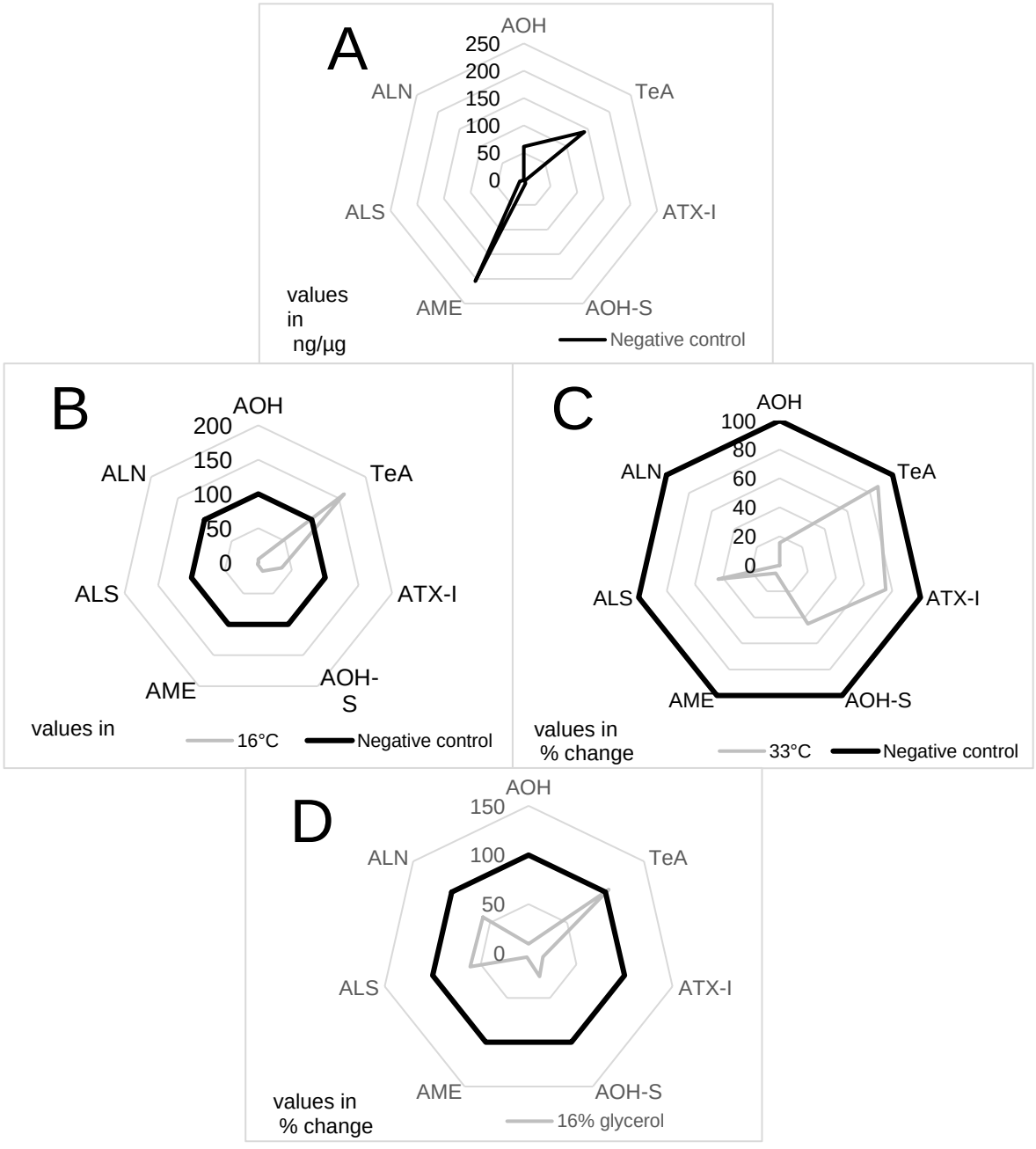

*Figure 48: **A**: Net diagram showing the mean amounts of the mycotoxins l AOH, TeA, ATX-I, AOH-S, AME, ALS, and ALN measured in the strains APBR, APBO, APCY, APKA, APSA, and APSA2 after incubation in darkness. **B**: Net diagram showing the average relative change of the detected mycotoxins after incubation at 16°C compared to the negative control. **C**: Net diagram showing the average relative change of the detected mycotoxins after incubation at 33°C compared to the negative control. **D:** Net diagram showing the average relative change of the detected mycotoxins after incubation at a water activity of 0.9 (16% glycerol) compared to the negative control.*

3.5 Alternariol sulfate

When *A. alternata* infects plants such as the tomato, mycotoxins synthesized by *A. alternata* are excreted into the plant to help with the infection. One of the defense mechanisms of plants against xenobiotics is the glycosylation or sulfation of those compounds, which makes them more water soluble and makes it possible for the plant to either store the detoxified conjugate in its cell wall or vesicle or even excrete it. Yet, it was found that even in the absence of a host plant, *A. alternata* synthesized a sulfated version of Alternariol that is called alternariol sulfate. In order to do so, the fungus needs a sulfotransferase. Yet, at this point in time, with the exception of PH-1 in Fusarium graminearum, no SULT has been identified within the phylum of ascomycota. Hence, in this work, we attempted to identify the sulfotransferase that is connected to the sulfation of AOH in order to find clues in the function of AOH-S.

3.5.1 Analysis of putative sulfotransferases

3.5.1.1 *Protein-Membrane prediction with TMHMM*

After finding potential candidates that are putative SULTs, the N-best prediction of TMHMM, a protein membrane prediction tool, was used in order to investigate to which of the two known groups (“membrane-bound” or “cytosolic”) the putative SULTs belong. This holds significance, since the second group is known to play a role in metabolic processes, making them more likely to be a valid target for our research (Weinshilboum & Otterness, 1994). The first putative SULT we tested was SULT1, which, as seen in Fig. 49, has about 230 amino acids outside the membrane and about 20 amino acids located within the membrane. Together, they suggested that SULT1 is a membrane-bound protein.

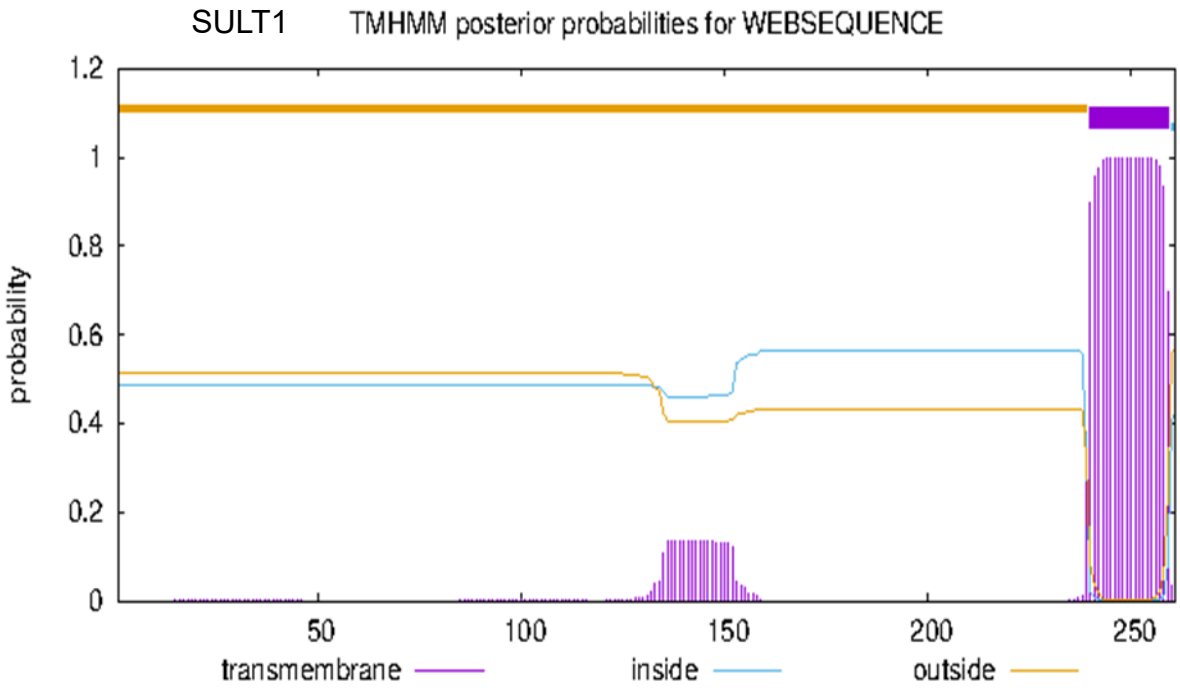

Figure 49: Diagram of TMHMM showing the probabilities of the positioning of the target protein relative to the cell membrane for SULT1

Thereafter, the same was tested with SULT2. Fig. 50 shows that the entire length of the protein is located outside the membrane, making SULT2 likely to be a member of the cytosolic SULTs.

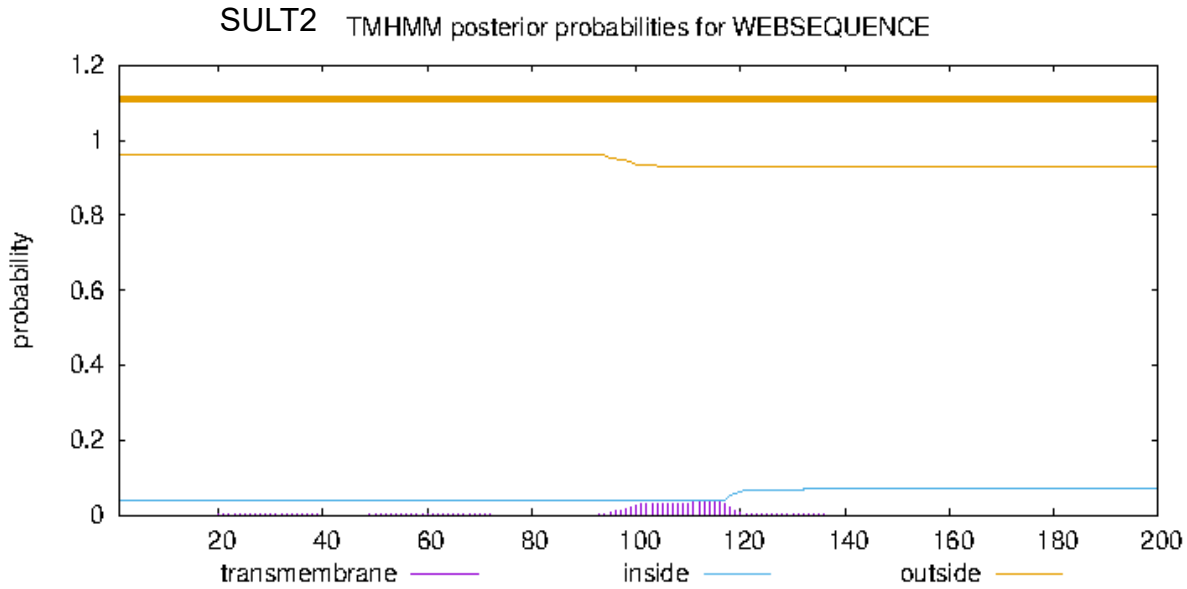

Figure 50: Diagram of TMHMM showing the probabilities of the positioning of the target protein relative to the cell membrane for SULT2

Next, as seen in Fig. 40, SULT3 was analyzed. In this case, about 250 Amino acids are located outside the membrane, while the following 25 amino acids are located within the membrane, and the last 25 amino acids are located inside the membrane. Hence, SULT3 is also likely to be a membrane-bound protein. Then, SULT5 was investigated, as shown in Fig. 51. SULT5 consists of 235 amino acids located outside the membrane and approximately 20 amino acids located within the membrane, making SULT5 likely to be a membrane-bound SULT. Following this, the analysis of SULT6 is presented in Fig. 52. In SULT5, the first 20 amino acids have the N-best prediction to be located inside the membrane. The next 20 amino acids were then shown to be within the membrane. From amino acid 40 to about 250, all amino acids are outside the membrane, followed by 25 transmembrane amino acids, and 24 amino acids inside the membrane. This results in SULT5 being presumably membrane-bound. Thereafter, SULT9 was investigated, as shown in Fig. 53. Lastly, as depicted in Fig. 54, SULT15 was analyzed. Similar to SULT2, SULT15 is predicted to be outside the membrane with its entire length and, thereby, likely a cytosolic SULT as well. Then, SULT5 was investigated, as shown in Fig. 51. SULT5 consists of 235 amino acids located outside the membrane and approximately 20 amino acids located within the membrane, making SULT5 likely to be a membrane-bound SULT. Following this, the analysis of SULT6 is presented in Fig. 52. In SULT5, the first 20 amino acids have the N-best prediction to be located inside the membrane. The next 20 amino acids were then shown to be within the membrane. From amino acid 40 to about 250, all amino acids are outside the membrane, followed by 25 transmembrane amino acids, and 24

amino acids inside the membrane. This results in SULT5 being presumably membrane-bound. Thereafter, SULT9 was investigated, as shown in Fig. 53. Lastly, as depicted in Fig. 54, SULT15 was analyzed. Similar to SULT2, SULT15 is predicted to be outside the membrane with its entire length and, thereby, likely a cytosolic SULT as well.

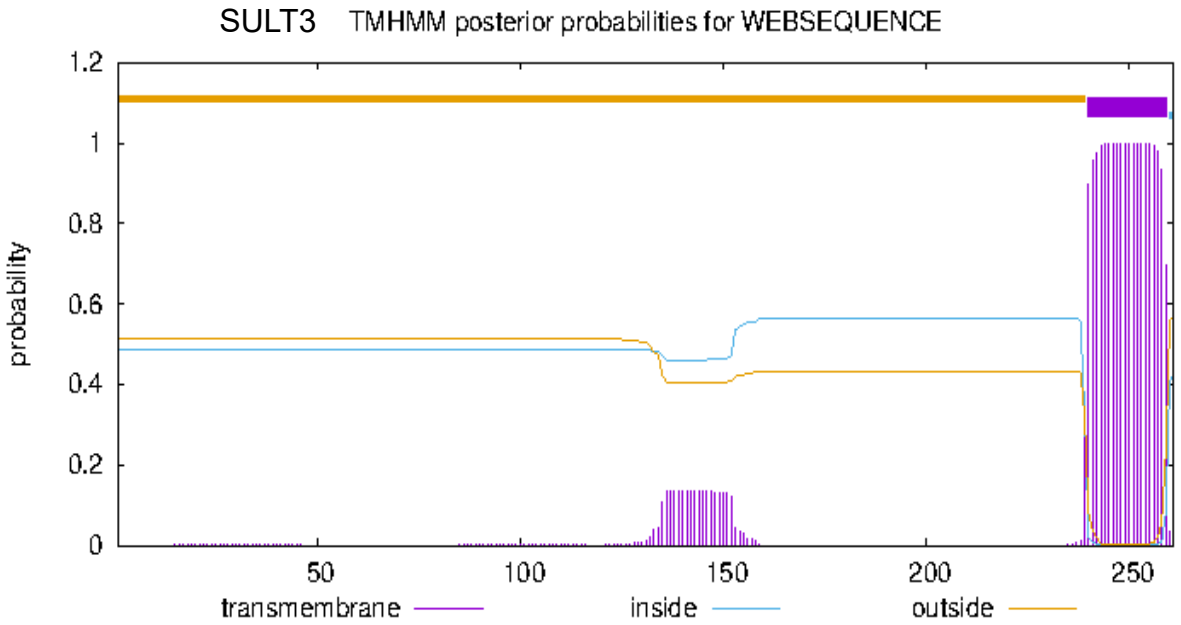

Figure 51: Diagram of TMHMM showing the probabilities of the positioning of the target protein relative to the cell membrane for SULT3

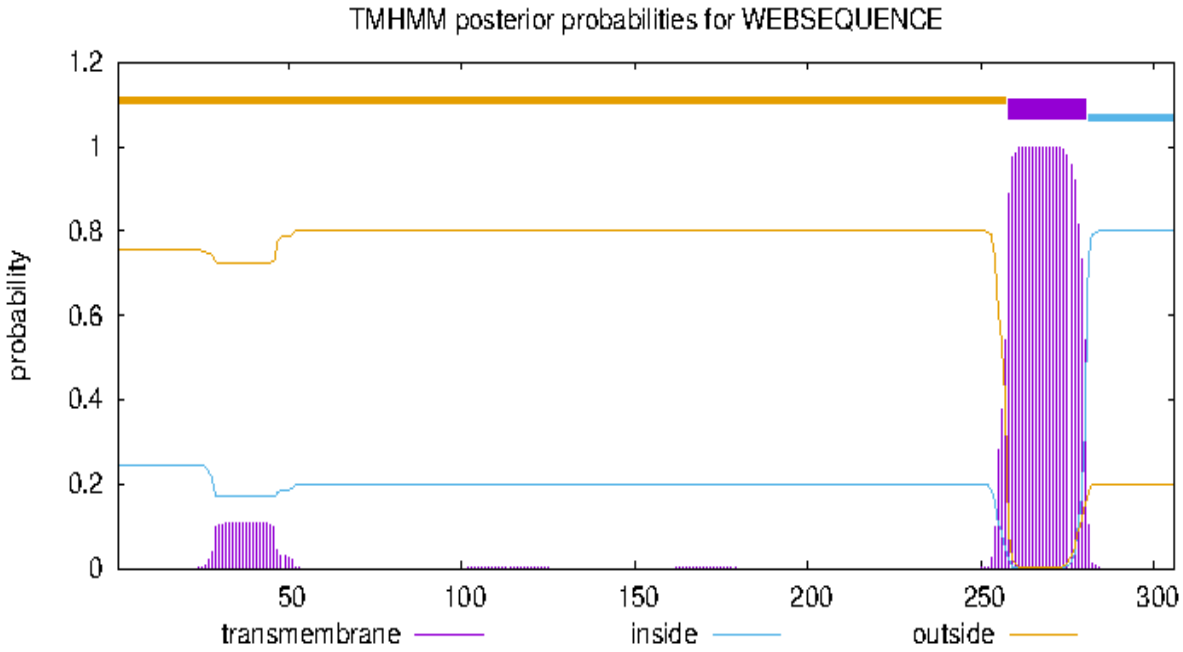

Figure 52: Diagram of TMHMM showing the probabilities of the positioning of the target protein relative to the cell membrane for SULT5

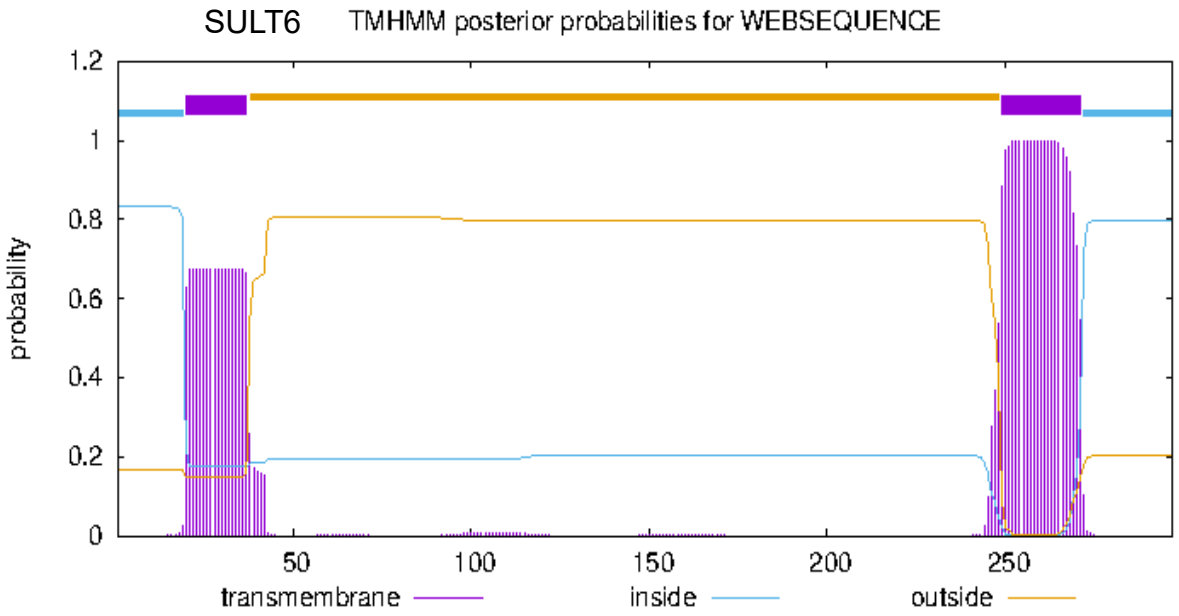

Figure 53: Diagram of TMHMM showing the probabilities of the positioning of the target protein relative to the cell membrane for SULT6

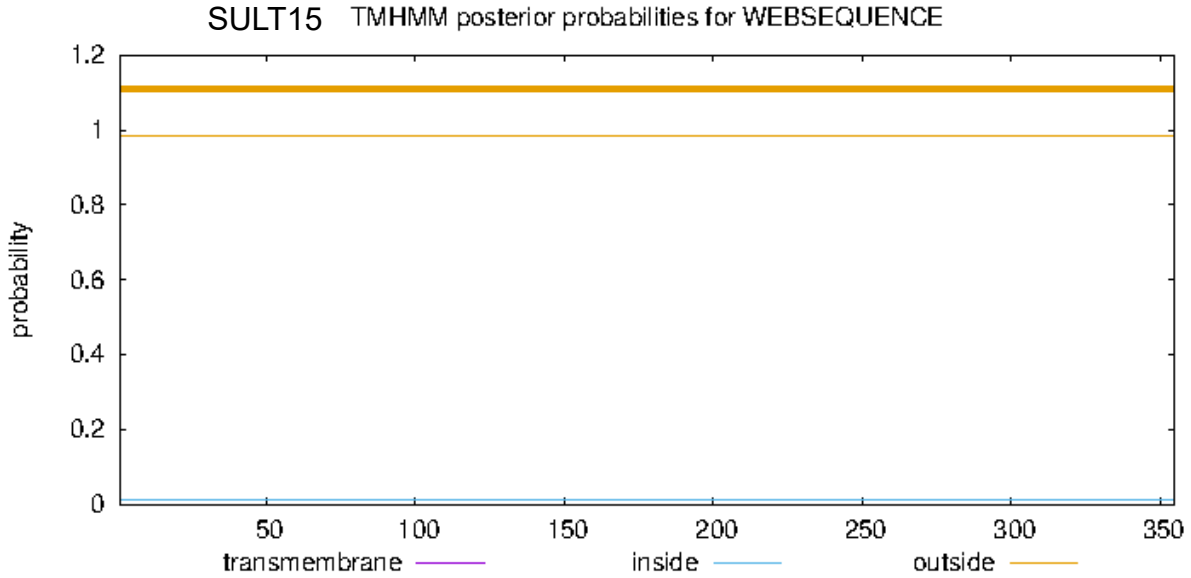

Figure 54: Diagram of TMHMM showing the probabilities of the positioning of the target protein relative to the cell membrane for SULT15

3.5.1.2 *Protein folding prediction with SWISS-MODEL expasy*

After analyzing the putative SULTs with TMHMM, the results were to be verified with SWISS-MODEL expasy. Models created with SWISS-MODEL expasy show a three-dimensional protein folding prediction, including likely membrane positioning. Fig. 55 shows the prediction of SULT1, SULT2, SULT3, and SULT5.

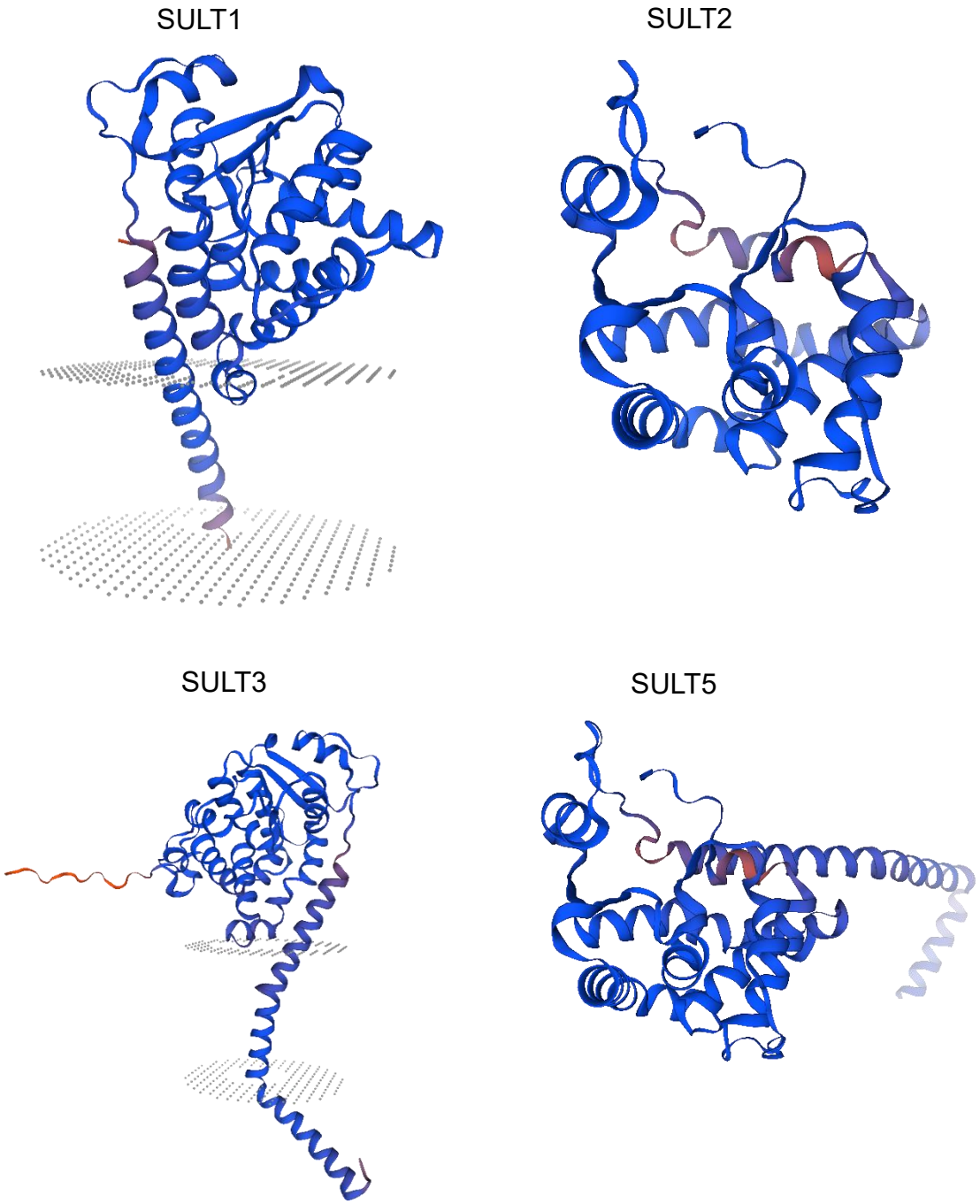

Figure 55: Protein folding prediction of SULT1, SULT2, SULT3 and SULT5 performed with SWISS-MODEL expasy

All models generated with SWISS-MODEL expasy that show transmembrane domains except for SULT5 also showed them in TMHMM, even though both SULT1 and SULT3 harbored two transmembrane domains in the SWISS-MODEL prediction. In contrast, they only showed a single one in TMHMM. Hence, SULT1 and SULT3 were assigned to the membrane-bound SULTs, whereas SULT2 belongs to the cytosolic SULTs, and SULT5 remains unclear. Furthermore, Fig. 56 shows the models of SULT6 and SULT15. SULT6 possesses two membrane domains, which align with the predictions of TMHMM. Lastly, SULT15 lacks transmembrane domains, which is also in accordance with the TMHMM prediction, thereby verifying both predictions mentioned above and leading to the conclusion that SULT6 belongs to the membrane-bound SULTs, while SULT15 belongs to the cytosolic SULTs. Templates used by SWISS-MODEL expasy are listed in Table 17.

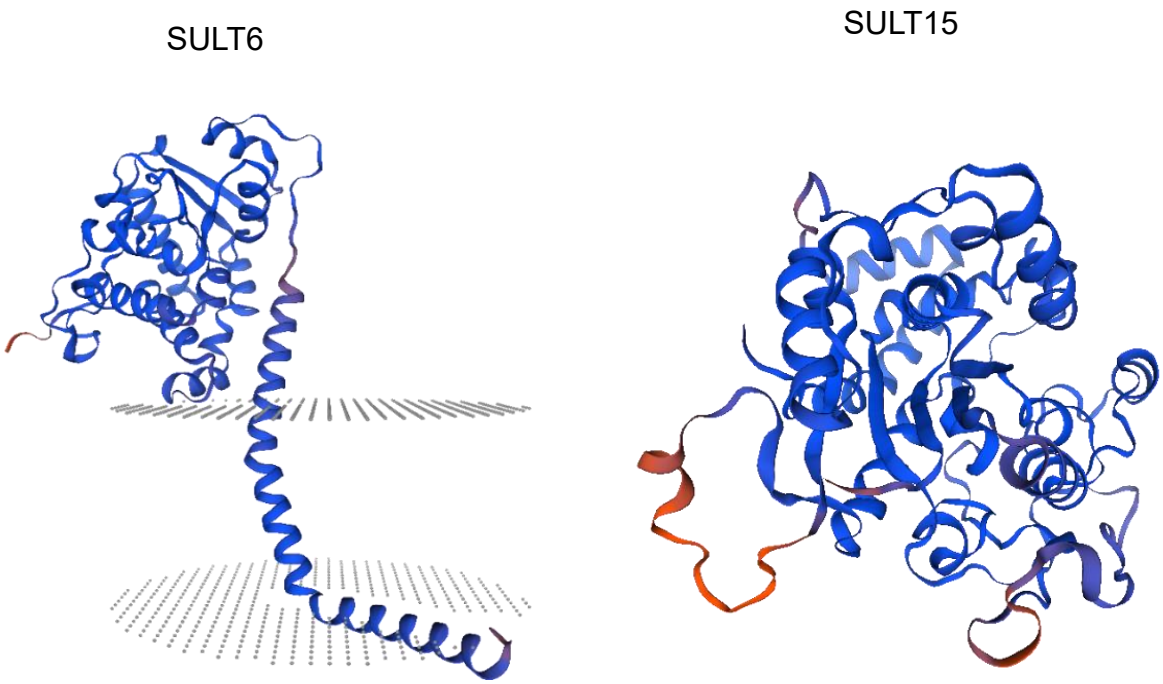

Figure 56: Protein folding prediction of SULT1, SULT2, SULT3 and SULT5 performed with SWISS-MODEL expasy

Table 17: Templates used by SWISS-MODEL expasy

Protein	Template	Seq identity
SULT1	A0A4Q4MER7.1. A NAD-dependent epimerase/dehydratase	100.00%
SULT2	A0A6A5SLG3.1. A NAD-dependent epimerase/dehydratase	81.88%
SULT3	W6ZDA4.1. A P-loop containing nucleoside triphosphate hydrolase protein	78.82
SULT6	A0A4Q4R8P3.1. A P-loop containing nucleoside triphosphate hydrolase protein	98.99%
SULT15	W6XL94.1. A Sulfotransferase domain-containing protein	88.17%

3.6 Sulfotransferase Knockout

3.6.1 Sulfotransferase gene expression

Since cytosolic SULTs are more likely to be involved in metabolic processes, we decided to use the CRISPR/Cas9 system to inactivate the corresponding genes for cytosolic SULTS2 and SULT15, as well as the membrane-bound SULT1, for a more comprehensive result.

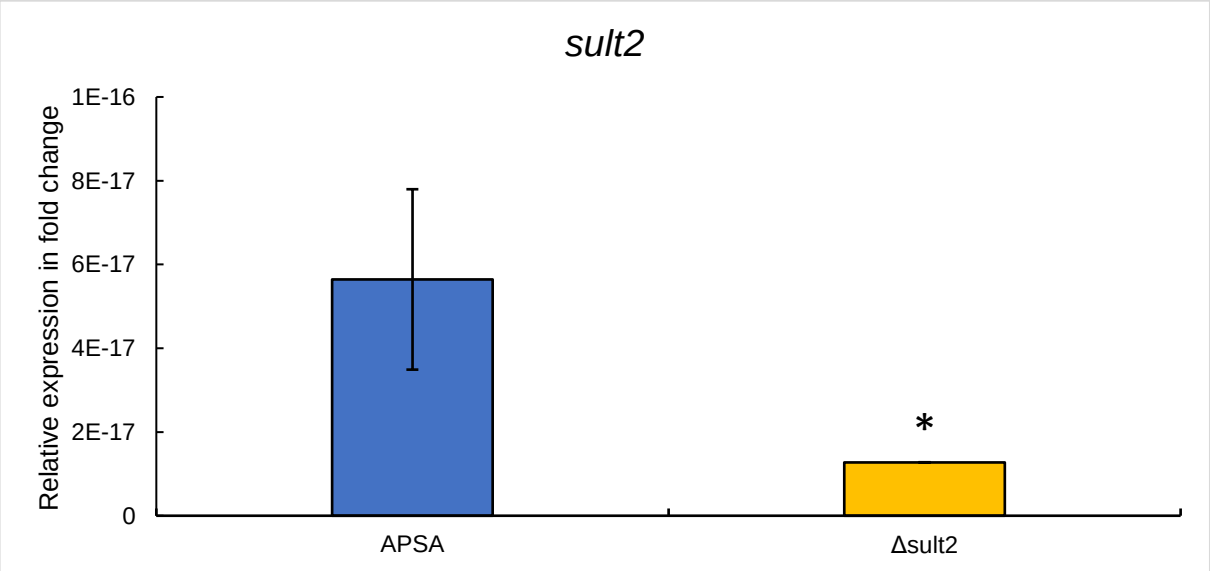

Figure 57: relative expression relative measured relative to the gene expression of the housekeeping gene beta Tubulin. The expression of sult2 in the wildtype APSA is shown in blue and the gene expression of sult2 in the sult2 knockout strain is shown in yellow (unpaired t-test :P= 00,5).*

Fig. 57 shows the gene relative gene expression of *sult2* in APSA and the *Δsult2* mutant. The expression of *sult2* in the *Δsult2* mutant was significantly lower than the expression in the wildtype APSA, indicating a successful gene knockout in the *Δsult2* mutant. Furthermore, the relative gene expression of *sult15* in APSA and the *Δsult15* mutant is shown in Fig. 58. Apparently, the expression of *sult15* in the *Δsult15* mutant was significantly lower than in the wildtype APSA, indicating a successful gene knockout in the *Δsult15* mutant as well. This suggests that both mutants exhibit the desired genotype and can therefore be used for follow-up experiments to determine the impact of the different knockouts on the metabolite. fingerprint.

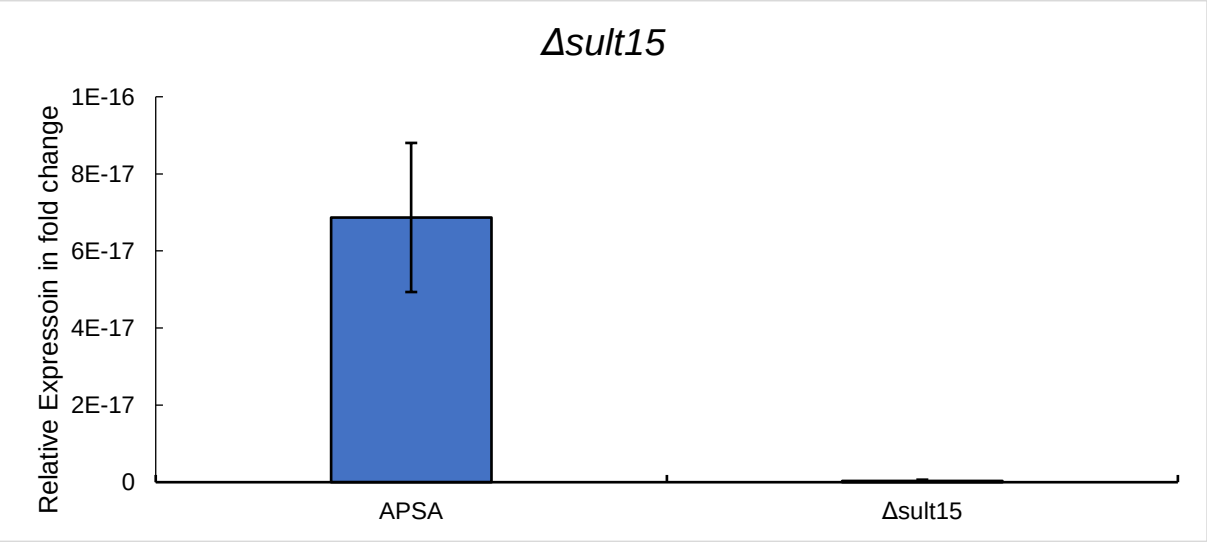

Figure 58: relative expression relative measured relative to the gene expression of the housekeeping gene beta Tubulin. The expression of sult2 in the wildtype APSA is shown in blue and the gene expression of sult2 in the sult2 knockout strain is shown in yellow.

3.6.1.1 *Sulfotransferase untargeted metabolite fingerprint*

After the successful knockout of *sult15* shown in Fig. 58, it was to be tested whether a mycotoxin extract of *Δsult2* still contains detectable amounts of AOH-S. Fig. 59 shows the mycotoxin extract of *Δsult2* and the AOH-S standard, irradiated at 254 nm and 366 nm. The *Δsult2* mutant clearly shows an AOH-S band at both wavelengths, meaning the knockout of the *sult2* gene did not result in an absence of AOH-S.

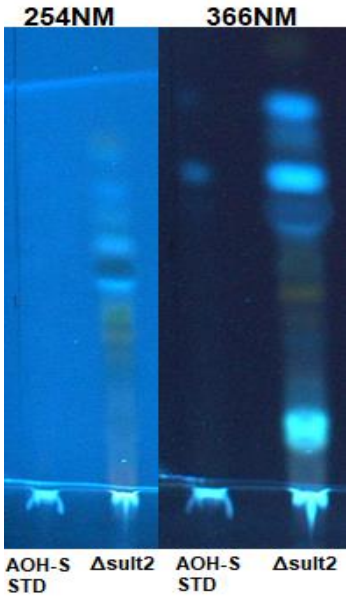

Figure 59: TLC plate with AOH-S standard and a mycotoxin extract of the Δsult2 mutant. Shown at 254 nm and 366 nm wavelengths.

Yet, a reduction is still possible, but has to be analyzed using HPLC quantification. Similar to what was done with the *Δsult2* mutant, a mycotoxin extract of the *Δsult15* mutant was applied along with the AOH-S standard shown in Fig. 60. Although less visible at a 254 nm wavelength, the 366 nm wavelength indicates that the *Δsult15* mutant still synthesized AOH-S. Hence, just as with the *Δsult2* mutant, an HPLC analysis was necessary to investigate how the genetic alteration affects the amount of AOH-S.

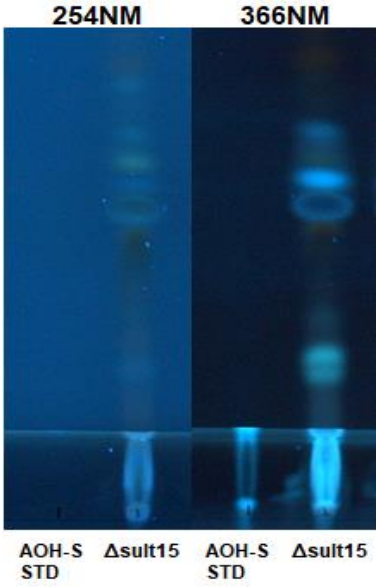

Figure 60: TLC plate with AOH-S standard and a mycotoxin extract of the Δsult2 mutant. Shown at 254 nm and 366 nm wavelengths.

3.6.1.2 *Sulfotransferase Targeted Metabolite Fingerprint*

After the untargeted approach using TLC was performed, we employed HPLC analysis to quantify relevant mycotoxins, including TeA, AOH-S, AOH, ATX-I, AME, ALN, and ALS, to investigate the impact of the knockout on the concentration of AOH-S and other AOH derivatives. Hence, Fig. 61 shows the measured concentrations of the aforementioned mycotoxins in the *Δsult1* mutant as well as the wild-type APSA. While AOH-S, AOH, ALN, and ALS showed no significant differences in concentrations between wildtype and mutant whatsoever, AME shows a very significant increase in AME in the mutant strain compared to the wildtype.

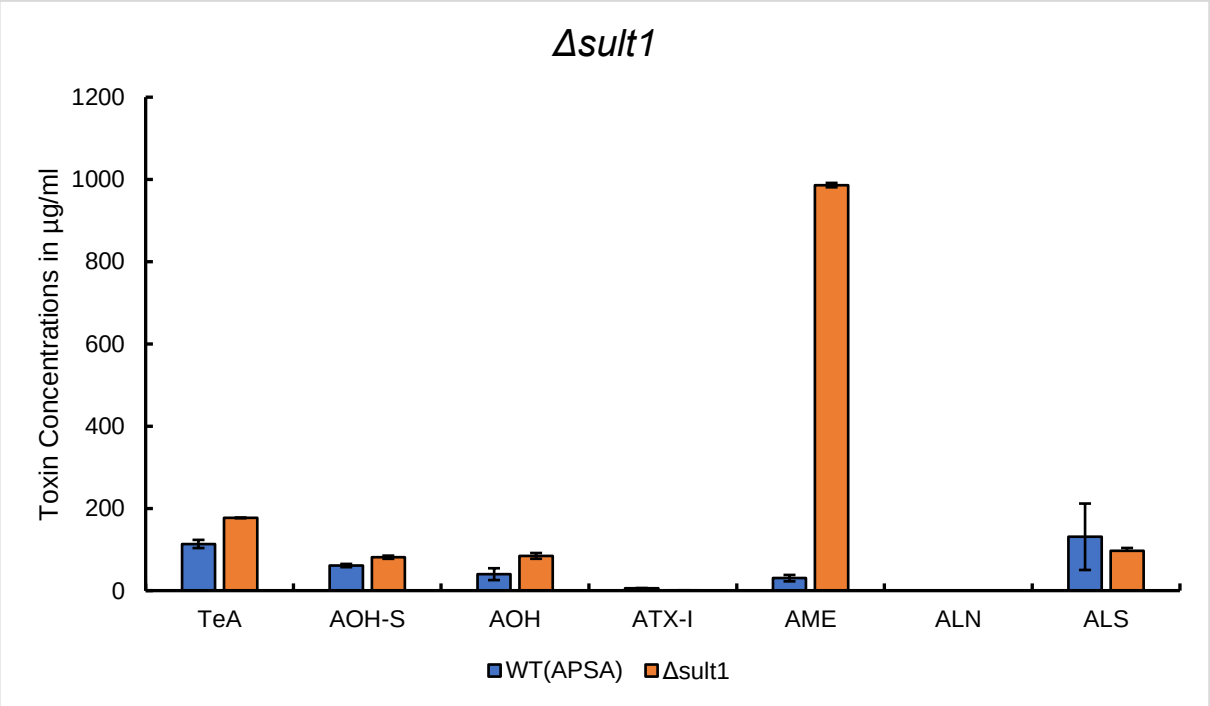

Figure 61: Quantitative analysis of wildtype strain APSA and mutant strain Δsult1. Quantification was performed using HPLC to measure TeA, AOH-S, AOH, ATX-I, AME, ALN and ALS.

Following up, the *Δsult2* mutant was compared to the wild-type APSA. Fig. 62 shows that there are no significant differences in the concentrations of AOH-S, AOH, and ALN between APSA and the *Δsult2* mutant. Whereas AME and ALS show substantial increases in concentrations of the mutant strain compared to the wild type. Finally, the same was done for the *Δsult15* mutant shown in the Fig. 63.

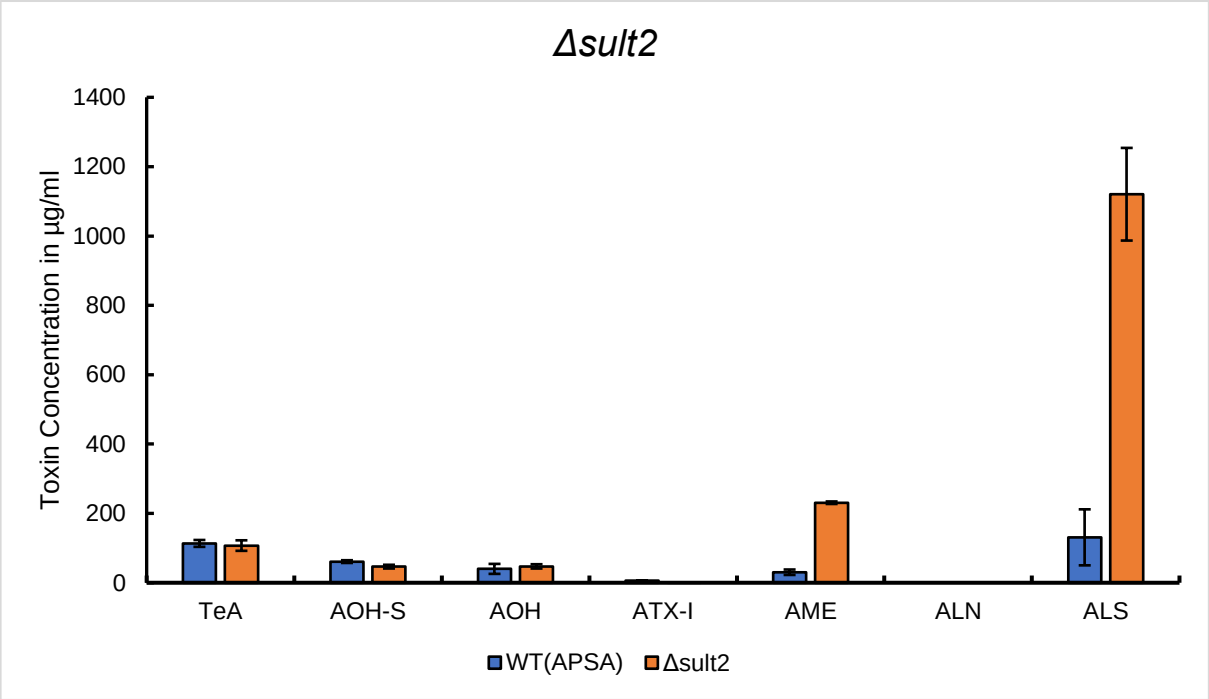

Figure 62: Quantitative analysis of wildtype strain APSA and mutant strain Δsult2. Quantification was performed using HPLC to measure TeA, AOH-S, AOH, ATX-I, AME, ALN and ALS.

Interestingly, the comparison of the wildtype to the *Δsult15* resulted in a pattern comparable to that of the comparison of the *Δsult2* mutant and the wildtype, which was defined by a significant change in concentrations limited to AME and ALS, while the other toxin concentrations remained unchanged.

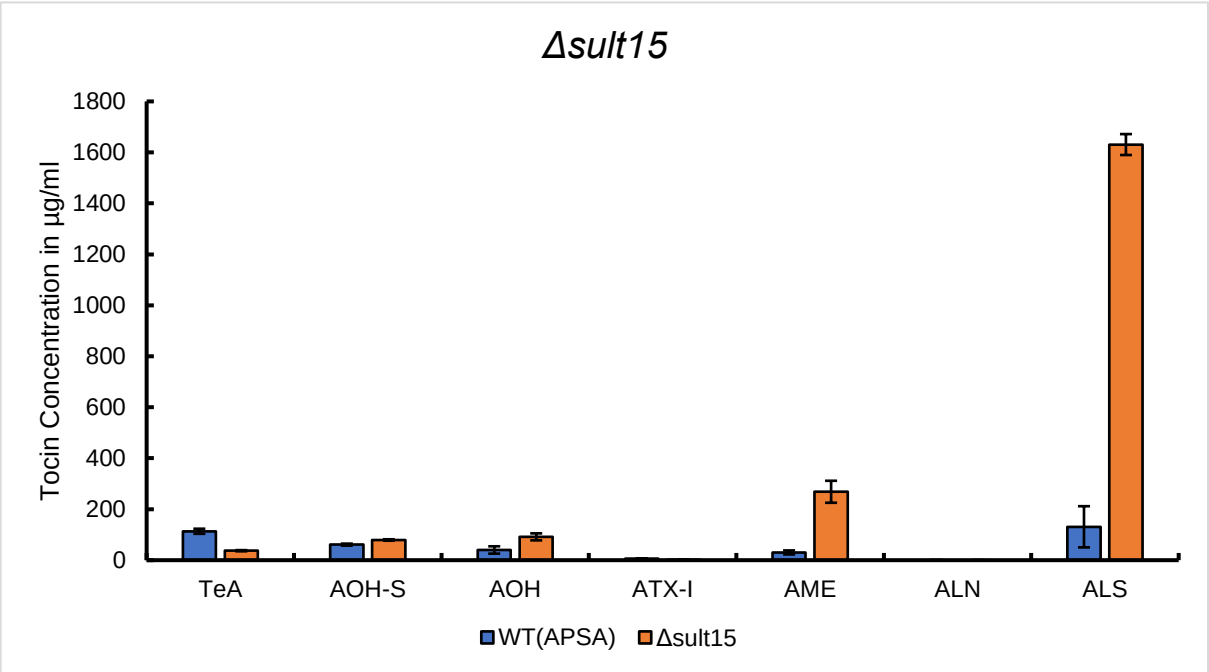

Figure 63: Quantitative analysis of wildtype strain APSA and mutant strain Δsult15. Quantification was performed using HPLC to measure TeA, AOH-S, AOH, ATX-I, AME, ALN and ALS.

3.7 Alternariol sulfate toxicity

Currently, the toxicity of AOH-S is unknown. Yet, since studies on the toxicity of AOH, we decided to compare their respective toxicity. This way, we were able to investigate how the derivatization of AOH affects its toxicity.

3.7.1 Comet-Assay

Since AOH is known for its mutagenic properties, at first, a comet assay was performed in order to test how much DNA damage is caused by AOH and how it compares to the damage caused by AOH-S. Eagle´s minimum essential medium with added 1 % DMSO was used as a negative control, while 30 µM hematine was used as a positive control. Fig. 64 clearly shows that with the concentrations tested, neither AOH nor AOH-S impacted the tail intensity in a significantly different manner than the negative control. Meaning, no DNA damage done by AOH or AOH-S was registered in this assay.

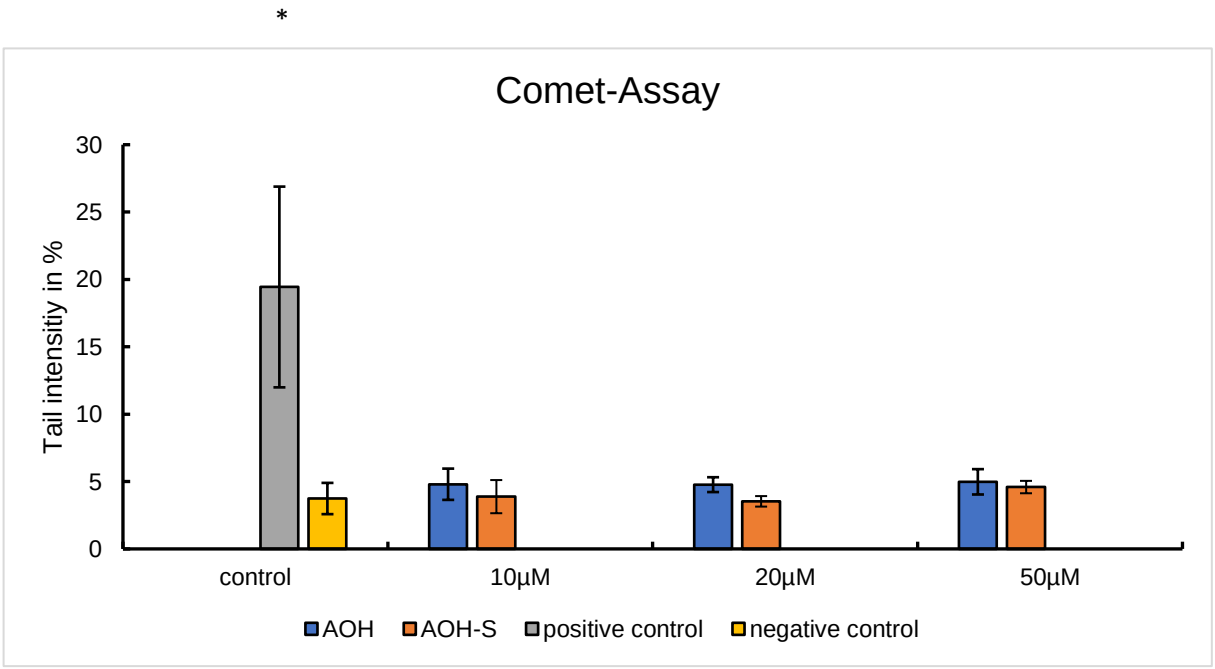

Figure 64: Results of a Comet Assay which was performed with CaCo2-cells after treatment with AOH and AOH-S. EMEM+1% DMSO was used as a negative control and hematine was used as a positive control

3.7.2 WST-Assay

Afterwards, a WST-Assay was performed to test how different concentrations of AOH and AOH-S influence the cell vitality of CaCo-2-cells, which can be seen in Fig. 65. Both AOH and AOH-S had no significant effect on the cell vitality in the concentrations between 0 and 20 µM. Yet, at 50 µM, both metabolites caused a significant decrease in cell vitality, which is reduced to approximately 84 % in AOH-S and about 43 % in AOH. From 50 µM to 200 µM, the influence of AOH-S and AOH on vitality was inverse, meaning that while the vitality decreased with higher AOH-S concentrations, it increased with higher AOH concentrations. At 200 µM, both metabolites had a similar effect on Caco-2 cell vitality, which was reduced to approximately 65 %. The concentrations between 300 µM and 500 µM do not exhibit any further significant changes in cell vitality. Hence, within the tested concentrations, AOH had the highest effect on cell vitality at 50 µM, while AOH-S had the highest impact at 200 µM, which is similar to that of AOH at this concentration.

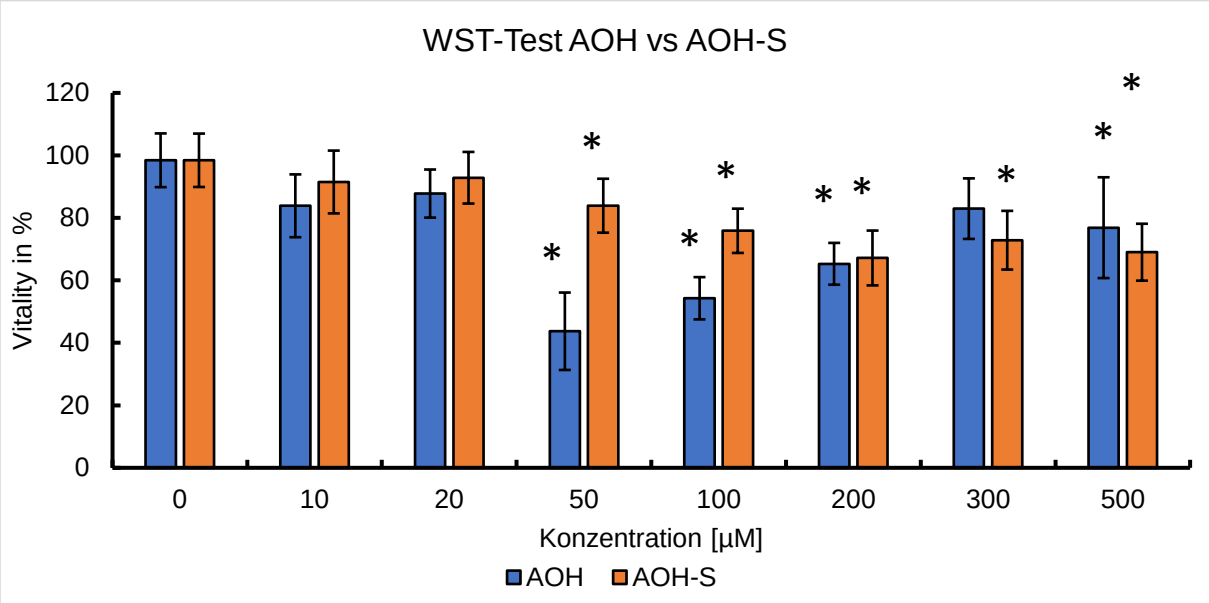

Figure 65: WST-Assay: Cell vitality of CaCO-2-Cells is measured after treatment with different concentrations of AOH and AOH-S. The negative control is EMEM+1 % DMSO

3.8 *Alternaria* apple virulence

Since apples are an important fruit in Germany and part of the *A. alternata* host range, we decided to investigate the virulence of *A. alternata* when infecting apples more thoroughly. Accordingly, we aimed to determine how deeply the fungus penetrates the fruit during infection, how deeply mycotoxins diffuse into the apple, and how these factors correlate with the lesion caused by the infection.

3.8.1 Fungal penetration into the apple

Intending to determine the penetration depth of the fungus after 14 days of inoculation, we used the Schmorl stain to color the fungus dark brown/black, while the parts of the apple in which no fungus is present were stained light blue. Fig. 66 shows two halves of the same apple, with the left half being Schmorl-stained, while the right half was left untreated and hence still showing the lesion.

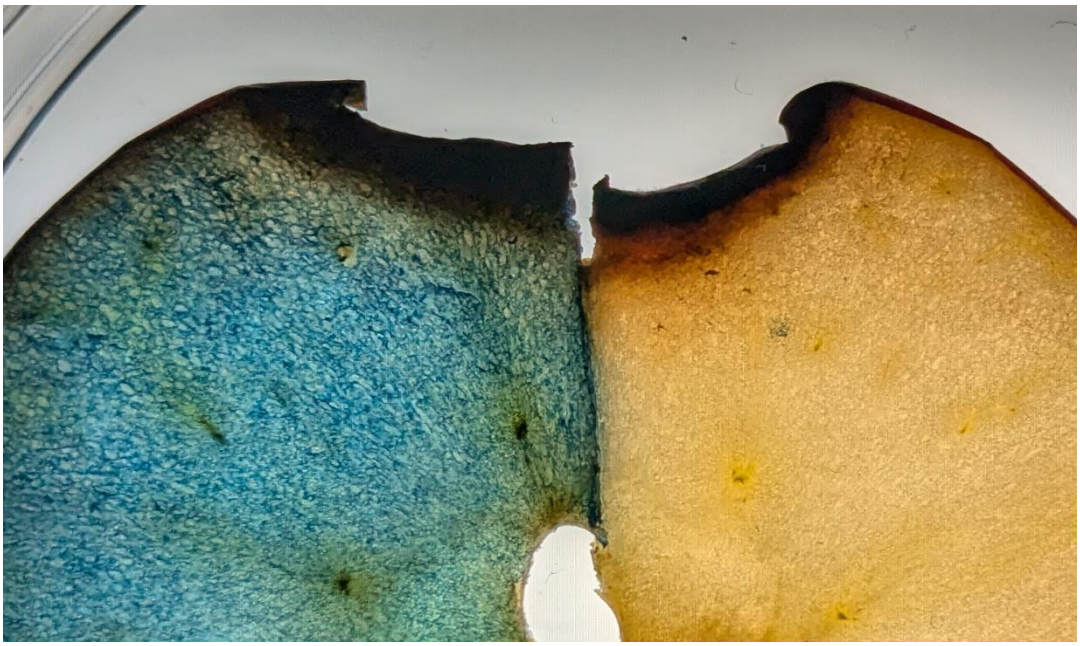

Figure 66: Picture of two halves of the same apple after being infected with A. alternata for 14 days. The apple was cut, and the left half was stained using the Schmorl melanin stain. The right half was not stained in order to allow for a direct comparison.

Here, it can be seen that the black-stained part of the left half of the apple ends well before the lesion of the right half of the apple, which led us to the conclusion that the lesion, which develops during the infection, envelops a larger area than the area infected by the fungus. For a more precise determination of the penetration depth of the fungus, with the help of GIMP, a pixel threshold was set, which displays any pixel that is brighter than the set threshold as white, thereby showing exactly up to which pixel the staining had colored the fungus dark and where it stopped. This can be seen in Fig. 67. After the threshold was set, a ruler, which was used as a scale in the original picture, was used as the reference for the measurement tool in GIMP, resulting in a measured penetration depth of 0.41cm.

Figure 67: Picture of the apple stained with Schmorl stain and set to black and white with the GIMP "threshold" function. On the right side there is a ruler which is used as a size reference.

3.8.2 Mycotoxin migration into the apple

Since toxins like AOH are known to be virulence factors, we aimed to investigate which toxins are synthesized when *A. alternata* infects an apple fruit and how deeply those toxins diffuse into the fruit. To do so, apple slices of 0,5 cm up to the depth of three cm were extracted, and AOH, AME, AOH-S, TeA, ATX-I-, ALN, and ALS were measured with HPLC. This way, the penetration depth and mycotoxin concentration were

determined. Fig. 68 shows that out of the seven mycotoxins we measured, only AOH and AME were found in quantifiable concentrations. Furthermore, it was apparent that the first apple slice, which covered the depth of the surface to 0,5cm, had the highest concentrations of both AME and AOH. Thereafter, the two slices making up the depth from 0,5 to 1,5 cm had similarly low amounts of AOH and AME. Despite the lower quantities of AME and AOH measured in the previous slices, the slice at a depth of 1.5-2 cm harbored higher concentrations of AME and AOH than those between 0.5 and 1.5 cm. The following slices, covering depths of 2-2.5 cm and 2.5-3 cm, did not contain measurable concentrations of the mycotoxins mentioned earlier.

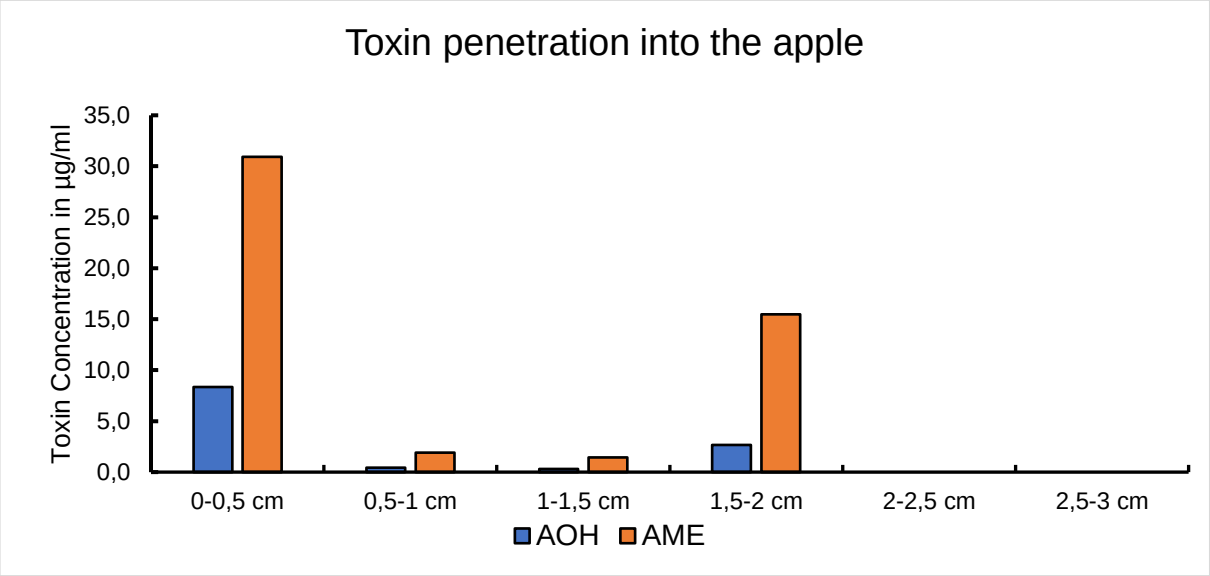

Figure 68: Toxin concentrations of 0,5cm thick apple slices extracted and measured using HPLC.

Hence, we ended up with a pattern in which in the part closest to the surface, there are the highest mycotoxin concentrations then the intermediate part with lower mycotoxin concentrations followed by the last part with elevated mycotoxin levels compared to the intermediate part but lower levels than the part closest to the surface and finally the part into which none of the mycotoxins we measured diffused.

4 Discussion

4.1 *Alternaria* identification

In this thesis, we compared the common methods of *Alternaria* identification by visualizing chemotype, phenotype, and genotype, with the intention of examining the validity of these methods (Emory G Simmons, 2007). To enhance the quality of our results, we included eight isolates from this study and commercially available strains obtained from the DSMZ. Thereby, we were able to compare the different methods beyond *Alternaria alternata* and include other species of the genus *Alternaria such as Alternaria citri, Alternaria brassicicola, Alternaria carotiincultae, and Alternaria tenuissima*. Furthermore, we investigated the concatenation of up to five well-established molecular markers to determine whether the use of more markers is actually advantageous compared to using fewer markers (Adeyemo & Schmidt-Heydt, 2024).

4.1.1 Comparison of morphology and chemotype

Spore morphology and chemotype of isolates are commonly used synergistically to identify *Alternaria* isolates. Since spore morphology is a factor used for identification, it might be expected that strains that share a common spore morphology are likely to have a more similar chemotype (Loganathan et al., 2016) (Zwickel et al., 2018). Yet, while most samples isolated in this study share a similar spore morphology, their chemotypes differ significantly. Striking examples are APSA2, which appears to produce hardly any detectable metabolites, as confirmed on different growth media (Fig. 20, Fig. 21) and repeated several times. Meanwhile, all other strains show at least three or four bands on the TLC plate. Moreover, half of the isolates, namely APKA, APSA, APPI, and APCY, produce the band likely to be ATX-II with a higher retention

time than AOH, which is not present in the other isolates. This non-correlation is even more apparent regarding the commercial strains used as a reference. Even though DSM12633, DSM62013, and DSM63360 share the same spore morphology, their chemotypes are tremendously different from one another. The differences between the chemotypes of strains with similar spore morphology are indistinguishable from those of strains possessing dissimilar morphologies. Additionally, when considering the colony phenotype, it can be observed that isolates with a specific phenotype do not have a chemotype more similar to those sharing the same phenotype. Therefore, our findings contradict research that attempts to link morphology or phenotypical factors, such as coloration, to valid approaches of identification (Andersen et al., 2005). It can be stated that chemotype and phenotype are highly dependent on environmental influences and hence exhibit a significant range of variation, as seen in Section 3.1.1, which makes them immensely challenging as singular factors of identification.

4.1.2 Comparison of morphology and molecular markers

As previously mentioned, the two strains that stand out in terms of spore shape are DSM62029 and DSM62008. Hence, we deemed it likely that those two strains might be the least closely related to all others. Yet, this idea was proven faulty when, regardless of the number of markers used, both DSM62029 and DSM62008 had the closest relation to strain DSM62013, which shares its morphology with the rest of the strains and isolates. Additionally, neither APSA, which stood out due to its darker spore color, nor DSM63360 stood out as the only strain lacking longitudinal septa; instead, they clustered with the other strains. Furthermore, DSM62008, DSM63360, APKA, and APCY, which have similarly longer conidia chains than the other strains, do not show any noticeable clustering. When colony phenotype is observed, we can see once again

that a similar phenotype is not an indicator of a closer genetic relation, which APPI and APKA strikingly showcase. Both possess the same phenotype as shown in Fig. 14, yet are very far from one another regarding genetic relation, which can be seen in Fig. 23. The morphological features do not correlate with the genetic clustering, which can potentially be attributed to the general issue that many morphological factors are very variable within *Alternaria* species (Emory G. Simmons, 2007; Emory G Simmons, 2007). Furthermore, factors such as the amount of conidia, germination, conidial length, and conidial width (Vakalounakis & Christias, 1985), as well as melanization, are strongly dependent on environmental factors, including light and the presence of antifungal drugs (Fernandes et al., 2016). When the conidia chains are observed in terms of similarity, the second-largest morphological subgroup detected comprises APKA, APCY, DSM 62008, and DSM 63360. Again, even though it could be expected that some form of clustering of those strains would occur in the phylogenetic trees, neither a single molecular marker nor any of the concatenations shown led to even a slight form of clustering. Those findings again vigorously challenge morphological factors as a means of independent identification.

4.1.3 Comparison of chemotype and molecular markers

Following the trend of the previous comparisons, the differences in chemotype and genetic relations are tremendous. The most constant, closely related groups, regardless of the number of molecular markers, exhibit greater differences in chemotype within their own groups than compared to other strains. An example of this is the group consisting of APKA, APSA, APBO, and APSA2. When incubated on PDA, APBO lacks the ATX-II band above AOH, whereas APKA and APSA both possess this band, with APSA2 hardly having any visible bands. The other group that shows a

comparable pattern of bands consists of DSM620008, DSM62013, and DSM62029. These strains appear to be closely related, but they exhibit a distinctly different chemotype. Similar to what was assessed regarding morphology as a means of identification, due to the chemotype being highly dependent on the environment (Adeyemo & Schmidt-Heydt, 2024; Häggblom & Unestam, 1979; Pose et al., 2010; Prendes et al., 2017), it alone is insufficient for independent identification.

4.1.4 Variation and comparability in chemotype and phenotype

One significant issue that arises in both chemotyping and phenotyping is the variation that depends on the growth medium (Ahmed et al., 2023; Kelman et al., 2020; Tymon et al., 2015). While examining phenotypes, it became apparent in Section 3.3.1 that changing the growth substrate can influence the colony phenotype of strains, leading to either a more similar phenotype or a greater difference in phenotype. This can potentially cause issues in terms of comparability, depending on the media used. Strains may appear to have a very similar phenotype on a particular medium, while possessing a very different one on another medium, leading to misidentifications (Tymon et al., 2015). Chemotyping, on the other hand, not only suffers from the issues of metabolite variation that can be seen in Fig. 19 and Fig. 20, but the issue of methodology is added, which can be seen in Fig. 21, in which the same method caused a smear due to Maillard products, which do not occur as disturbing factors when samples are incubated and extracted from PDA. Since the different types of media can also affect metabolite separation via TLC, as shown in Fig. 21, every medium tested would require a specific method, which would likely be detrimental to their comparability.

4.1.5 Number of molecular markers

When using molecular markers, it becomes pretty apparent that certain markers excel at distinguishing between specific genera and species, yet lack the ability to differentiate between others. This is particularly evident when only one marker is used, as shown in Fig. 22. Therefore, the concatenation of markers, which is regularly performed, makes a lot of sense since the more markers with different specificities are used, the better the final result (Kokaeva & Elansky, 2022; Sadeghi & Mirzaei, 2018; Stewart et al., 2014). Hence, we used ITS, GDP, RPB2, EndoPG, and Alta-1, all of which are well-established markers for *Alternaria spp.* identification (Andersen et al., 2009; Ntasiou et al., 2015; H. F. Sun et al., 2022; Zheng & Wu, 2013). Although subsets of the previously mentioned markers have been used in other studies, neither a comparison of the single markers nor the combination of all of them has been done before (Li et al., 2021; Wachowska et al., 2021; Yu et al., 2016). By comparing the phylogenetic trees of marker subsets with three and four markers, we realized that the specificity of the singular markers can significantly alter the positions of species in a phylogenetic tree by adding just one additional marker. This phenomenon is very conspicuous in the case of APCY which is marked red in all three phylogenetic trees shown in Fig. 23. Additionally, as mentioned before there is a significant variation in the ability of different makers to distinguish between markers which could lead to the use of insufficient markers in certain strains which is showcased in Fig. 22 in which it can be seen, how DSM62008, DSM62013 and DSM62029 do not cluster appropriately when the wrong markers are used. Hence, we think it is quite likely that, to this day, a significant number of *Alternaria spp* are assigned to the wrong species due to identification with insufficient molecular markers.

4.1.6 Spore morphology, phenotype, and chemotype as means of identification

The comparisons conducted in this thesis reveal that spore morphology, colony phenotype, and especially chemotyping exhibit high variation within the *A. alternata* species, comparable to the variations observed within the genus *Alternaria spp*. leading us to believe that, with given exceptions, identification attempts using only spore morphology, phenotype, or chemotype to a species level are very likely to be futile or very error-prone. Furthermore, this variation is intensified by external factors such as different media, temperatures, and light. Additionally, the issue of variation is also accompanied by potential methodological issues, as discussed in Section 4.1.4. Hence, we conclude that spore morphology, colony phenotype, and chemotype are less stable and reliable than molecular markers. Yet, in some cases, they can be potentially helpful in distinguishing between seemingly genetically identical strains as complementary factors to molecular markers for identification.

4.1.7 Improved usage of molecular markers in *A. alternata*

While examining the phylogenetic trees with varying numbers of markers, it becomes clear that, as expected, increasing the number of markers enhances the precision of possible species assignments within the genus *Alternaria*. Yet, stacking more and more markers is likely to disproportionately increase the amount of work in relation to the improvement in precision, especially when several strains are investigated simultaneously. Hence, we conclude that using five well-established markers is likely a sufficient compromise for a more precise identification of *Alternaria* spp. while requiring an appropriate amount of work.

4.2 Impact of external stress factors on mycotoxin concentrations in *A. alternata*

Food and feed have to pass a whole process chain before consumers or animals get to eat them; those products, along with the microbiome hosted by the product, are exposed to a variety of external stress factors. Those external factors can impact the product itself but also influence the behavior of the microbiome carried by the product (Klunklin & Savage, 2017; Meiramkulova et al., 2023) (Oliveira et al., 2013) (Park et al., 2023) (Spern et al., 2025). Hence, we investigated a number of external factors known to induce physiological stress in fungal cells, as previous studies (Schmidt-Heydt et al., 2008) have shown that such stress could trigger mycotoxin biosynthesis. We focused on their impact on mycotoxin synthesis in *A. alternata*. On one hand, we investigated different parts of the light spectrum (Suzuki, 2018) (Schmidt-Heydt et al., 2011) (L. Wang et al., 2022), and on the other hand, we investigated different non-light stress factors (Á. Medina et al., 2015) (Mannaa & Kim, 2017) (Paterson & Lima, 2011). We aim to be able to give recommendations on which stress factors are to be avoided due to their stimulating effect on mycotoxin synthesis and which are to be incurred because of their inhibiting effect on mycotoxin synthesis.

4.2.1 Blue light

Blue light is known for its effect on mycotoxin synthesis (Fanelli et al., 2012; Priesterjahn et al., 2020a; Schmidt-Heydt et al., 2011; Suzuki, 2018); however, conflicting results have been reported in the past. On the one hand, Häggblom and Unestam (1979) reported an inhibitory effect of blue light on AOH and AME, while on the other hand, Prüss et al. (2014) found blue light to have a stimulating impact on AOH, AME, and ATX-I. Contrasting both, we found that neither AOH nor AME are affected by blue light. Yet, we were able to confirm the stimulation of ATX-I and expand

those by the additional stimulation of AOH-S, ALN, and ALS synthesis. Furthermore, we were able to confirm Wang et al (2022) findings of TeA not being influenced by blue light.

4.2.2 Red light

Similar to blue light, red light is known to impact the secondary metabolism of fungi (Schmidt-Heydt et al., 2011). Yet, in contrast to the findings published in (Igbalajobi et al., 2019) which stated that red light only influences the AOH synthesis positively but seems to otherwise lead to a metabolite profile indistinguishable from the metabolite profile that develops when incubated in darkness, we determined that while AOH, AME, and ATX-I concentrations are in accordance with this statement, TeA, AOH-S, ALS, and ALN show increased concentrations and therefore contradict the publication above. Those behavioral discrepancies can be caused by factors such as light intensity, wavelength of radiation, and severity, as well as characteristics of adaptation mechanisms, such as melanin, which protects the organism from UV light (Casadevall et al., 2017). Additionally, we investigated these changes in several different strains, not just a single one, which would be more prone to irregularity.

4.2.3 Yellow light

Just as the other parts of the light spectrum, yellow light can influence the fungal metabolism (Fanelli et al., 2016). However, regarding the genus *Alternaria,* yellow light is only known to suppress lesion formation in *Alternaria tenuissima* (Rahman et al., 2003). However, there was no inhibition of any of the toxins we measured. While some toxins, such as AOH, ALS, and AME, remained at a similar concentration level compared to the negative control, others, including ALN and ATX-I, increased to significantly higher concentrations. This does not directly contradict the publication

mentioned above, but since mycotoxins such as AOH are known to be virulence factors for *A. alternata*, it would be expected that the mycotoxins causing lesion formation are significantly decreased in concentration. Although AOH is slightly reduced, the reduction is not significant and is therefore unlikely to impact the potential virulence significantly. This leads us to believe that yellow light would not reduce lesion formation in *A. alternata.*

4.2.4 Green light

Akin to the other wavelengths, green light can affect metabolites synthesized by fungi (Schmidt-Heydt et al., 2012). We mostly confirmed the findings of Igbalajobi et al. (2019), who state that green light induces most of the *Alternaria* toxins, including ATX-I, AOH-S, ALS, and ALN. However, in contrast to their TLC results, which suggest a lower amount of AOH, our HPLC measurements show a substantial 94% increase in AOH, which can again be attributed to our use of several strains simultaneously. Furthermore, to date, not much research has been devoted to the green light receptor, opsin, and its function in *A. alternata* (Igbalajobi et al., 2019; Panzer et al., 2019; Wang et al., 2018). Yet, since most mycotoxins are synthesized more abundantly when exposed to green light and are either virulence factors, like AOH, or derivatives of virulence factors, such as ALN, ALS, and AOH-S, green light is likely to have a function in regulating virulence factors (Wenderoth et al., 2019)

4.2.5 White light

As the culmination of the light spectrum and the representation of sunlight, white light holds significant importance. Furthermore, it also influences the metabolites synthesized by fungi (Fanelli et al., 2012). While Igbalajobi et al. (2019) claim that white light has no drastic impact on the metabolism of *A. alternata*, we agree with this

statement concerning TeA, AME, and ALN. Despite this, in contrast to the other results, we found several metabolites with increased concentrations, namely AOH (induced by 94 %), ATX-I (induced by 400 %), AOH-S (induced by 68 %), and ALS (induced by 445 %). Since white light consists of every wavelength of the visible light spectrum, and our results for the individual wavelengths mostly showed increases in mycotoxin concentrations (Sliney, 2016), it was to be expected that exposure to white light would lead to increases in concentration of a number of metabolites. Since it stems from the melanin biosynthesis pathway, an increase in this mycotoxin is likely linked to the need for protection against UV radiation, which is usually caused by sunlight (Gao et al., 2022).

4.2.6 pH-shift

Another external stress factor that impacts the fungal metabolism is the pH value of the fungal environment (Schmidt-Heydt et al., 2008). Regarding pH shifts in solid media research, data are unfortunately scarce. However, Brzonkalik et al. (2012) investigated different pH values in submerged cultures and then measured AOH, TeA, and AME concentrations. Their experiments showed that the highest concentrations of AOH and TeA were measured at a pH of 4,5 while the lowest amounts of the respective metabolites were measured at a pH of 7,5. Yet, our measurements show that pH values of 4 and 8 similarly inhibit the AOH synthesis. Additionally, our results show an inverse behavior in TeA. However, since Brzonkalik et al. (2012) used submerged cultures, and we used agar plates, the results are hardly comparable. As can be seen, they did not find any AME independent of their chosen pH values, whereas we found AME in all strains tested.

4.2.7 Oxidative stress

Oxidative stress is a major factor for most plant pathogenic fungi, particularly due to the plant's oxidative burst reaction, a defense mechanism against infections (Singh et al., 2021). Consequently, oxidative stress is known to play a role in controlling fungal metabolites (Geisen et al., 2018). Our results indicate that oxidative stress appears to inhibit the synthesis of most mycotoxins we measured, except for ATX-I, which is only induced by stronger oxidative stress, and ALN, which is induced by both weaker and stronger oxidative stress. Curiously, ATX-I is also strongly induced by blue light, which causes the fungus to experience oxidative Stress (Yu et al., 2021). Beyond its function as a UV protectant, melanin also has antioxidant properties, which are relevant for the fungus (Jacobson & Tinnell, 1993). Since ATX-I stems from the melanin biosynthesis pathway, it can be suggested that, similar to melanin, ATX-I might also have antioxidant properties, due to which a connection of its synthesis to oxidative stress could be explained. Meanwhile, Wenderoth et al. (2017) suggest that ATX-I is regulated via the polyketide synthetase A (pksA), like AOH and its derivatives; it would be expected for them to react at least somewhat similarly, which, apart from ALN, they do not.

4.2.8 High and low temperatures

Just like other environmental stress factors, the temperature of the environment can impact the metabolism of fungi (A. Medina et al., 2015). Oviedo et a. (2017) stated that compared to the incubation at 25 °C, both the incubation at lower temperatures, in this case, 18 °C, and higher temperatures, in this case, 30 °C, negatively impact the measured concentrations of AOH and AME synthesized by the analyzed strains. Our results align with their findings. Additionally, according to our results, ATX-I, AOH-S, ALS, and ALN react the same way. When considering TeA, Pose et al. (2010) showed

that the highest TeA concentration is achieved at 25 °C. In contrast, we measured a 60 % increase at 16 °C compared to 28 °C, contradicting their results.

4.2.9 Low water activity

Similar to other stress factors, the water activity can impact metabolite synthesis in fungi (Priesterjahn et al., 2020). Magan et al. (1984) stated that the synthesis of AOH, AME, and ALN is reduced by incubation in an environment with low water activity, a finding further confirmed by our measurements. Meanwhile, Prendes et al. (2017) share the same results concerning AOH and AME. Yet, according to them, TeA concentrations drastically decrease with lower water activity before a water activity of 0.9, which disagrees with our measured results. However, instead, we were able to confirm the results of Etcheverry et al. (1994), which showed that a water activity of 0.9 does not significantly change the measured amount of TeA. Those differences in data may be influenced by variations in strains and media used in these studies. Since a low water activity leads to osmotic stress in organisms due to the lack of viable water, the HOG-regulated stress response can be expected in *A. alternata* (Gustin Michael et al., 1998) (Lin & Chung, 2010). While it has been shown that HOG regulates several different mycotoxins (Zhang et al., 2010) (Ochiai et al., 2007), our findings align with Graf et al. (2012) who showed that the water activity influences AOH and AME since AOH is mainly needed in the presence of a host, which is indicated by higher water activity since it is an colonization factor.

4.2.10 Impact of light on the mycotoxin concentration in *A. alternata*

When measuring changes in toxin concentrations, we sought to identify wavelengths that particularly increase or decrease the concentrations, as described in Section 4.2. Interestingly, none of our measurements showed any significant decrease in toxin

concentrations. Instead, we observed either consistent levels of toxin concentrations or increases caused by irradiation with different wavelengths. Firstly, red light holds quite the significance because mornings and evenings have a light spectrum shifted towards it (Young, 1981). Our particular interest in observing the changes caused by red light ultimately focused on the increase in TeA. Even though its toxicity is controversially discussed (den Hollander et al., 2022) (Rychlik et al., 2016), its sheer abundance is cause for caution. In the case of green light, which emulates the light the fungus is exposed to when growing as an endophyte inside green plants, the strong increases in ATX-I and AOH are of major interest, as both are relevant factors for human health due to their cytotoxic and mutagenic properties (Burkhardt et al., 2011). Blue light, which is close enough to UV light to be a slight indicator of how the fungus might react to UV light, is still in the visible part of the light spectrum. Here, the perylenequinone ATX-I is induced by far the most, at about 600 %, coupled with its potent toxicity, providing a valid reason for caution (Zhu et al., 2022). Yet, interestingly, this induction can also be an indicator of the potential ATX-I holds, to be a light protectant and antioxidant, since a similar behavior was observed in *Penicillium spp* in which citrinin turned out to act as a light protectant and antioxidant (Heider et al., 2006) (Schmidt-Heydt et al., 2015). Finally, since the sun is a source of white light that exposes fruits and vegetables to stress, the inductions caused by white light are of special interest. Foremost, the approximate doubling of AOH as well as the near quadrupling of ATX-I both pose a serious health risk for human beings. In summary, since all parts of the light spectrum induce at least certain mycotoxins in *A. alternata*, avoiding light as much as possible might be a valid strategy to decrease mycotoxin contaminations in food or feed.

4.2.11 Impact of non-light stress on the mycotoxin concentration in *Alternaria alternata*

The non-light stress factors include oxidative stress, changes in pH, temperature outside the growth optimum of *A. alternata*, and low water activity. Those stress factors are less reliant in the wilderness, such as the change in pH value, which can depend on the host the fungus infects. Yet, in transport and storage circumstances, they are usually easier to control than light. Interestingly, those stress factors primarily decrease the concentrations of mycotoxins measured. It is worth noting that, although those stress factors primarily decreased the mycotoxin concentrations measured, a spike in at least one mycotoxin was detected in most cases. This issue can be observed when external factors, such as oxidative stress, pH values outside the optimum for *A. alternata*, and incubation temperatures about 10 °C below the optimum, are encountered. Observing the data, it becomes quite apparent that the only external factors that inhibit the toxin biosynthesis of most measured toxins without causing a spike in others are the incubation above the optimal growth temperature of *A. alternata,* as well as low water activity. This leads us to believe that these two stress factors can serve as grounds for designing effective strategies to reduce mycotoxin contamination in food or animal feed. Since temperature and water activity can be controlled relatively precisely, in a closed system, those two factors should be applied when produce is transported or stored. Beyond our findings, it would be of great interest to investigate how mycotoxin concentrations might be impacted by a combination of several external stress factors, such as heat and low water activity, similar to what Pose et al. (2010) did, but on a broader spectrum. This may be of particular interest if a specific external stress factor, such as light, which increases toxin concentrations, cannot be avoided. Here, determining which other stress factors most

efficiently antagonize the effect of light on toxin synthesis would be valuable information, especially in regions with limited resources.

4.3 Comparison of Peruvian and Chilean strains to German strains

4.3.1 Colony phenotype

When the colony phenotypes of the Peruvian/Chilean strains and the German strains are compared, some differences can be immediately determined. While the German strains vary between a dark brown and a significantly less dark green on PDA, the Peruvian and Chilean strains all exhibit a dark brown phenotype on PDA without exception. Since the color of the colony correlates with the melanization of the fungus, we postulate that the Chilean/Peruvian strains synthesize higher levels of melanin. So, if the function of melanin as a UV protectant is considered, elevated levels are necessary in an environment where the fungi are subject to higher UV stress. UV stress can be determined by the UV Index, which is influenced by a multitude of factors, including altitude and the thickness of the ozone layer (Fioletov et al., 2010). While Germany has an average altitude of about 250 m, Peru has an average altitude of about 1555 m, and Peru even about 1870 m making the altitude difference between Germany and Peru or Chile over 1300 m on average (Central-Intelligence-Agency, 2025), meaning that factoring in altitude alone, Peru and Chile are supposed to have a considerably higher UV index than Germany. Furthermore, it has been found that the ozone layer, which can also influence the UV Index by its thickness, is thinner near the equator. This means that Peru and northern Chile have a thinner ozone layer, providing another reason for a higher UV Index (Ball et al., 2018). Hence, we conclude that the stronger UV radiation prevalent in Peru and Chile is the factor the fungi must adapt to, forcing them to synthesize more melanin, resulting in an all-around darker phenotype.

4.3.2 Secondary metabolites

In accordance with Section 4.3.1, it is expected that the measured metabolites show elevated levels for those who are either derivatives of the melanin synthesis pathway, such as ATX and its derivatives, or those that are similar to melanin and can fulfill the role of a UV protectant (Gao et al., 2022). Regarding elevated levels of ATX-I, the targeted approach shown in Fig. 44 reveals that many of the Peruvian and Chilean strains exhibit the expected strongly elevated ATX-I concentrations compared to the German reference strain. Furthermore, if we look at Fig. 29 and Fig. 30, which show the untargeted approach, the bands that we suspect to be ATX-II are very prevalent, which also supports the suggestion of a stronger innate ability to synthesize ATX and derivatives due to the UV stress the strains are exposed to in their natural habitat. A similar effect of elevated ATX-I levels was observed when the German isolates were exposed to blue light, as shown in Fig. 46 C. Furthermore, the most abundant metabolite, particularly in the Peruvian and Chilean strains, is TeA, which is not known to be a UV protectant. Yet, TeA happens to be a tetrameric acid, and there are other tetrameric acids that are known to have photoprotective properties. This, along with its absorption peak being at 225 nm and 290 nm, might suggest TeA to at least play a role as a UV protectant to a certain extent (Li et al., 2020; Mercurio et al., 2015). The final metabolite that is standing out in the Peruvian and Chilean strains is AME. Until now, beyond its toxicity, little is known about the function AME provides for the fungus. Yet, since AME, as well as the other AOH derivatives, are polyphenols, which are known to absorb UV light, they may provide the fungus with additional UV protection in addition to their other functions (Del Valle et al., 2020; L. Li et al., 2023). Hence, testing the different *Alternaria* toxins for their photoprotective properties might help deepen the understanding of the functionality of the various metabolites. Especially regarding their different absorption peaks, it would be fascinating to see whether they

can protect the organism exceptionally well against specific wavelengths when combined.

4.4 Alternariol sulfate

4.4.1 *A. alternata* sulfotransferases

4.4.1.1 *Assignment of putative sulfotransferases*

SULTs are enzymes that are likely linked to the sulfation of AOH to AOH-S. Yet, until recently, no SULTs were identified in any member of the Ascomycota. This changed when Xie et al. (2020) discovered the SULT PH-1 in *Fusarium graminearum*. Hence, we employed a similar approach to identify potential SULT candidates in *A. alternata*. We identified the putative SULTs presented in Chapter 3.4 through several concatenated BLAST searches. Since cytosolic SULTs are known to play a role in the metabolism of compounds (Kurogi et al., 2024; Suiko et al., 2017), we hypothesized that this group would be the most likely to be involved in the sulfation of AOH. Accordingly, we focused our experiments primarily on the putative cytosolic SULTs, specifically SULT2 and SULT15.

4.4.1.2 *Functional analysis of putative sulfotransferase gene Knockouts*

After successfully deactivating the *sult1*, *sult2*, and *sult15* genes, respectively, we analyzed the changes in mycotoxin synthesis caused by these alterations. For *Δsult1*, Fig. 61 shows that the amounts of AOH-S synthesized in the deletion strain are not significantly different from those in the wild-type strain. Meanwhile, Fig. 62 shows the same behavior in *Δsult2*, and finally, Fig. 63 exhibits the same pattern in *Δsult15*. Since the protein folding models shown in Section 3.1.1 defined all three of our SULTs as

monomers, it is unlikely for them to be part of a heterodimer, concluding that even though a change in the mycotoxin synthesis was apparent, none of the putative SULTs found in this study are responsible for the sulfation of AOH to AOH-S. Yet, there is still the question of what function those proteins fulfill since a knockout of their encoding gene showed such a clear chemotype. Interestingly, a significant increase in the AME concentration was determined in all three mutant strains. Wenderoth et al. 2019 found that (OmtI)O-methyltransferase forms a methyl ether with the 9-hydroxy group of AOH, resulting in AME, which is then transformed into 4-OH-AME by the addition of a hydroxyl group at position 4, likely by SdrI. Additionally, in the Knockout strains of *sult2* and *sult15*, we detected massive amounts of ALS, which is another AOH derivative. Since the change in toxin concentrations in the mutants is limited to some of the AOH-derivatives, we suggest that the proteins encoded by the deleted genes directly or indirectly influence some of the tailoring enzymes that play a role in this pathway. In order to verify this, the gene expression of the tailoring enzymes involved in the AOH pathway, such as moxI, doxI, and sdrI, would have to be measured in the mutant strains. Furthermore, all AOH derivatives, like 4-OH-AME, which were not measured, ought to be measured since there might be a redistribution of intermediates if the activity of the tailoring enzymes is altered. Yet, since the putative SULTs we investigated were not the ones responsible for the sulfation of AOH, further research is necessary to identify those enzymes, as their functionality and expression may also provide clues to the function AOH-S fulfills for the fungus.

4.4.2 AOH-S toxicity

The Comet-assay shown in Fig. 64 shows that neither AOH nor its derivative AOH.-S possesses the ability to directly induce DNA damage, following what was shown in their work, stating that the mutagenic properties of AOH are very low and only gain significance through long-term exposure, which was also confirmed by (Miao et al., 2022). Although we are currently unable to verify that the long-term effect of AOH is similar in AOH-S, we strongly recommend testing AOH-S for mutagenicity through long-term exposure. Beyond mutagenicity, the WST-Assay performed in Section 3.6.2 shows that both AOH-S and AOH can significantly impact cell vitality. AOH has three free hydroxy groups, which are capable and known to interact with other proteins like the DNA topoisomerase-I or the Human serum albumin (hsa) (Fehr et al., 2009) (Fliszár-Nyúl et al., 2019). Compared to that, due to the sulfate group being bonded to the hydroxy group of AOH-S, one hydroxy group less is free for interaction. This might be why AOH-S has less impact on cell vitality at lower concentrations due to fewer interaction sites, which is comparable to a competitive inhibition of the toxin. Furthermore, this would explain why both mycotoxins end up having the same impact on cell vitality, as at a certain concentration, the sheer abundance of active moieties would compensate for the difference.

4.5 *A. Alternata* apple infection

When fungi infect their host plant, several things are known to happen. In the case of *A. alternata*, mycotoxins are synthesized, as some of them serve as virulence factors that help the fungus infect the host plant in the first place (Wenderoth et al., 2019). The synthesized toxins vary from host to host since some hosts, like the apple fruit, are capable of defending themselves against the fungus by means of oxidative stress

applied through an oxidative burst reaction (Meena & Samal, 2019) (Torres et al., 2003). Since the toxins synthesized by *A. alternata* are host-specific and chemically vary strongly, the question of which mycotoxins diffuse how deeply into the apple fruit arises (Coton & Dantigny, 2019). After a certain time, a lesion forms, which can be seen on the surface of the apple surrounding the infection site. Additionally, if the apple is cut, the lesion usually continues beyond the surface into the apple (Patriarca, 2019). The mentioned lesion forms after the fungus successfully infects the host plant and grows on the surface, as well as usually inside the host. This leads us to realize that three factors must be considered: the depth of fungus penetration, the depth of mycotoxin diffusion, and the size and depth of the lesion. In chapter 3.7, we show that the fungus penetrates the apple up to 0.41 cm, while the lesion reaches a depth of 0.577 cm, and the mycotoxins diffuse to a depth of approximately 2.0 cm. Interestingly, we expected the lesion to be a result of mycotoxin diffusion, since the measured mycotoxins AOH and AME both possess phytotoxic properties, leading to cell death and thereby causing the lesion in the apple fruit (H. Wang et al., 2022). Yet, we determined that AOH and AME diffuse beyond the lesion, making it likely that many fruits are contaminated with higher concentrations than previously determined, since some studies only investigated the parts of the fruit with visible lesions (Puntscher et al., 2020) (Hasan, 1996). In conclusion, it can be said that even though lesions are a helpful tool for consumers to identify fungal contaminations, any recommendations given to consumers must take into consideration that mycotoxin diffusion can extend far beyond the visible lesion, depending on the fruit and the diffusing mycotoxin.

4.6 Conclusion and outlook

In the course of this work, we were able to improve the current system of identification for *A. alternata* as well as shed light on the weaknesses and issues of other systems and subsystems. Yet, with the occurrence of new molecular markers in the future, it will be necessary time and time again to invoke novelties into the developed system in order to further improve it.

The generation of data concerning the mycotoxin synthesis in *A. alternata* and how it is affected by external stress factors enables us to provide data to help set up federal limits for *Alternaria* toxins. Furthermore, the knowledge on how to modify the toxin synthesis in *A. alternata* can be used to design strategies for mycotoxin prevention. On the basis of the data generated in this thesis, it would be interesting to investigate whether the efficiency of the mycotoxin reduction caused by certain external stress factors can be further increased by the combination with another stress factor. Furthermore, if research were to be conducted on whether mycotoxin-inducing stress factors, such as light, can be antagonized by other stress factors, the culmination of this research would have the potential to greatly reduce consumer intake of *Alternaria* toxins.

Even though the target SULT was not identified in this work, our data can, on one hand, serve as a basis to find new putative SULTs and, on the other hand, show that due to AOH-S having a similar toxic potential as AOH, more research should be conducted. Finally, since our experiments on the penetration depth and mycotoxin migration only focused on the apple fruit, extending those experiments to other fruits and vegetables, especially those that are more prone to microbial contamination due to weaker means of defense, could help further deepen the understanding of the infection process of *A. alternata* and how different distinct groups of hosts react.

5 References

Abdessemed, N., Kerroum, A., Bahet, Y. A., Talbi, N., & Zermane, N. (2019). First report of *Alternaria* leaf spot caused by *Alternaria alternata* (Fries.) Kiessler on *Sonchus oleraceus L. and Convolvulus arvensis L*. in Algeria. *J. Phytopathol.*, ***167***, 321-325.

Abe, K., & Gomi, K. (2007). Food products fermented by *Aspergillus oryzae*. In The *Aspergilli* (pp. 449-460). CRC Press.

Adeyemo, A., & Schmidt-Heydt, M. (2024). Expansion of the multi-locus gene alignment approach to improve identification of the fungal species *Alternaria alternata*. *Int. J. Food Microbiol.*, ***421***, 110746.

Ahmed, A. J. S., Aljarah, N. S., & Merzah, N. R. (2023). The Effect of Different Culture Media and Different Environmental Conditions on the *Alternaria solani* Sporulation. *IOP Conference Series: Earth and Environmental Science*, ***1262***, 032055.

Ahmed, E., Arshad, M., Khan, M. Z., Amjad, M. S., Sadaf, H. M., Riaz, I., Sabir, S., & Ahmad, N. (2017). Secondary metabolites and their multidimensional prospective in plant life. *J. Pharmacogn.*, ***6***, 205-214.

Ali, A., Shehzad, A., Khan, M. R., Shabbir, M. A., & Amjid, M. R. (2012). Yeast, its types and role in fermentation during the bread-making process. *Pak. J. Food Sci.*, ***22***, 171-179.

Andersen, B., Hansen, M. E., & Smedsgaard, J. (2005). Automated and Unbiased Image Analyses as Tools in Phenotypic Classification of Small-Spored *Alternaria spp. Phytopathol.*, ***95***, 1021-1029.

Andersen, B., Sørensen, J. L., Nielsen, K. F., van den Ende, B. G., & de Hoog, S. (2009). A polyphasic approach to the taxonomy of the *Alternaria infectoria* species–group. *Fungal Genet. Biol.*, ***46***, 642-656.

Angel, J., Authority, E. F. S., Arcella, D., Eskola, M., & Ruiz, G. (2016). Dietary exposure assessment to *Alternaria* toxins in the European population. *EFSA J.*, ***14***, e04654.

Antony, M., Gupta, K. P., Janardanan, K., & Mehrotra, N. (1991). Inhibition of mouse skin tumor promotion by tenuazonic acid. *Cancer lett.*, ***61***, 21-25.

Audenaert, K., Vanheule, A., Höfte, M., & Haesaert, G. (2013). Deoxynivalenol: a major player in the multifaceted response of *Fusarium* to its environment. *Toxins*, ***6***, 1-19.

Bai, X., Sheng, Y., Tang, Z., Pan, J., Wang, S., Tang, B., Zhou, T., Shi, L. e., & Zhang, H. (2023). Polyketides as secondary metabolites from the genus *Aspergillus*. *J. Fungi*, ***9***, 261.

Ball, W. T., Alsing, J., Mortlock, D. J., Staehelin, J., Haigh, J. D., Peter, T., Tummon, F., Stübi, R., Stenke, A., Anderson, J., Bourassa, A., Davis, S. M., Degenstein, D., Frith, S., Froidevaux, L., Roth, C., Sofieva, V., Wang, R., Wild, J.,…Rozanov, E. V. (2018). Evidence for a continuous decline in lower stratospheric ozone offsetting ozone layer recovery. *Atmos. Chem. Phys.*, ***18***, 1379-1394.

Balsalobre, L., Blanco, A., & Alarcón, T. (2019). Beta-Lactams. In *Antibiotic Drug Resistance* (pp. 57-72).

Bautista-Baños, S., Sivakumar, D., Bello-Pérez, A., Villanueva-Arce, R., & Hernández-López, M. (2013). A review of the management alternatives for controlling fungi on papaya fruit during the postharvest supply chain. *Crop Prot.*, ***49***, 8-20.

Berthiller, F., Crews, C., Dall'Asta, C., Saeger, S. D., Haesaert, G., Karlovsky, P., Oswald, I. P., Seefelder, W., Speijers, G., & Stroka, J. (2013). Masked mycotoxins: A review. *Mol. Nutr. Food Res.*, ***57***, 165-186.

Blackwell, M. (2011). The Fungi: 1, 2, 3… 5.1 million species? *Am. J. Bot.*, ***98***, 426-438.

Bonerba, E., Ceci, E., Conte, R., & Tantillo, G. (2010). Survey of the presence of patulin in fruit juices. *Food Addit. Contam.*, ***3***, 114-119.

Bottin, J. H., Swann, J. R., Cropp, E., Chambers, E. S., Ford, H. E., Ghatei, M. A., & Frost, G. S. (2016). Mycoprotein reduces energy intake and postprandial insulin release without altering glucagon-like peptide-1 and peptide tyrosine-tyrosine concentrations in healthy overweight and obese adults: a randomised-controlled trial. *Br. J. Nutr.*, ***116***, 360-374.

Bräse, S., Encinas, A., Keck, J., & Nising, C. F. (2009). Chemistry and Biology of Mycotoxins and Related Fungal Metabolites. *Chem. Rev.*, ***109***, 3903-3990.

Bräse, S., Gläser, F., Kramer, C., Lindner, S., Linsenmeiser, A. M., Masters, K.-S.,, & Meister, A. C., Ruff, B. M. & Zhong, S. (2013). *The chemistry of mycotoxins, pp. 1–2, 1st edn*. Springer.I

Bullerman, L. B., & Bianchini, A. (2007). Stability of mycotoxins during food processing. *Int. J. Food Microbiol.*, ***119***, 140-146.

Burkhardt, B., Wittenauer, J., Pfeiffer, E., Schauer, U. M., & Metzler, M. (2011). Oxidative metabolism of the mycotoxins alternariol and alternariol-9-methyl ether in precision-cut rat liver slices in vitro. *Mol. Nutr. Food Res.*, ***55***, 1079-1086.

Caldwell, R. W., Tuite, J., Stob, M., & Baldwin, R. (1970). Zearalenone production by *Fusarium* species. *Appl. Microbiol.*, ***20***, 31-34.

Carvalho, C., Santos, R. X., Cardoso, S., Correia, S., Oliveira, P. J., Santos, M. S., & Moreira, P. I. (2009). Doxorubicin: the good, the bad and the ugly effect. *Curr. Med. Chem.*, ***16***, 3267-3285.

Casadevall, A., Cordero Radames, J. B., Bryan, R., Nosanchuk, J., & Dadachova, E. (2017). Melanin, Radiation, and Energy Transduction in Fungi. *Microbiol. Spectr.*, ***5***, 10.1128/microbiolspec.funk-0037-2016.

Cendoya, E., Chiotta, M. L., Zachetti, V., Chulze, S. N., & Ramirez, M. L. (2018). Fumonisins and fumonisin-producing *Fusarium* occurrence in wheat and wheat by products: A review. *J. Cereal Sci.*, ***80***, 158-166.

Central-Intelligence-Agency. (2025). *filed Listing-Elevation*. Retrieved 12.05.2025 from https://www.cia.gov/the-world-factbook/field/elevation/

Chain, E. P. o. C. i. t. F. (2011). Scientific Opinion on the risks for animal and public health related to the presence of *Alternaria* toxins in feed and food. *EFSA J.*, ***9***, 2407.

Chen, S., Yin, C., Dai, X., Qiang, S., & Xu, X. (2008). Action of tenuazonic acid, a natural phytotoxin, on photosystem II of spinach. *Environ. Exp. Bot.*, ***62***, 279-289.

Chroumpi, T., Mäkelä, M. R., & de Vries, R. P. (2020). Engineering of primary carbon metabolism in filamentous fungi. *Biotechnol. Adv.*, ***43***, 107551.

Coton, M., & Dantigny, P. (2019). Mycotoxin migration in moldy foods. *Curr. Opin. Food Sci.*, ***29***, 88-93.

Crudo, F., Partsch, V., Braga, D., Blažević, R., Rollinger, J. M., Varga, E., & Marko, D. (2025). Discovery of the *Alternaria* mycotoxins alterperylenol and altertoxin I as novel immunosuppressive and antiestrogenic compounds in vitro. *Arch. Toxicol.*, ***99***, 407-421.

Dall'Asta, C., Cirlini, M., & Falavigna, C. (2014). Chapter Three - Mycotoxins from *Alternaria*: Toxicological Implications. In J. C. Fishbein & J. M. Heilman (Eds.), *Adv. Mol. Toxicol.* (**Vol.** 8, pp. 107-121). Elsevier.

Dawlal, P., Barros, E., & Marais, G. J. (2012). Evaluation of maize cultivars for their susceptibility towards mycotoxigenic fungi under storage conditions. *J. Stored Prod. Res.*, ***48***, 114-119.

de Reu, J. C., Marcel ten Wolde, R., de Groot, J., Nout, M. R., Rombouts, F. M., & Gruppen, H. (1995). Protein hydrolysis during soybean tempe fermentation with *Rhizopus oligosporus*. *J. Agric. Food Chem.*, ***43***, 2235-2239.

Del Valle, J. C., Buide, M. L., Whittall, J. B., Valladares, F., & Narbona, E. (2020). UV radiation increases phenolic compound protection but decreases reproduction in *Silene littorea*. *PLoS One*, ***15***, e0231611.

den Hollander, D., Holvoet, C., Demeyere, K., De Zutter, N., Audenaert, K., Meyer, E., & Croubels, S. (2022). Cytotoxic effects of alternariol, alternariol monomethyl-ether, and tenuazonic acid and their relevant combined mixtures on human enterocytes and hepatocytes. *Front. Microbiol.*, ***Volume 13 - 2022***, 849243.

Doyle, M. P., Applebaum, R. S., Brackett, R., & Marth, E. (1982). Physical, chemical and biological degradation of mycotoxins in foods and agricultural commodities. *J. Food Prot.* , ***45***, 964-971.

Dunlop, M. V., Kilroe, S. P., Bowtell, J. L., Finnigan, T. J., Salmon, D. L., & Wall, B. T. (2017). Mycoprotein represents a bioavailable and insulinotropic non-animal-derived dietary protein source: a dose–response study. *Br. J. Nutr.*, ***118***, 673-685.

Eisenman, H. C., & Casadevall, A. (2012). Synthesis and assembly of fungal melanin. *Appl. Microbiol. Biotechnol.*, ***93***, 931-940.

Etcheverry, M., Chulze, S., Dalcero, A., Varsavsky, E., & Magnoli, C. (1994). Effect of water activity and temperature on Tenuazonic acid production by *Alternaria alternata* on sunflower seeds. *Mycopathologia*, ***126***, 179-182.

Fanelli, F., Geisen, R., Schmidt-Heydt, M., Logrieco, A., & Mulè, G. (2016). Light regulation of mycotoxin biosynthesis: New perspectives for food safety. *World Mycotoxin J.*, ***9***, 129-146.

Fanelli, F., Schmidt-Heydt, M., Haidukowski, M., Susca, A., Geisen, R., Logrieco, A., & Mulè, G. (2012). Influence of light on growth, conidiation and fumonisin production by *Fusarium verticillioides*. *Fungal Biol.*, ***116***, 241-248.

Fang, J., Sheng, L., Ye, Y., Ji, J., Sun, J., Zhang, Y., & Sun, X. (2023). Recent advances in biosynthesis of mycotoxin-degrading enzymes and their applications in food and feed. *Crit Rev Food Sci Nutr.*, 1-17.

Farrar, J. J., Pryor, B. M., & Davis, R. M. (2004). *Alternaria* diseases of carrot. *Plant Dis.*, ***88***, 776-784.

Fehr, M., Pahlke, G., Fritz, J., Christensen, M. O., Boege, F., Altemöller, M., Podlech, J., & Marko, D. (2009). Alternariol acts as a topoisomerase poison, preferentially affecting the IIα isoform. *Mol. Nutr. Food Res.*, ***53***, 441-451.

Fernandes, C., Prados-Rosales, R., Silva Branca, M. A., Nakouzi-Naranjo, A., Zuzarte, M., Chatterjee, S., Stark Ruth, E., Casadevall, A., & Gonçalves, T. (2016). Activation of Melanin Synthesis in *Alternaria infectoria* by Antifungal Drugs. *Antimicrob. Agents Chemother.*, ***60***, 1646-1655.

Fernández-Blanco, C., Font, G., & Ruiz, M.-J. (2014). Oxidative stress of alternariol in Caco-2 cells. *Toxicol. lett.*, ***229***, 458-464.

Fernández-Blanco, C., Juan-García, A., Juan, C., Font, G., & Ruiz, M.-J. (2016). Alternariol induce toxicity via cell death and mitochondrial damage on Caco-2 cells. *Food Chem. Toxicol.*, ***88***, 32-39.

Fink-Gremmels, J. (2008). Mycotoxins in cattle feeds and carry-over to dairy milk: A review. *Food Addit. Contam. Part A*, ***25***, 172-180.

Finnigan, T. J. A., Wall, B. T., Wilde, P. J., Stephens, F. B., Taylor, S. L., & Freedman, M. R. (2019). Mycoprotein: The Future of Nutritious Nonmeat Protein, a Symposium Review. *Curr. dev. nutr.*, ***3***, nzz021.

Fioletov, V., Kerr, J. B., & Fergusson, A. (2010). The UV index: definition, distribution and factors affecting it. *Can. J. Public Health.*, ***101***, I5-9.

Fliszár-Nyúl, E., Lemli, B., Kunsági-Máté, S., Dellafiora, L., Dall'Asta, C., Cruciani, G., Pethő, G., & Poór, M. (2019). Interaction of Mycotoxin Alternariol with Serum Albumin. *Int. J. Mol. Sci.*, ***20***.

Fontaine, K., Fourrier-Jeandel, C., Armitage, A. D., Boutigny, A.-L., Crépet, M., Caffier, V., Gnide, D. C., Shiller, J., Le Cam, B., & Giraud, M. (2021). Identification and pathogenicity of *Alternaria* species associated with leaf blotch disease and premature defoliation in French apple orchards. *PeerJ.*, ***9***, e12496.

Gao, J., Wenderoth, M., Doppler, M., Schuhmacher, R., Marko, D., & Fischer, R. (2022). Fungal melanin biosynthesis pathway as source for fungal toxins. *MBio.*, ***13***, e00219-00222.

Gavahian, M., & Cullen, P. (2020). Cold plasma as an emerging technique for mycotoxin-free food: Efficacy, mechanisms, and trends. *Food Rev. Int.*, ***36***, 193-214.

Geisen, R., Schmidt-Heydt, M., Touhami, N., & Himmelsbach, A. (2018). New aspects of ochratoxin A and citrinin biosynthesis in *Penicillium. Curr. Opin. Food Sci.*, ***23***, 23-31.

Geisen, R., Touhami, N., & Schmidt-Heydt, M. (2017). Mycotoxins as adaptation factors to food related environments. *Curr. Opin. Food Sci.*, ***17***, 1-8.

Gow, N. A., Latge, J.-P., & Munro, C. A. (2017). The fungal cell wall: structure, biosynthesis, and function. *Microbiol. Spectr.*, ***5***, 10.1128/microbiolspec. funk-0035-2016.

Griffin, G. F., & Chu, F. (1983). Toxicity of the *Alternaria* metabolites alternariol, alternariol methyl ether, altenuene, and tenuazonic acid in the chicken embryo assay. *Appl. Environ. Microbiol.*, ***46***, 1420-1422.

Gustin Michael, C., Albertyn, J., Alexander, M., & Davenport, K. (1998). MAP Kinase Pathways in the Yeast *Saccharomyces cerevisiae*. *Microbiol. Mol. Biol.*, ***62***, 1264-1300.

Harley, J. (1971). Fungi in ecosystems. *J. Ecol.*, ***59***, 653-668.

Hasan, H. A. (1996). *Alternaria* mycotoxins in black rot lesion of tomato fruit: conditions and regulation of their production. *Acta Microbiol. Immunol. Hung*, ***43***, 125-133.

Hawksworth, D. (1988). The variety of fungal-algal symbioses, their evolutionary significance, and the nature of lichens. *Bot. J. Linn. Soc.*, ***96***, 3-20.

He, J., Evans, N. M., Liu, H., Zhu, Y., Zhou, T., & Shao, S. (2021). UV treatment for degradation of chemical contaminants in food: A review. *Compr Rev Food Sci Food Saf.*, ***20***, 1857-1886.

Heider, E. M., Harper, J. K., Grant, D. M., Hoffman, A., Dugan, F., Tomer, D. P., & O'Neill, K. L. (2006). Exploring unusual antioxidant activity in a benzoic acid derivative: a proposed mechanism for citrinin. *Tetrahedron*, ***62***, 1199-1208.

Herskowitz, I. (1988). Life cycle of the budding yeast *Saccharomyces cerevisiae. Microbiol. Rev.*, ***52***, 536-553.

Hetrick, K. J., & van der Donk, W. A. (2017). Ribosomally synthesized and post-translationally modified peptide natural product discovery in the genomic era. *Curr. Opin. Chem. Biol.* , ***38***, 36-44.

Hou, L., Mori, D., Takase, Y., Meihua, P., Kai, K., & Tokunaga, O. (2009). Fumagillin inhibits colorectal cancer growth and metastasis in mice: In vivo and in vitro study of anti-angiogenesis. *Pathol. Int.*, ***59***, 448-461.

Hu, W., Liu, Z., Fu, B., Zhang, X., Qi, Y., Hu, Y., Wang, C., Li, D., & Xu, N. (2022). Metabolites of the soy sauce Koji making with *Aspergillus niger* and *Aspergillus oryzae*. *Int. J. Food Sci. Technol.*, ***57***, 301-309.

Huang, C.-H., Wang, F.-T., & Chan, W.-H. (2021). Alternariol exerts embryotoxic and immunotoxic effects on mouse blastocysts through ROS-mediated apoptotic processes. *Toxicol. Res.*, ***10***, 719-732.

Hyvärinen, M., Härdling, R., & Tuomi, J. (2002). Cyanobacterial lichen symbiosis: the fungal partner as an optimal harvester. *Oikos*, ***98***, 498-504.

Igbalajobi, O., Yu, Z., & Fischer, R. (2019). Red- and Blue-Light Sensing in the Plant Pathogen *Alternaria alternata* Depends on Phytochrome and the White-Collar Protein LreA. *MBio*, ***10***, 10.1128/mbio.00371-00319.

Isshiki, A., Akimitsu, K., Yamamoto, M., & Yamamoto, H. (2001). Endopolygalacturonase Is Essential for Citrus Black Rot Caused by *Alternaria citri* but Not Brown Spot Caused by *Alternaria alternata*. *Mol. Plant Microbe Interact.*, ***14***, 749-757.

Jackson, L. S., Hlywka, J. J., Senthil, K. R., & Bullerman, L. B. (1996). Effect of thermal processing on the stability of fumonisins. *Adv Exp Med Biol.*, 345-353.

Jacobson, E. S., & Tinnell, S. B. (1993). Antioxidant function of fungal melanin. *J. Bacteriol.*, ***175***, 7102-7104.

Keller, N. P., & Hohn, T. M. (1997). Metabolic pathway gene clusters in filamentous fungi. *Fungal Genet. Biol.*, ***21***, 17-29.

Keller, N. P., Turner, G., & Bennett, J. W. (2005). Fungal secondary metabolism—from biochemistry to genomics. *Nat. Rev. Microbiol.*, ***3***, 937-947.

Kelman, M. J., Renaud, J. B., Seifert, K. A., Mack, J., Yeung, K. K. C., & Sumarah, M. W. (2020). Chemotaxonomic Profiling of Canadian *Alternaria* Populations Using High-Resolution Mass Spectrometry. *Metabolites*, ***10*****(6)**.

Klunklin, W., & Savage, G. (2017). Effect on quality characteristics of tomatoes grown under well-watered and drought stress conditions. *Foods*, ***6***, 56.

Koide, R. T., & Mosse, B. (2004). A history of research on arbuscular mycorrhiza. *Mycorrhiza*, ***14***, 145-163.

Kokaeva, L. Y., & Elansky, S. N. (2022). First Report of *Alternaria alternariacida* Causing Potato Leaf Blight in the Far East, Russia. *Plant Dis.*, ***107***, 938.

Kolawole, O., Meneely, J., Petchkongkaew, A., & Elliott, C. (2021). A review of mycotoxin biosynthetic pathways: Associated genes and their expressions under the influence of climatic factors. *Fungal Biol. Rev.*, ***37***, 8-26.

Kornienko, A., Evidente, A., Vurro, M., Mathieu, V., Cimmino, A., Evidente, M., van Otterlo, W. A., Dasari, R., Lefranc, F., & Kiss, R. (2015). Toward a cancer drug of fungal origin. *Med. Res. Rev.*, ***35***, 937-967.

Kurogi, K., Suiko, M., & Sakakibara, Y. (2024). Evolution and multiple functions of sulfonation and cytosolic sulfotransferases across species. *Biosci. Biotechnol. Biochem.*, ***88***, 368-380.

Lahue, C., Madden, A. A., Dunn, R. R., & Smukowski Heil, C. (2020). History and domestication of *Saccharomyces cerevisiae* in bread baking. *Front. genet.*, ***11***, 584718.

Lee, H. B., Patriarca, A., & Magan, N. (2015). *Alternaria* in food: ecophysiology, mycotoxin production and toxicology. *Mycobiology*, ***43***, 93-106.

Lee, J., Her, J.-Y., & Lee, K.-G. (2015). Reduction of aflatoxins (B1, B2, G1, and G2) in soybean-based model systems. *Food Chem.*, ***189***, 45-51.

Lehmann, L., Wagner, J., & Metzler, M. (2006). Estrogenic and clastogenic potential of the mycotoxin alternariol in cultured mammalian cells. *Food Chem. Toxicol.*, ***44***, 398-408.

Li, J.-F., Jiang, H.-B., Jeewon, R., Hongsanan, S., Bhat, D. J., Tang, S.-M., Lumyong, S., Mortimer, P. E., Xu, J.-C., & Camporesi, E. (2023). *Alternaria*: Update on species limits, evolution, multi-locus phylogeny, and classification. *Stud. Fungi.*, ***8***, 1-61.

Li, L., Chong, L., Huang, T., Ma, Y., Li, Y., & Ding, H. (2023). Natural products and extracts from plants as natural UV filters for sunscreens: A review. *AMEM*, ***6***, 183-195.

Li, Q., Bai, D., Qin, L., Shao, M., Zhang, S., Yan, C., Yu, G., & Hao, J. (2020). Protective effect of d-tetramannuronic acid tetrasodium salt on UVA-induced photo-aging in HaCaT cells. *Biomed. Pharmacother.*, ***126***, 110094.

Li, S., Shen, Q., Wang, H., He, F., Xiao, Z., Peng, X., Zhou, M., & Tang, X. (2021). First Report of *Alternaria alternata* Causing Leaf Spot of Tartary Buckwheat in China. *Plant Dis.*, ***105***, 3751.

Lin, C.-H., & Chung, K.-R. (2010). Specialized and shared functions of the histidine kinase- and HOG1 MAP kinase-mediated signaling pathways in *Alternaria alternata*, a filamentous fungal pathogen of citrus. *Fungal Genet. Biol.*, ***47***, 818-827.

Liu, Y. X., Cui, Z. P., Zhao, H. P., Li, Y. H., Gu, Y. C., & Wang, Q. M. (2014). Synthesis and Biological Activities of 3-Substituted Analogues of Tenuazonic Acid. *J. Heterocycl. Chem.*, ***51***, E209-E215.

Lodolo, E. J., Kock, J. L., Axcell, B. C., & Brooks, M. (2008). The yeast *Saccharomyces cerevisiae*–the main character in beer brewing. *FEMS yeast res.*, ***8***, 1018-1036.

Loganathan, M., Venkataravanappa, V., Saha, S., Rai, A. B., Tripathi, S., Rai, R. K., Pandey, A. K., & Chowdappa, P. (2016). Morphological, Pathogenic and Molecular Characterizations of *Alternaria* Species Causing Early Blight of Tomato in Northern India. *Proc Natl Acad Sci India Sect B Biol Sci.*, ***86***, 325-330.

López Sáncheza, P., de Nijsa, M., Spanjerb, M., Pietric, A., Bertuzzic, T., Starski, A., Postupolski, J., Castellari, M., & Hortós, M. (2017). Generation of occurrence data on citrinin in food. *EFSA support. publ.*, ***14***, 1177E.

Louro, H., Vettorazzi, A., López de Cerain, A., Spyropoulou, A., Solhaug, A., Straumfors, A., Behr, A.-C., Mertens, B., Žegura, B., & Fæste, C. K. (2024). Hazard characterization of *Alternaria* toxins to identify data gaps and improve risk assessment for human health. *Arch. Toxicol.*, ***98***, 425-469.

Mannaa, M., & Kim, K. D. (2017). Influence of temperature and water activity on deleterious fungi and mycotoxin production during grain storage. *Mycobiology*, ***45***, 240-254.

Markham, P., & Collinge, A. J. (1987). Woronin bodies of filamentous fungi. *FEMS Microbiol. Rev.*, ***3***, 1-11.

McKenzie, K., Sarr, A., Mayura, K., Bailey, R., Miller, D., Rogers, T., Norred, W., Voss, K., Plattner, R., & Kubena, L. (1997). Oxidative degradation and detoxification of mycotoxins using a novel source of ozone. *Food Chem. Toxicol.*, ***35***, 807-820.

Medina, Á., Rodríguez, A., & Magan, N. (2015). Climate change and mycotoxigenic fungi: Impacts on mycotoxin production. *Current Opinion in Food Science*, ***5***, 99-104.

Medina, A., Schmidt-Heydt, M., Rodríguez, A., Parra, R., Geisen, R., & Magan, N. (2015). Impacts of environmental stress on growth, secondary metabolite biosynthetic gene clusters and metabolite production of xerotolerant/xerophilic fungi. *Curr. Genet.*, ***61***, 325-334.

Meena, M., & Samal, S. (2019). *Alternaria* host-specific (HSTs) toxins: An overview of chemical characterization, target sites, regulation and their toxic effects. *Toxicol. Rep.*, ***6***, 745-758.

Meiramkulova, K., Devrishov, D., Adylbek, Z., Kydyrbekova, A., Zhangazin, S., Ualiyeva, R., Temirbekova, A., Adilbektegi, G., & Mkilima, T. (2023). The impact of various LED light spectra on tomato preservation. *Sustainability*, ***15***, 1111.

Merckx, V., Bidartondo, M. I., & Hynson, N. A. (2009). Myco-heterotrophy: when fungi host plants. *Ann. Bot.*, ***104***, 1255-1261.

Mercurio, D. G., Wagemaker, T. A. L., Alves, V. M., Benevenuto, C. G., Gaspar, L. R., & Maia Campos, P. M. B. G. (2015). In vivo photoprotective effects of cosmetic formulations containing UV filters, vitamins, *Ginkgo biloba* and red algae extracts. *J. Photochem. Photobiol. B.* , ***153***, 121-126.

Miao, Y., Wang, D., Chen, Y., Zhu, X., Tang, X., Zhang, J., Zhang, L., & Chen, J. (2022). General toxicity and genotoxicity of alternariol: a novel 28-day multi-endpoint assessment in male Sprague-Dawley rats. *Mycotoxin Res.*, ***38***, 231-241.

Mohr, K. I. (2016). *History of antibiotics research*.I

Nazari, K., Ebadi, M. J., & Berahmand, K. (2022). Diagnosis of *Alternaria* disease and leafminer pest on tomato leaves using image processing techniques. *J. Sci. Food Agric.*, ***102***, 6907-6920.

NCBI. (2025). *PubChem Compound Summary for CID 6918469, Altenusin*. https://pubchem.ncbi.nlm.nih.gov/compound/Altenusin.

Nout, M. J. R., & Aidoo, K. E. (2011). Asian Fungal Fermented Food. In M. Hofrichter (Ed.), *Industrial Applications* (pp. 29-58). Springer Berlin Heidelberg.

Ntasiou, P., Myresiotis, C., Konstantinou, S., Papadopoulou-Mourkidou, E., & Karaoglanidis, G. S. (2015). Identification, characterization and mycotoxigenic ability of *Alternaria spp*. causing core rot of apple fruit in Greece. *Int. J. Food Microbiol.*, ***197***, 22-29.

Ochiai, N., Tokai, T., Takahashi-Ando, N., Fujimura, M., & Kimura, M. (2007). Genetically engineered *Fusarium* as a tool to evaluate the effects of environmental factors on initiation of trichothecene biosynthesis. *FEMS Microbiol. Lett.*, ***275***, 53-61.

Oliveira, A. B., Moura, C. F., Gomes-Filho, E., Marco, C. A., Urban, L., & Miranda, M. R. A. (2013). The impact of organic farming on quality of tomatoes is associated to increased oxidative stress during fruit development. *PLoS One*, ***8***, e56354.

Oviedo, M. S., Ramirez, M. L., Barros, G. G., & Chulze, S. N. (2010). Impact of Water Activity and Temperature on Growth and Alternariol and Alternariol Monomethyl Ether Production of *Alternaria alternata* Isolated from Soybean. *J. Food Prot.*, ***73***, 336-343.

Panzer, S., Brych, A., Batschauer, A., & Terpitz, U. (2019). Opsin 1 and Opsin 2 of the corn smut fungus *Ustilago maydis* are green light-driven proton pumps. *Front. Microbiol.*, ***10***, 735.

Park, H. S., Han, H. Y., & Cho, T. J. (2023). Fruit Quality Changes and Microbiome Dynamics of Natural Microflora of Peaches (*Prunus persica*) during Visible Blue-light Irradiation. *한국식품영양과학회 학술대회발표집*, 501-501.

Parkinson, D. (1994). Filamentous Fungi. In Methods of Soil Analysis (pp. 329-350).

Paterson, R. R. M., & Lima, N. (2011). Further mycotoxin effects from climate change. *Food Research International*, ***44***, 2555-2566.

Patriarca, A. (2019). Fungi and mycotoxin problems in the apple industry. *Curr. Opin. Food Sci.*, ***29***, 42-47.

Pavicich, M. A., Nielsen, K. F., & Patriarca, A. (2022). Morphological and chemical characterization of *Alternaria* populations from apple fruit. *Int. J. Food Microbiol.*, ***379***, 109842.

Pfeiffer, E., Schebb, N. H., Podlech, J., & Metzler, M. (2007). Novel oxidative in vitro metabolites of the mycotoxins alternariol and alternariol methyl ether. *Mol. Nutr. Food Res.*, ***51***, 307-316.

Ponts, N. (2015). Mycotoxins are a component of *Fusarium graminearum* stress-response system. In **(Vol. 6, pp. 1234)**: Frontiers Media SA.

Priesterjahn, E.-M., Geisen, R., & Schmidt-Heydt, M. (2020). Influence of Light and Water Activity on Growth and Mycotoxin Formation of Selected Isolates of *Aspergillus flavus* and *Aspergillus parasiticus*. *Microorganisms*, ***8*****(12)**.

Puntscher, H., Marko, D., & Warth, B. (2020). First determination of the highly genotoxic fungal contaminant altertoxin II in a naturally infested apple sample. *Emerg. Contam.*, ***6***, 82-86.

Qin, X., Su, X., Tu, T., Zhang, J., Wang, X., Wang, Y., Wang, Y., Bai, Y., Yao, B., & Luo, H. (2021). Enzymatic degradation of multiple major mycotoxins by dye-decolorizing peroxidase from *Bacillus subtilis*. *Toxins*, ***13***, 429.

Rahman, M. Z., Honda, Y., & Arase, S. (2003). Red-Light-Induced Resistance in Broad Bean (*Vicia faba L.*) to Leaf Spot Disease Caused by *Alternaria tenuissima*. *J. Phytopathol.*, ***151***, 86-91.

Raters, M., & Matissek, R. (2008). Thermal stability of aflatoxin B 1 and ochratoxin A. *Mycotoxin Res.*, ***24***, 130-134.

Read, D. (1999). *Mycorrhiza—the state of the art*.I

Robeson, D. J., & Jalal, M. A. (1991). Tenuazonic acid produced by an *Alternaria alternata* isolate from *Beta vulgaris*. *J. Inorg. Biochem.*, ***44***, 109-116.

Rychlik, M., Lepper, H., Weidner, C., & Asam, S. (2016). Risk evaluation of the *Alternaria* mycotoxin tenuazonic acid in foods for adults and infants and subsequent risk management. *Food Control*, ***68***, 181-185.

Sadeghi, B., & Mirzaei, S. (2018). First Report of *Alternaria* Leaf Spot Caused by *Alternaria chlamydosporigena* on Tomato in Iran. *Plant Dis.*, ***102***, 1175.

Saha, D., Fetzner, R., Burkhardt, B., Podlech, J., Metzler, M., Dang, H., Lawrence, C., & Fischer, R. (2012). Identification of a polyketide synthase required for alternariol (AOH) and alternariol-9-methyl ether (AME) formation in *Alternaria alternata*. *PLoS One*, ***7***, e40564.

Salimova, D., Dalinova, A., Dubovik, V., Senderskiy, I., Stepanycheva, E., Tomilova, O., Hu, Q., & Berestetskiy, A. (2021). Entomotoxic activity of the extracts from the fungus, *Alternaria tenuissima* and its major metabolite, tenuazonic acid. *J. Fungus*, ***7***, 774.

Samtiya, M., Aluko, R. E., Puniya, A. K., & Dhewa, T. (2021). Enhancing Micronutrients Bioavailability through Fermentation of Plant-Based Foods: A Concise Review. *Fermentation*, ***7*(2)**.

Sands, D. C., McINTYRE, J. L., & Walton, G. S. (1976). Use of activated charcoal for the removal of patulin from cider. *Appl. Environ. Microbiol.*, ***32***, 388-391.

Schmidt-Dannert, C. (2015). *Biosynthesis of terpenoid natural products in fungi*.I

Schmidt-Heydt, M., Cramer, B., Graf, I., Lerch, S., Humpf, H.-U., & Geisen, R. (2012). Wavelength-dependent degradation of ochratoxin and citrinin by light in vitro and in vivo and its implications on *Penicillium*. *Toxins*, ***4***, 1535-1551.

Schmidt-Heydt, M., Magan, N., & Geisen, R. (2008). Stress induction of mycotoxin biosynthesis genes by abiotic factors. *FEMS Microbiol. Lett.*, ***284***, 142-149.

Schmidt-Heydt, M., Rüfer, C., Raupp, F., Bruchmann, A., Perrone, G., & Geisen, R. (2011). Influence of light on food relevant fungi with emphasis on ochratoxin producing species. *nt. J. Food Microbiol.*, ***145***, 229-237.

Schmidt-Heydt, M., Stoll, D., Schütz, P., & Geisen, R. (2015). Oxidative stress induces the biosynthesis of citrinin by *Penicillium verrucosum* at the expense of ochratoxin. *Int. J. Food Microbiol.*, ***192***, 1-6.

Schrader, T., Cherry, W., Soper, K., & Langlois, I. (2006). Further examination of the effects of nitrosylation on *Alternaria alternata* mycotoxin mutagenicity in vitro. *Mutat. Res. Genet. Toxicol. Environ. Mutagen.*, ***606***, 61-71.

Selhub, E. M., Logan, A. C., & Bested, A. C. (2014). Fermented foods, microbiota, and mental health: ancient practice meets nutritional psychiatry. *J. Physiol. Anthropol.*, ***33***, 1-12.

Setälä, H., & McLean, M. A. (2004). Decomposition rate of organic substrates in relation to the species diversity of soil saprophytic fungi. *Oecologia*, ***139***, 98-107.

Shigeura, H. T., & Gordon, C. N. (1963). The biological activity of tenuazonic acid. *Biochem.*, ***2***, 1132-1137.

Simmons, E. G. (2007). *Alternaria* an identification manual, fully illustrated and with catalogue raisonné 1796-2007.

Singh, V. (2015). *Alternaria* diseases of vegetable crops and its management control to reduce the low production. *Int. J. Agric Sci.*, 0975-3710.

Solhaug, A., Eriksen, G. S., & Holme, J. A. (2016). Mechanisms of Action and Toxicity of the Mycotoxin Alternariol: A Review. *Basic Clin. Pharmacol. Toxicol.*, ***119***, 533-539.

Solhaug, A., Holme, J. A., Haglund, K., Dendele, B., Sergent, O., Pestka, J., Lagadic-Gossmann, D., & Eriksen, G. S. (2013). Alternariol induces abnormal nuclear morphology and cell cycle arrest in murine RAW 264.7 macrophages. *Toxicol. lett.*, ***219***, 8-17.

Solhaug, A., Vines, L., Ivanova, L., Spilsberg, B., Holme, J., Pestka, J., Collins, A., & Eriksen, G. (2012). Mechanisms involved in alternariol-induced cell cycle arrest. *Mutat. Res.-Fund. Mol. M.*, ***738***, 1-11.

Solhaug, A., Wisbech, C., Christoffersen, T. E., Hult, L., Lea, T., Eriksen, G. S., & Holme, J. A. (2015). The mycotoxin alternariol induces DNA damage and modify macrophage phenotype and inflammatory responses. *Toxicol. lett.*, ***239***, 9-21.

Songsermsakul, P., & Razzazi-Fazeli, E. (2008). A Review of Recent Trends in Applications of Liquid Chromatography-Mass Spectrometry for Determination of Mycotoxins. *J. Liq. Chromatogr. Relat. Technol.*, ***31***, 1641-1686.

Soukup, S. T., Kohn, B. N., Pfeiffer, E., Geisen, R., Metzler, M., Bunzel, M., & Kulling, S. E. (2016). Sulfoglucosides as Novel Modified Forms of the Mycotoxins Alternariol and Alternariol Monomethyl Ether. *J. Agric. Food Chem.*, ***64***, 8892-8901.

Spern, C. J., Hummerick, M. E., Khodadad, C. L., Morales, C., Dixit, A. R., Spencer, L. E., Mitchell, C., Morrow, B., Douglas, G. L., & Wheeler, R. M. (2025). The Microbiome of A Tomato Crop Grown Under Different Lighting Regimes on the International Space Station.

Sreeramulu, G., Zhu, Y., & Knol, W. (2000). Kombucha Fermentation and Its Antimicrobial Activity. *J. Agric. Food Chem.*, ***48***, 2589-2594.

Stahl, W., & Sies, H. (2002). Carotenoids and Protection against Solar UV Radiation. *Skin Pharmacol. Appl. Skin Physiol.*, ***15***, 291-296.

Stewart, J. E., Timmer, L. W., Lawrence, C. B., Pryor, B. M., & Peever, T. L. (2014). Discord between morphological and phylogenetic species boundaries: incomplete lineage sorting and recombination results in fuzzy species boundaries in an asexual fungal pathogen. *BMC Evol. Biol.*, ***14***, 38.

Steyn, P. S., & Rabie, C. J. (1976). Characterization of magnesium and calcium tenuazonate from *Phoma sorghina*. *Phytochemistry*, ***15***, 1977-1979.

Suiko, M., Kurogi, K., Hashiguchi, T., Sakakibara, Y., & Liu, M. C. (2017). Updated perspectives on the cytosolic sulfotransferases (SULTs) and SULT-mediated sulfation. *Biosci. Biotechnol. Biochem.*, ***81***, 63-72.

Sun, F., Cao, X., Yu, D., Hu, D., Yan, Z., Fan, Y., Wang, C., & Wu, A. (2022). AaTAS1 and AaMFS1 Genes for Biosynthesis or Efflux Transport of Tenuazonic Acid and Pathogenicity of *Alternaria alternata*. *MPMI*, ***35***, 416-427.

Sun, H. F., Wang, H., Yan, Y., & Yang, H. Y. (2022). First Report of *Alternaria alternata* Causing Leaf Spot of *Cynanchum atratum* in China. *Plant Dis.*, ***107***, 1226.

Suthar, M., Dufossé, L., & Singh, S. K. (2023). The enigmatic world of fungal melanin: a comprehensive review. *J. Fungi*, ***9***, 891.

Suzuki, T. (2018). Light-Irradiation Wavelength and Intensity Changes Influence Aflatoxin Synthesis in Fungi. *Toxins*, ***10***, 31.

Takahashi, R., Isshiki, S.-N., Hakozaki, M., Kanno, Y., Uesugi, S., Koseki, T., & Shiono, Y. (2024). Altenuene derivatives produced by an endophyte *Alternaria alternata*. *Nat. Prod. Res.*, 1-8.

Tang, X., Chen, Y., Zhu, X., Miao, Y., Wang, D., Zhang, J., Li, R., Zhang, L., & Chen, J. (2022). Alternariol monomethyl ether toxicity and genotoxicity in male Sprague-Dawley

rats: 28-Day in vivo multi-endpoint assessment. *Mutat. Res. Genet. Toxicol. Environ. Mutagen.*, ***873***, 503435.

Taralova, E. H., Schlecht, J., Barnard, K., & Pryor, B. M. (2011). Modelling and visualizing morphology in the fungus *Alternaria*. *Fungal Biol.*, ***115***, 1163-1173.

Thomma, B. P. H. J. (2003). *Alternaria spp*.: from general saprophyte to specific parasite. *Mol. Plant Pathol.*, ***4***, 225-236.

Tiessen, C., Fehr, M., Schwarz, C., Baechler, S., Domnanich, K., Böttler, U., Pahlke, G., & Marko, D. (2013). Modulation of the cellular redox status by the *Alternaria* toxins alternariol and alternariol monomethyl ether. *Toxicol. lett.*, ***216***, 23-30.

Tola, M., & and Kebede, B. (2016). Occurrence, importance and control of mycotoxins: A review. *Cogent food agric.*, ***2***, 1191103.

Torres, R., Valentines, M. C., Usall, J., Viñas, I., & Larrigaudiere, C. (2003). Possible involvement of hydrogen peroxide in the development of resistance mechanisms in 'Golden Delicious' apple fruit. *Postharvest Biol. and Technol.*, ***27***, 235-242.

Troncoso-Rojas, R., & Tiznado-Hernández, M. E. (2014a). *Alternaria alternata* (black rot, black spot). In *Postharvest decay* (pp. 147-187). Elsevier.

Troncoso-Rojas, R., & Tiznado-Hernández, M. E. (2014b). Chapter 5 - *Alternaria alternata* (Black Rot, Black Spot). In S. Bautista-Baños (Ed.), *Postharvest Decay* (pp. 147-187). Academic Press.

Tymon, L. S., Peever, T. L., & Johnson, D. A. (2015). Identification and Enumeration of Small-Spored *Alternaria* Species Associated with Potato in the U.S. Northwest. *Plant Dis.*, ***100***, 465-472.

Vakalounakis, D. J., & Malathrakis, N. E. (1988). A Cucumber Disease Caused by *Alternaria alternata* and its Control. *J. Phytopathol.*, ***121***, 325-336.

Van Egmond, H. P., & Jonker, M. A. (2004). Worldwide regulations on aflatoxins—The situation in 2002. *J. Toxicol. Toxin Rev.*, ***23***, 273-293.

Wachowska, U., Kwiatkowska, E., & Pluskota, W. (2021). *Alternaria alternata* as a Seed-Transmitted Pathogen of *Sida hermaphrodita* (*Malvaceae*) and Its Suppression by *Aureobasidium pullulans*. *Agriculture*, ***11*****(12)**.

Wallace Hayes, A. (1980). Mycotoxins: a review of biological effects and their role in human diseases. *Clin. Toxicol.*, ***17***, 45-83.

Wang, H., Guo, Y., Luo, Z., Gao, L., Li, R., Zhang, Y., Kalaji, H. M., Qiang, S., & Chen, S. (2022). Recent advances in *Alternaria* phytotoxins: a review of their occurrence, structure, bioactivity, and biosynthesis. *J. Fungi*, ***8***, 168.

Wang, L., Wang, M., Jiao, J., & Liu, H. (2022). Roles of AaVeA on Mycotoxin Production via Light in *Alternaria alternata* [Original Research]. *Front. Microbiol.*, ***13***, 842268.

Wang, Z., Wang, J., Li, N., Li, J., Trail, F., Dunlap, J. C., & Townsend, J. P. (2018). Light sensing by opsins and fungal ecology: NOP-1 modulates entry into sexual reproduction in response to environmental cues. *Mol. Ecol.*, ***27***, 216-232.

Wei, B., Du, A.-Q., Ying, T.-T., Hu, G.-A., Zhou, Z.-Y., Yu, W.-C., He, J., Yu, Y.-L., Wang, H., & Xu, X.-W. (2023). Secondary metabolic potential of *Kutzneria*. *J. Nat. Prod.*, ***86***, 1120-1127.

Weinshilboum, R., & Otterness, D. (1994). Sulfotransferase Enzymes. In F. C. Kauffman (Ed.), Conjugation—Deconjugation Reactions in Drug Metabolism and Toxicity (pp. 45-78). Springer Berlin Heidelberg.

Weinshilboum, R. M. (1986). Phenol sulfotransferase in humans: properties, regulation, and function. *Fed. Proc.*, ***45***, 2223-2228.

Wenderoth, M., Garganese, F., Schmidt-Heydt, M., Soukup, S. T., Ippolito, A., Sanzani, S. M., & Fischer, R. (2019). Alternariol as virulence and colonization factor of *Alternaria alternata* during plant infection. *Mol. Microbiol.*, ***112***, 131-146.

Wenderoth, M., Pinecker, C., Voß, B., & Fischer, R. (2017). Establishment of CRISPR/Cas9 in *Alternaria alternata*. *Fungal Genet. Biol.*, ***101***, 55-60.

Wilson, H. E., Carroll, G. C., Roy, B. A., & Blaisdell, G. K. (2014). Tall fescue is a potential spillover reservoir host for *Alternaria* species. *Mycologia*, ***106***, 22-31.

Wyatt, M. A., Wang, W., Roux, C. M., Beasley, F. C., Heinrichs, D. E., Dunman, P. M., & Magarvey, N. A. (2010). *Staphylococcus aureus* nonribosomal peptide secondary metabolites regulate virulence. *Science*, ***329***, 294-296.

Xu, C., Li, C. Y.-T., & Kong, A.-N. T. (2005). Induction of phase I, II and III drug metabolism/transport by xenobiotics. *Arch. Pharm. Res.*, ***28***, 249-268.

Yekeler, H., Bitmiş, K., Ozçelik, N., Doymaz, M. Z., & Calta, M. (2001). Analysis of toxic effects of *Alternaria* toxins on esophagus of mice by light and electron microscopy. *Toxicol. Pathol.*, ***29***, 492-497.

Young, A. T. (1981). Rayleigh scattering. *Applied Optics*, ***20***, 533-535.

Yu, Y., Zeng, L., Huang, L., Yan, Z., Sun, K., Zhu, T., & Zhu, A. (2016). First Report of Black Leaf Spot Caused by *Alternaria alternata* on Ramie in China. *J Phytopathol.*, ***164***, 358-361.

Yu, Z., Streng, C., Seibeld, R. F., Igbalajobi, O. A., Leister, K., Ingelfinger, J., & Fischer, R. (2021). Genome-wide analyses of light-regulated genes in *Aspergillus nidulans* reveal a complex interplay between different photoreceptors and novel photoreceptor functions. *PLoS Genet.*, ***17***, e1009845.

Zhang, H., Murzello, C., Sun, Y., Kim, M.-S., Xie, X., Jeter, R. M., Zak, J. C., Dowd, S. E., & Paré, P. W. (2010). Choline and osmotic-stress tolerance induced in *Arabidopsis* by the soil microbe *Bacillus subtilis* (GB03). *MPMI*, ***23***, 1097-1104.

Zheng, H. H., & Wu, X. H. (2013). First Report of *Alternaria* Blight of Potato Caused by *Alternaria tenuissima* in China. *Plant Dis.*, ***97***, 1246-1246.

Zhu, X., Chen, Y., Tang, X., Wang, D., Miao, Y., Zhang, J., Li, R., Zhang, L., & Chen, J. (2022). General toxicity and genotoxicity of altertoxin I: A novel 28-day multiendpoint assessment in male Sprague–Dawley rats. *J. Appl. Toxicol.*, ***42***, 1310-1322.

Zwickel, T., Kahl, S. M., Rychlik, M., & Müller, M. E. H. (2018). Chemotaxonomy of Mycotoxigenic Small-Spored *Alternaria* Fungi – Do Multitoxin Mixtures Act as an Indicator for Species Differentiation?. *Front. Microbiol.*, ***9***.

List of scientific publications

Publications in peer-reviewed Journals

1. **Adeyemo, A., & Schmidt-Heydt, M. (2024).** Expansion of the multi-locus gene alignment approach to improve identification of the fungal species *Alternaria alternata*. *International Journal of Food Microbiology*, *421*, 110746.

Publications under review in peer-reviewed Journals

1. **A.W. Adeyemo, M. Schmidt-Heydt. (2025)** Sequencing and Analysis of the entire Genome of the Toxigenic Fungus *Alternaria alternata*. Under review at: Microbiology Resource Announcements
2. **A.W. Adeyemo, M. Schmidt-Heydt (2025) Impact** of External Stress Factors on Mycotoxin Synthesis in *Alternaria alternata*.

Presentations

1. **Adeyemo, A.W, & Schmidt-Heydt, M. (2023).** Environmental influences on the production of Alternariol-Sulfate in *Alternaria alternata*. Mycotoxin Workshop, Celle, Germany, 05.07.2023 - 07.07.2023
2. **Adeyemo, A.W, & Schmidt-Heydt, M. (2023).** *Alternaria* toxins and their influence on human health. Vivid GRK 2576, Karlsruhe, Germany, 24.0720.23
3. **Adeyemo, A.W, & Schmidt-Heydt, M. (2024).** Filamentous fungi as food contaminants. VAAM Special Group Quality Management Meeting, Pohlheim, Germany,12.09.2024 -13.09.2024
4. **Adeyemo, A.W, & Schmidt-Heydt, M. (2024).** Expansion of the multi-locus gene alignment approach to improve identification of the fungal species

Alternaria alternata Mycotoxin Workshop, Vienna, Austria, 02.06.2024 - 05.06.2024

5. **Adeyemo, A.W, & Schmidt-Heydt, M. (2025).** Impact of External Stress Factors on Mycotoxin Synthesis in *Alternaria alternata*. Mycotoxin Workshop, Martina Franca, Italy, 25.05.2025 – 28.5.2025

Poster Presentations

1. **Adeyemo, A.W, & Schmidt-Heydt, M. (2023).** Environmental influences on the production of alternariol-Sulfate in *Alternaria alternata*. PhD Seminar, Karlsruhe, Germany
2. **Schmey, T., Adeyemo, A. W., Stam, R. (**Small spored *Alternaria* infecting wild tomatoes show genetic and chemical diversity. European Conferences on Fungal Genetics Dublin, Ireland, 02.03.2025 - 05.03-2025
3. **Maul, R., Schmidt-Heydt, M. Adeyemo, A.W, Lie, K.** Preparation Strategy for Enniatins to be used in Toxicological and Transfer Studies

Publications in the sequence database of the NCBI

Whole genome sequences (assemblies) on GenBank and raw sequencing data on the Sequence
Read Archive (SRA):

1. **Adeyemo, A.W, & Schmidt-Heydt, M.** *Alternaria alternata* ATCC 66981. , BioSample: SAMN45053446, GenBank: JBLEAD000000000

Publications of gene sequences in the sequence database of the NCBI

1. **Adeyemo, A.W, & Schmidt-Heydt, M.** *Alternaria alternata* ATCC 66981.

Alternaria alternata culture ATCC:66981 putative sulfotransferase gene, complete cds, ACCN: PP982769

Danksagung

Zunächst möchte ich mich bei meinem Doktorvater PD Markus Schmidt-Heydt bedanken, nicht nur dafür, dass ich dank ihm an diesem hochinteressanten Thema, das der Allgemeinheit zugutekommt, arbeiten durfte, sondern auch für die anregenden Gespräche über fachliche und nicht fachliche Dinge, den Umgang und das Verständnis, die mir entgegengebracht wurden.

Des Weiteren möchte ich Prof. Dr. Reinhard Fischer sowohl für die Übernahme des Korreferats als auch für die positive Zusammenarbeit im Zuge der Studentenbetreuung am KIT meinen Dank aussprechen.

Einige Mitarbeitende des MRI müssen hier auch Dankend erwähnt werden da diese fachliche und experimentelle Unterstützung geliefert haben welche meine Arbeit bereichert haben. Somit möchte ich Dr. med. Karlis Briviba und seinen Mitarbeitern für die Hilfe bei der Durchführung der Toxizitätstests danken. Genauso gilt mein Dank Dr. Sebastian Soukup und Volker Müller für Ihre Zuarbeit beim Unterfangen der Identifikation unbekannter Metaboliten.

Ein weiterer Dank geht an die Arbeitsgruppe Mykologie und ihre Mitarbeiter, von denen jeder für sich einen Beitrag zu meiner Zeit am MRI geleistet hat. Ein besonderer Dank gilt Marianne Urbanek, die nicht nur immer ein Ohr für interessante Gespräche hatte, sondern auch die Messung dieser großen Menge an Proben in dieser Zeit ermöglicht hat. Auch den anderen Mitgliedern gilt mein Dank, Karla Hell und Heidi Brandel, die sich nie zu schade waren, sich Zeit zu nehmen, um ihre Erfahrung mit anderen zu teilen; Nicole Mischke, die so nett war, mich in die Gepflogenheiten des MRI einzuführen; außerdem meinem Bürogenossen Christian Roder, dessen Ausstrahlung immer ein willkommener Ruhepol an stressigen Tagen war. Nicht zu vergessen die Neuzugänge Katharina Neumeier, Nicolai Glockner und Nico Mühling, mit denen es immer etwas zu lachen gab.

Auch den anderen Doktoranden des OG mit denen ich so manche Mittagspause verbracht habe in der sich über alles Mögliche, aber vor allem über Essen ausgetauscht wurde. Allen voran Lea Böckstiegel, Jens Knauth, Oliver Wittek und Elisa Streitenberger haben meinen Horizont immer wieder erweitert.

Natürlich möchte ich es mir nicht nehmen lassen, meinen Freunden und meiner Familie zu danken. Leider wäre es zu viel, jeden Einzelnen hier zu nennen, dem ich danken möchte, aber diejenigen wissen es, da bin ich mir sicher. Sie alle waren immer für mich da, um mich zu motivieren und einen Ausgleich zu den langen Stunden im Labor zu schaffen. Allen voran danke ich Isabel Gräber dafür, dass sie mich in den letzten Jahren begleitet und immer unterstützt hat. Sie hat mich nicht nur immer wieder daran erinnert, dass es ein Leben außerhalb des Labors gibt, sondern sie hat die schwierigsten Zeiten erträglich und die guten Zeiten zu den besten gemacht.

Außerdem möchte ich mich bei meinen Eltern Seyi und Ulrike sowie meinen Geschwistern Dayo und Kemi dafür bedanken, dass sie mich auf meinem Weg immer nach Kräften unterstützt haben.

Zum Schluss möchte ich mich bei meiner Großmutter Friederike bedanken die meinen Werdegang immer voller Euphorie beobachtet hat und meinem leider verstorbener Großvater Alfred der mir zu Lebzeiten nahegebracht hat, dass sich harte Arbeit und Durchhaltevermögen immer auszahlen.